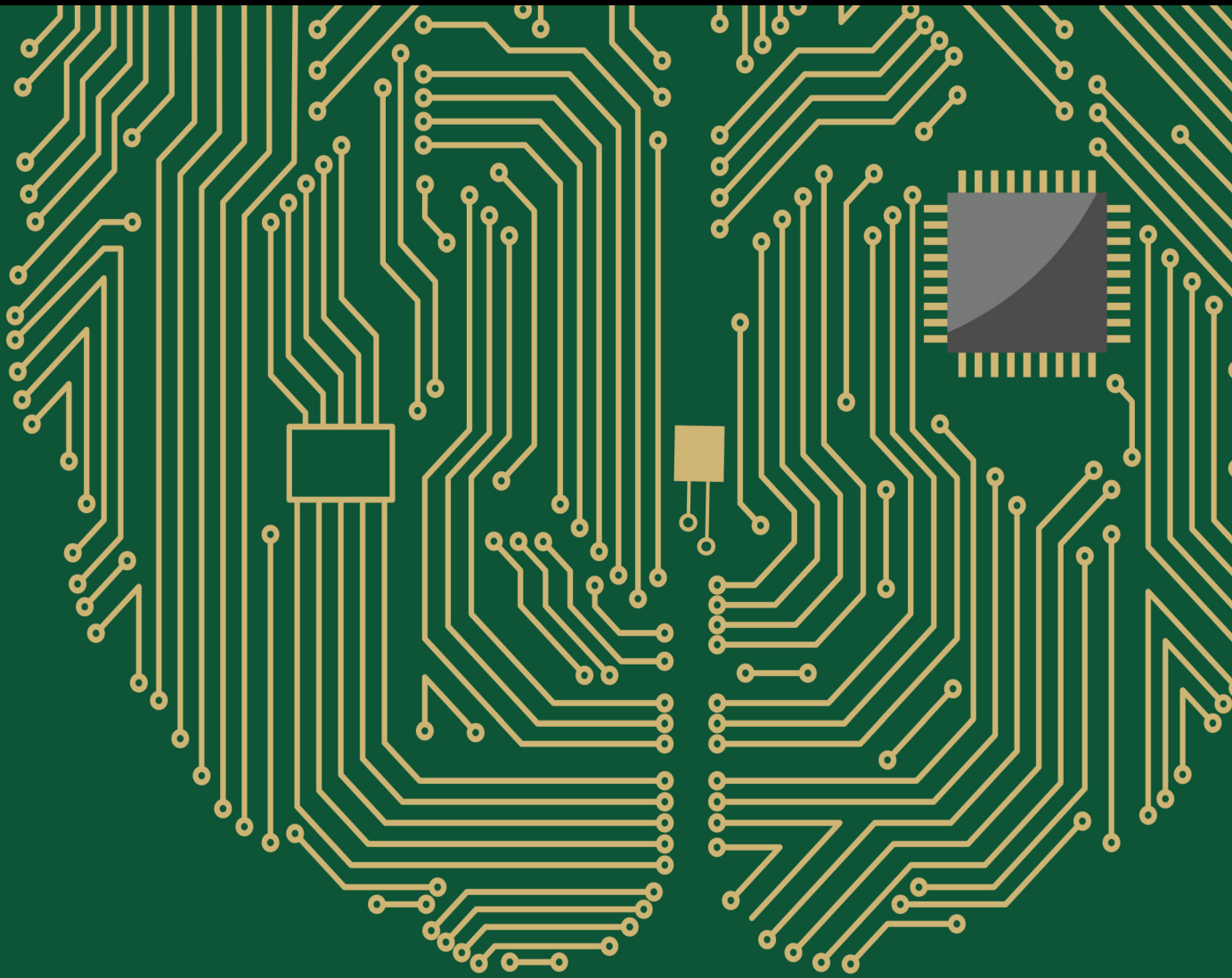


Brain-Computer Interface Applications for Improving the Quality of Elderly Living

Lead Guest Editor: Abdelkader Nasreddine Belkacem

Guest Editors: Yasuharu Koike, Tiago H. Falk, and Jason Palmer





Brain-Computer Interface Applications for Improving the Quality of Elderly Living

Computational Intelligence and Neuroscience

Brain-Computer Interface Applications for Improving the Quality of Elderly Living

Lead Guest Editor: Abdelkader Nasreddine
Belkacem

Guest Editors: Yasuharu Koike, Tiago H. Falk, and
Jason Palmer



Copyright © 2021 Hindawi Limited. All rights reserved.

This is a special issue published in "Computational Intelligence and Neuroscience." All articles are open access articles distributed under the Creative Commons Attribution License, which permits unrestricted use, distribution, and reproduction in any medium, provided the original work is properly cited.

Chief Editor

Andrzej Cichocki, Poland

Associate Editors

Arnaud Delorme, France
Cheng-Jian Lin , Taiwan
Saeid Sanei, United Kingdom

Academic Editors




Mohamed Abd Elaziz , Egypt
Tariq Ahanger , Saudi Arabia
Muhammad Ahmad, Pakistan
Ricardo Aler , Spain
Nouman Ali, Pakistan
Pietro Aricò , Italy
Lerina Aversano , Italy
Ümit Ağbulut , Turkey
Najib Ben Aoun , Saudi Arabia
Surbhi Bhatia , Saudi Arabia
Daniele Bibbo , Italy
Vince D. Calhoun , USA
Francesco Camastra, Italy
Zhicheng Cao, China
Hubert Cecotti , USA
Jyotir Moy Chatterjee , Nepal
Rupesh Chikara, USA
Marta Cimitile, Italy
Silvia Conforto , Italy
Paolo Crippa , Italy
Christian W. Dawson, United Kingdom
Carmen De Maio , Italy
Thomas DeMarse , USA
Maria Jose Del Jesus, Spain
Arnaud Delorme , France
Anastasios D. Doulamis, Greece
António Dourado , Portugal
Sheng Du , China
Said El Kafhali , Morocco
Mohammad Reza Feizi Derakhshi , Iran
Quanxi Feng, China
Zhong-kai Feng, China
Steven L. Fernandes, USA
Agostino Forestiero , Italy
Piotr Franaszczuk , USA
Thippa Reddy Gadekallu , India
Paolo Gastaldo , Italy
Samanwoy Ghosh-Dastidar, USA

Manuel Graña , Spain
Alberto Guillén , Spain
Gaurav Gupta, India
Rodolfo E. Haber , Spain
Usman Habib , Pakistan
Anandakumar Haldorai , India
José Alfredo Hernández-Pérez , Mexico
Luis Javier Herrera , Spain
Alexander Hošovský , Slovakia
Etienne Hugues, USA
Nadeem Iqbal , Pakistan
Sajad Jafari, Iran
Abdul Rehman Javed , Pakistan
Jing Jin , China
Li Jin, United Kingdom
Kanak Kalita, India
Ryotaro Kamimura , Japan
Pasi A. Karjalainen , Finland
Anitha Karthikeyan, Saint Vincent and the
Grenadines
Elpida Keravnou , Cyprus
Asif Irshad Khan , Saudi Arabia
Muhammad Adnan Khan , Republic of
Korea
Abbas Khosravi, Australia
Tai-hoon Kim, Republic of Korea
Li-Wei Ko , Taiwan
Raşit Köker , Turkey
Deepika Koundal , India
Sunil Kumar , India
Fabio La Foresta, Italy
Kuruva Lakshmana , India
Maciej Lawrynczuk , Poland
Jianli Liu , China
Giosuè Lo Bosco , Italy
Andrea Loddo , Italy
Kezhi Mao, Singapore
Paolo Massobrio , Italy
Gerard McKee, Nigeria
Mohit Mittal , France
Paulo Moura Oliveira , Portugal
Debajyoti Mukhopadhyay , India
Xin Ning , China
Nasimul Noman , Australia
Fivos Panetsos , Spain

Evgeniya Pankratova , Russia
Rocío Pérez de Prado , Spain
Francesco Pistolesi , Italy
Alessandro Sebastian Podda , Italy
David M Powers, Australia
Radu-Emil Precup, Romania
Lorenzo Putzu, Italy
S P Raja, India
Dr.Anand Singh Rajawat , India
Simone Ranaldi , Italy
Upaka Rathnayake, Sri Lanka
Navid Razmjooy, Iran
Carlo Ricciardi, Italy
Jatinderkumar R. Saini , India
Sandhya Samarasinghe , New Zealand
Friedhelm Schwenker, Germany
Mijanur Rahaman Seikh, India
Tapan Senapati , China
Mohammed Shuaib , Malaysia
Kamran Siddique , USA
Gaurav Singal, India
Akansha Singh , India
Chiranjibi Sitaula , Australia
Neelakandan Subramani, India
Le Sun, China
Rawia Tahrir , Iraq
Binhua Tang , China
Carlos M. Travieso-González , Spain
Vinh Truong Hoang , Vietnam
Fath U Min Ullah , Republic of Korea
Pablo Varona , Spain
Roberto A. Vazquez , Mexico
Mario Versaci, Italy
Gennaro Vessio , Italy
Ivan Volosyak , Germany
Leyi Wei , China
Jianghui Wen, China
Lingwei Xu , China
Cornelio Yáñez-Márquez, Mexico
Zaher Mundher Yaseen, Iraq
Yugen Yi , China
Qiangqiang Yuan , China
Miaolei Zhou , China
Michal Zochowski, USA
Rodolfo Zunino, Italy








Contents

Visual-Electrotactile Stimulation Feedback to Improve Immersive Brain-Computer Interface Based on Hand Motor Imagery

David Achancaray , Shin-Ichi Izumi , and Mitsuhiro Hayashibe 

Research Article (13 pages), Article ID 8832686, Volume 2021 (2021)

EEG Assessment in a 2-Year-Old Child with Prolonged Disorders of Consciousness: 3 Years' Follow-up

Gang Xu , Qianqian Sheng , Qinggang Xin , Yanxin Song , Gaoyan Zhang , Lin Yuan , Peng Zhao , and Jun Liang 

Research Article (8 pages), Article ID 8826238, Volume 2020 (2020)

The Time Course of Perceptual Closure of Incomplete Visual Objects: An Event-Related Potential Study

Chenyang Liu, Sha Sha, Xiujun Zhang , Zhiming Bian, Lin Lu, Bin Hao, Lina Li, Hongge Luo, Xiaotian Wang, Changming Wang, and Chao Chen 

Research Article (7 pages), Article ID 8825197, Volume 2020 (2020)

Effect of Emotion on Prospective Memory in Those of Different Age Groups

Jinhua Xian, Yan Wang , and Buxin Han 

Research Article (8 pages), Article ID 8859231, Volume 2020 (2020)

Towards an Accessible Use of a Brain-Computer Interfaces-Based Home Care System through a Smartphone

Koun-Tem Sun, Kai-Lung Hsieh , and Syuan-Rong Syu

Research Article (17 pages), Article ID 1843269, Volume 2020 (2020)

Research Article

Visual-Electrotactile Stimulation Feedback to Improve Immersive Brain-Computer Interface Based on Hand Motor Imagery

David Achancaray ¹, Shin-Ichi Izumi ^{2,3} and Mitsuhiro Hayashibe ¹

¹Neuro-Robotics Laboratory, Department of Robotics, Tohoku University, Sendai 980-8579, Japan

²Department of Physical Medicine and Rehabilitation, Tohoku University Graduate School of Medicine, Sendai 980-8575, Japan

³Graduate School of Biomedical Engineering, Tohoku University, Sendai 980-8574, Japan

Correspondence should be addressed to David Achancaray; david.ad@dc.tohoku.ac.jp

Received 21 August 2020; Revised 9 February 2021; Accepted 15 February 2021; Published 25 February 2021

Academic Editor: Abdelkader Nasreddine Belkacem

Copyright © 2021 David Achancaray et al. This is an open access article distributed under the Creative Commons Attribution License, which permits unrestricted use, distribution, and reproduction in any medium, provided the original work is properly cited.

In the aging society, the number of people suffering from vascular disorders is rapidly increasing and has become a social problem. The death rate due to stroke, which is the second leading cause of global mortality, has increased by 40% in the last two decades. Stroke can also cause paralysis. Of late, brain-computer interfaces (BCIs) have been garnering attention in the rehabilitation field as assistive technology. A BCI for the motor rehabilitation of patients with paralysis promotes neural plasticity, when subjects perform motor imagery (MI). Feedback, such as visual and proprioceptive, influences brain rhythm modulation to contribute to MI learning and motor function restoration. Also, virtual reality (VR) can provide powerful graphical options to enhance feedback visualization. This work aimed to improve immersive VR-BCI based on hand MI, using visual-electrotactile stimulation feedback instead of visual feedback. The MI tasks include grasping, flexion/extension, and their random combination. Moreover, the subjects answered a system perception questionnaire after the experiments. The proposed system was evaluated with twenty able-bodied subjects. Visual-electrotactile feedback improved the mean classification accuracy for the grasping ($93.00\% \pm 3.50\%$) and flexion/extension ($95.00\% \pm 5.27\%$) MI tasks. Additionally, the subjects achieved an acceptable mean classification accuracy (maximum of $86.5\% \pm 5.80\%$) for the random MI task, which required more concentration. The proprioceptive feedback maintained lower mean power spectral density in all channels and higher attention levels than those of visual feedback during the test trials for the grasping and flexion/extension MI tasks. Also, this feedback generated greater relative power in the μ -band for the premotor cortex, which indicated better MI preparation. Thus, electrotactile stimulation along with visual feedback enhanced the immersive VR-BCI classification accuracy by 5.5% and 4.5% for the grasping and flexion/extension MI tasks, respectively, retained the subject's attention, and eased MI better than visual feedback alone.

1. Introduction

The number of elderly people suffering from vascular disorders has increased rapidly in developed countries. It has become a social problem, which can cause paralysis and worsen living conditions. Paralysis could be due to medical conditions, such as stroke, spinal cord injury (SCI), amyotrophic lateral sclerosis, or multiple sclerosis [1]. Stroke is one of the most important causes of global mortality, and the death rate due to stroke has increased by 40% in the last two decades [2]. It was reported in 2016 as the second cause of death by the World Health Organization [3]; most poststroke patients experience partial paralysis mainly, often of the upper limbs [4].

Lately, brain-computer interfaces (BCIs) have been gathering attention in the rehabilitation field. They are focused on improving the life quality and health condition of paralyzed patients mostly. BCI for motor rehabilitation is an assistive technology that promotes neural plasticity and eases cortical reorganization in ipsilesional motor brain regions, when subjects perform motor imagery (MI) tasks. MI tasks can modulate brain activity in the sensorimotor cortex by eliciting an event-related desynchronization (ERD) and an event-related synchronization similar to movement execution during physical therapies. High ERD in the μ -(8–12 Hz) and central β -(16–24 Hz) bands can contribute to the recovery process [5, 6]. Also, BCIs can train

motor and cognitive skills of elderly people, with or without physical and cognitive diseases. BCIs attempted to prevent degenerative changes by aging. Thereby, an interactive interface could improve multitasking skills, and neurofeedback (or feedback) could enhance cognitive performance [7]. In addition, feedback is a significant factor to reach high performance and reliability in BCI-based assistive systems [8, 9]. Most BCI applications use visual feedback; however, it could be limited to subjects without visual disability or by the end-effector device. Alternative feedbacks can be auditory, vibrotactile, or electrical stimulation [10]. BCIs with visual and proprioceptive feedbacks contribute to MI learning in healthy subjects [11] and motor function restoration of poststroke patients [12].

In a BCI, visual feedback could induce fatigue and lead to a poor BCI performance owing to the monotony of performing MI tasks; thereby, subjects would lose interest and concentration [13]. Visual feedback modification can improve BCI performance by increasing the subject's motivation, attention, or engagement. An option is realistic visual feedback, which can induce an embodiment sense, promoting significant MI learning in the short term. The embodiment sense, which is the owning feeling of a controlled body, can reinforce the immersive experience of able-bodied subjects [14]. Moreover, virtual reality (VR) provides powerful graphical resources to improve feedback control by enhancing feedback presentation [15]. VR also increases patient engagement during the BCI training owing to enhancing feedback focus [16]. On the other hand, action observation of real or virtual body movements stimulates the corresponding motor-related cortical areas through the mirror neuron system [17–19]. Thus, the ERD is enhanced during MI tasks [20, 21].

BCIs in rehabilitation can replace and restore lost neurological function. On the one hand, BCIs for replacement restore the subject's skills to interact with environments and control devices to perform activities. On the other hand, BCIs for restoration are used with rehabilitation therapies to help the central nervous system restoration by inducing neural plasticity, synchronizing brain activity related to movement intent with motion, and feedback provided by end-effector devices [16]. The electrical stimulation also contributes to neural recovery from paralysis; functional electrical stimulation (FES) produces muscle contraction on paretic limbs and activates the sensory-motor system [5, 22], and electrotactile stimulation provides somatosensory feedback on human skin for sensory restoration [23]. Sensory restoration depends on cutaneous inputs for natural motor control by indicating state transitions and providing information about slip or contact force from manual interactions [24]. Thus, able-bodied and amputee subjects improved the perceptual embodiment in an artificial hand by participating in a modified version of the rubber hand illusion and received transcutaneous electrical nerve stimulation [25, 26]. In another study, Wilson et al. [27] proposed a lingual electrotactile stimulation feedback as a vision substitution system in a BCI based on MI to move a cursor, where subjects with or without visual disability obtained similar results. Also, a BCI used visual-haptic feedback [28],

which comprised a visual scene and electrical stimulation simultaneously. This feedback combination improved sensorimotor cortical activity and BCI performance during MI in able-bodied subjects.

Some studies combined VR with electrical stimulation. A VR hand rehabilitation platform with electrotactile stimulation feedback and surface electromyography modules in a closed-loop control improved the training efficiency and grasp control performance of healthy subjects compared to visual and no feedbacks [29]. FES-BCI [30, 31] and robot-BMI [32] showed virtual hands as realistic visual feedback. Both systems improved upper limb motor functions and increased the subject's motivation with SCI by achieving higher relative power (RP) [33–35] than those of conventional BCI systems. Other studies used a head-mounted display (HMD) to increase the immersive experience, which is considered as the subject's propensity to respond to the VR environment as it was real [36]. Researchers proposed an embodied BCI based on MI using an HMD to display an immersive VR environment to train able-bodied subjects. These systems improved their MI skills and BCI performance [37, 38], reaching classification results and power spectral density (PSD) [38] better than those of the classical MI approach [39].

The present work proposed an immersive BCI based on electroencephalography (EEG) signals to perform hand MI tasks in a VR environment displayed by an HMD, supplying realistic visual feedback along with electrotactile stimulation. The proposed VR-BCI framework with visual-electrotactile stimulation (VES) feedback could improve the system performance achieved with realistic visual feedback. Thereby, our BCI design attempts to obtain results to increase the system usability by able-bodied subjects. It can also assist in the motor rehabilitation of paralyzed patients.

2. Materials and Methods

2.1. Participants. Twenty able-bodied subjects participated in this study, 5 females and 15 males, aged between 18 and 39 years (mean = 26.20, standard deviation (SD) = 5.37); only one was left-handed. Ten of them participated in experiments with VES feedback, while the rest of them participated in experiments with visual feedback. The Ethical Committee from the School of Engineering at Tohoku University approved the experimental protocol.

All subjects signed an informed-consent document according to the Declaration of Helsinki guidelines before the experiment began. They were naive to perform MI tasks for a BCI and without previous experience using a similar device. In addition, none had a background in neurological disorders.

2.2. Experimental Setup. The experimental setup is illustrated in Figure 1(a). The brain activity was recorded using a 16-channel amplifier g.USBamp (g.tec Medical Engineering GMBH) with active electrodes. The electrodes were distributed over the scalp according to the 10–20 international system, using electrode positions AF3, AF4, FC3, FCz, FC4,

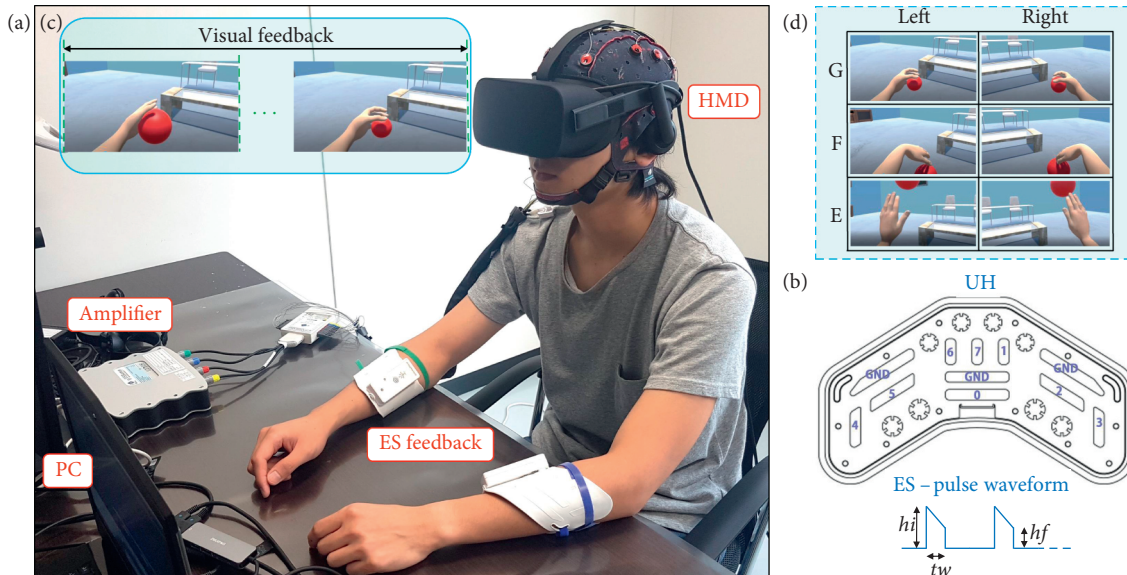


FIGURE 1: Immersive VR-BCI system. (a) The experimental setup comprised an EEG amplifier, an HMD, two electro-tactile stimulation (ES) devices, and a PC. (b) UnlimitedHand (UH) device to supply electro-tactile stimulation feedback. (c) Visual feedback displayed by an HMD. (d) Virtual arm animations of both limbs for the MI tasks (G: grasping, F: flexion, and E: extension).

C3, Cz, C4, T7, T8, CP3, CPz, CP4, Pz, O1, and O2; Fz was the ground electrode, and the right ear lobe was the reference electrode. Additionally, an HMD Oculus Rift (Facebook Technologies, LLC) with a display frequency of 90 Hz provided a higher immersion perception of the subjects. Also, two devices, UnlimitedHand (UH) (H2L Inc.), supplied electro-tactile stimulation and were mounted over each subject's forearm, as shown in Figure 1(a). This device worked to 40 Hz and provided electro-tactile stimulation for 1 second.

The devices were connected to a PC for recording and processing EEG data and developing the VR environment. The PC had the following features: Windows 10 operating system, Intel Core i7-8750H CPU at up to 4.1 GHz, 16 GB RAM, Nvidia GTX 1070 GPU. The VR-BCI system was integrated into Unity (Unity Technologies) and coded in C# language.

The VR environment, which comprised a virtual avatar and room, was shown through an HMD. Thus, the human avatar was designed in MakeHuman (The MakeHuman Team). The VR room was designed using Unity, and the virtual arm animations were done using Blender (Blender Foundation). They included a red ball that interacted with the virtual arms, as shown in Figure 1(d). Each arm animation comprised the movement itself (during 1 second) and the return (during 1 second) to the neutral position.

2.3. Experimental Procedure. The electro-tactile stimulation intensity was calibrated before the beginning of the experiment. The pulse width (tw) was 0.2 milliseconds, and the voltage bootup level (hi) of 5V over the voltage level (hf). The voltage level started at 1V and was increased by 1V repeatedly until the subject felt it, and before producing muscle contraction, it was between 1V and 3V for most subjects. The experiment did not

require contracting hand muscles, and electro-tactile stimulation was simply a means to provide interaction between the subject and the BCI. The eight electrode positions and their pulse waveforms are shown in Figure 1(b). The electrodes used for grasping were 0, 1, 3, 4, 6, 7, and flexion and extension were 0, 1, 6, 7. There was no difference between the stimulation pattern for both movements. These electrodes were chosen according to the MI task associated.

Active electrodes were positioned in a cap and mounted on the subject's scalp; then, the conductive gel was applied to each electrode. Then, an HMD was placed over the subject's head. The electrode's impedance was then checked to be below 10 k Ω . The experimental setup preparation took between 15 and 20 minutes.

The experiment was carried out following the timeline shown in Figure 2(a) during the BCI calibration stage. In the trial beginning, a green cross (side cue) was displayed randomly in the left or right position to indicate the MI task limb. Then, a virtual arm animation (MI cue) showed the MI task requested. The subject started the kinesthetic MI task when the virtual arm animation stopped, and the red ball disappeared; it is performed repeatedly for 6 seconds. After the virtual arm animation of the MI performed was shown as a visual reinforcement (R), the electro-tactile stimulation was added at the reinforcement beginning if the subject belongs to the group with electro-tactile stimulation. Afterward, a blue line (end cue) indicated the trial ends. This BCI system was calibrated for hand MI tasks, such as grasping, flexion, and extension. There were two runs for each MI task, each run of 20 trials (10 trials for each limb) with a break of 1 minute between runs. The flexion and extension MI tasks were performed in the same run. This stage lasted about 22 minutes.

The second stage was training and consisted of feature extraction and classifier training, as shown in Figure 2(b), using the EEG data recorded in the calibration session. The

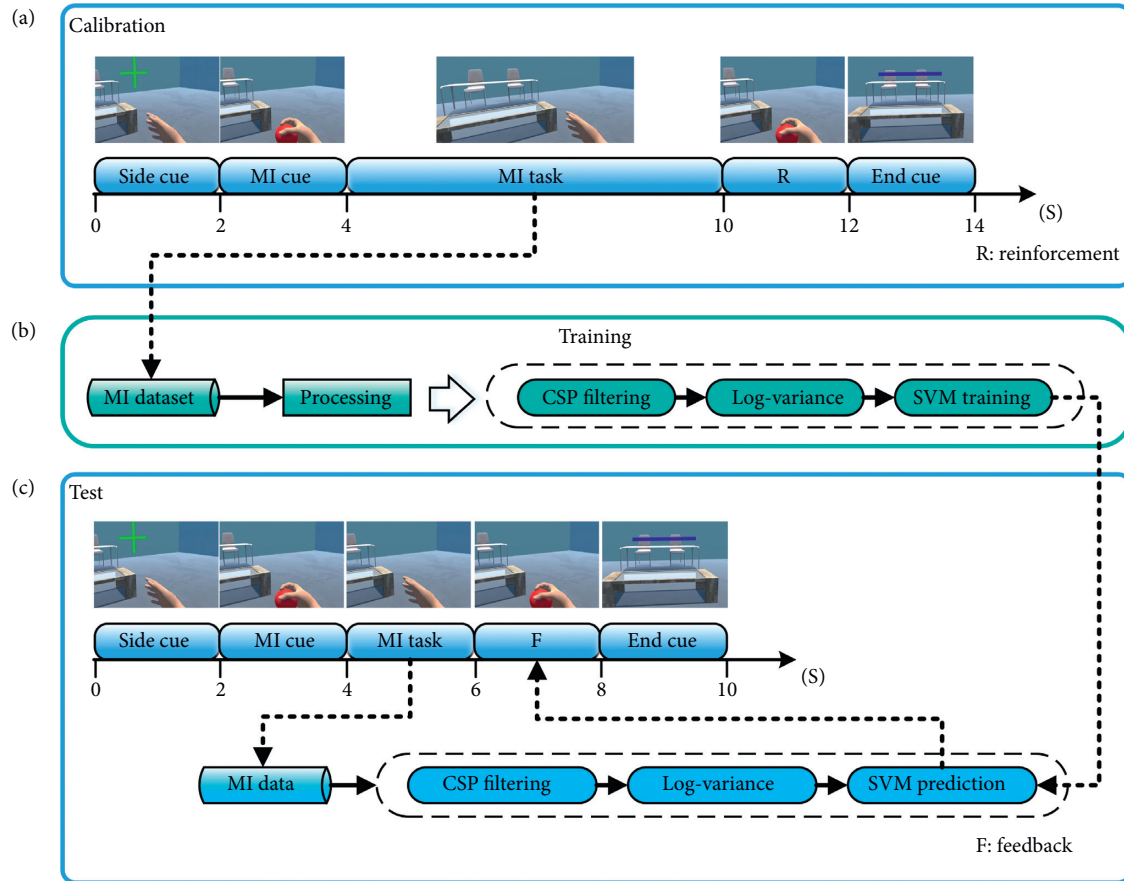


FIGURE 2: Timelines and flowcharts of the experiment sessions. (a) Calibration stage. (b) Training stage comprised feature extraction and classifier's training of the MI dataset recorded during the calibration stage. (c) Test stage.

feature extraction comprised common spatial pattern (CSP) filtering and normalized log-variance; then, a support vector machine (SVM) classifier was trained. These methods are detailed in the next section. There was a break of 5 minutes between the calibration and test sessions.

During the test stage, the trial followed the timeline shown in Figure 2(c). In the beginning, a green cross and the virtual arm animation indicated the MI task limb and the MI task, similar to the calibration session. The subject started the kinesthetic MI task when the virtual arm animation stopped, and the red ball disappeared; it is performed repeatedly for 2 seconds. After the virtual arm animation of the classifier's output was shown as visual feedback (F), the electro-tactile stimulation was added at the feedback beginning if the subject belongs to the group with electro-tactile stimulation. Afterward, a blue line indicated the trial ends. The VR-BCI system evaluated a run for each hand MI task, which were grasping, flexion/extension, and the random combination of them. The random MI task run used trained classifiers for the other MI tasks. Each run consisted of 20 trials (10 trials for each limb) with a break of 1 minute between runs. This stage lasted about 12 minutes.

Finally, subjects answered the questionnaire shown in Table 1 about system perception and detailed in Section

2.6. This stage lasted around 5 minutes. The time required to disassemble the experimental setup was around 10 minutes. Each subject carried out the whole experiment on the same day, and the total time was about 1 hour 15 minutes.

2.4. Signal Processing. Figures 2(b) and 2(c) show the signal processing for the training and test stages, respectively. EEG data were sampled at a frequency of 512 Hz and filtered using an eighth-order Butterworth bandpass filter with cutoff frequencies of 0.5 and 30 Hz and a fourth-order 50 Hz notch filter.

The feature extraction consisted of CSP and log-variance. CSP filtering is a popular and useful method applied in BCI systems based on oscillatory activity such as MI. It provides high classification performance, being numerically efficient, and a simple algorithm to implement [40]. The CSP method is based on the calculation of a transformation matrix W (equation (1)) that maximizes the variance of spatially filtered EEG data belonging to one class while minimizing it for the other class: in our case, EEG data of MI tasks of the left and right limbs. The matrix X is transformed into a matrix Z . W is a square matrix, the dimensions of which depend on the number of channels, and its columns are

TABLE 1: Questionnaire about the system perception.

Questions	
Q1	I felt as if the virtual hands might belong to my body
Q2	I felt that I controlled the virtual hands as if they were my own hands
Q3	Even though it did not look like me, when I saw the virtual hands moving, I felt as if they might be my own hands
Q4	I had the feeling that I was in the virtual environment
Q5	I was concentrating during the experiment
Q6	I felt that moving my visual focus inside the virtual environment was easy
Q7	I was often distracted by the virtual environment objects
Q8	I was frustrated, trying to imagine the movements
Q9	I felt tired because the virtual environment was very bright

spatial filters. Three pairs of spatial filters of the 16×16 CSP transformation matrix W were applied to EEG data. The first three spatial filters generate the maximum variance in filtered EEG signals during left limb MI, and the last three spatial filters generate it during right limb MI [11, 41–43].

$$Z = WX. \quad (1)$$

Then, the feature vector f involved the normalized variance logarithm, as shown in equation (2), where $p = 1, 2, \dots, 6$.

$$f_p = \log \left(\frac{\text{var}_p}{\sum_{p=1}^6 \text{var}_p} \right). \quad (2)$$

The SVM classifier has demonstrated to be efficient for discriminating between two motor-imagery classes, and it is the standard classification method used for binary-class BCIs based on MI owing to its fast and computationally efficient training [43–45]. An SVM classifier was trained to discriminate between the left and right limbs for the grasping and flexion/extension MI tasks. This classifier was configured with a radial basis function kernel using the library LibSVM [46] in C#.

In the SVM classifier training, each MI task EEG dataset recorded during the calibration stage was reordered randomly. Then, the dataset was divided into 80% and 20% for training and test, respectively. These subdatasets were reshaped to one-second segments with 90% overlapped (sliding window method [47–49]). The random reordering of subdatasets was optimized by genetic algorithms in MATLAB (The MathWorks, Inc.). The function to maximize was the classification accuracy of the trained SVM using the test subdataset. Then, the SVM model was validated using fivefold cross-validation using the training subdataset.

The optimized SVM classifier predicted MI tasks in the test stage; the EEG data during test trials were also reshaped to one-second segments, with 90% overlapping. The virtual arm animation displayed as visual feedback was shown partially (biased feedback [14]) depending on the percentage of one-second segments right classified. Then, the trial prediction depended on the one-second segments' accuracy. In addition, no animation was shown if the prediction was wrong (error-ignoring [14]).

2.5. Analysis. First of all, the classification accuracy and the overall BCI performance were calculated for the test stage. The overall BCI performance was measured by the

information transfer rate (ITR) [42]. The ITR depends on the accuracy and is defined by [50]

$$B = \left(\log N + P \log P + (1 - P) \log \frac{1 - P}{N - 1} \right) \left(\frac{60}{T} \right). \quad (3)$$

Here, N is the number of classes, P is the classification accuracy (%), T is the time required for one classification in seconds, and B is the ITR in bits per minute (bpm).

Second of all, the frequency spectrum was calculated and assessed by the following measurements. The ERD power generated was evaluated by the relative power for all channels. The relative power can normalize the PSD, eliminating offsets and reducing the power variability. Then, the relative power was computed using [33–35]

$$RP_x = \frac{P_x - P_{\text{baseline}}}{P_{\text{baseline}}} \times 100. \quad (4)$$

Here, P_x is the PSD in dB during the event x .

The coefficient of determination r^2 was computed to find power differences [51, 52] between the grand average PSDs of two groups. r^2 is defined as follows [53, 54]:

$$r^2 = \frac{\sigma_{xy}^2}{\sigma_x^2 \sigma_y^2}, \quad (5)$$

where x is the observed signal, y is the predicted signal, σ_x^2 is the variance of x , σ_y^2 is the variance of y , and σ_{xy}^2 is the covariance between x and y . r^2 range is from 0 to 1 [55]. If r^2 value is close to 1, there is very good discrimination, whereas if r^2 value is close to 0, it indicates that the signals can hardly be distinguished [54].

Additionally, the hemispheric asymmetry is related to the performance of fine motor tasks, and left hemisphere changes are related to motor learning. Then, the hemispheric asymmetry was calculated over the motor brain regions as the difference between the mean PSD of the right (FC4, C4, and CP4) and left (FC3, C3, and CP3) channels [38, 56].

Then, the statistical analysis looked into differences between groups. The Shapiro–Wilk (S–W) test ($p > 0.05$) was applied to verify the normal distribution; the S–W test is commonly used for a small sample of fewer than 50 data. If the S–W test was accomplished, analysis of variances (ANOVA) [55] was then used to find statistically significant differences. The repeated measures ANOVA evaluated the overall differences between groups; if the repeated measures model failed the Mauchly's test of sphericity ($p < 0.05$), the Greenhouse–Geisser correction was

computed. Then, the post hoc test Bonferroni correction was used for pairwise comparisons. The significance level was 5% for the methods mentioned above [38].

On the other hand, If the S–W test was not accomplished, nonparametric statistical tests analyzed it; Friedman test assessed the overall differences between groups. Then, the nonparametric Wilcoxon rank-sum test was adopted to find statistically significant differences between pairwise comparisons. The significance level was also 5% for the nonparametric methods [38, 55].

Finally, Spearman correlation found relationships between the relative power for each channel and the perception levels with a significance level of 5% [38].

2.6. Questionnaire. Each subject responded to the questionnaire presented in Table 1. The questionnaire consisted of nine questions, and the answers were on the Likert scale from 1 to 7 [57]. The questionnaire was directed to know the subject’s perception about the system during BCI sessions; the questions were designed to get levels for the ownership perception (mean of Q1 and Q2), immersion perception (mean of Q3 and Q4), attention (mean of Q5 and Q6), and difficulty (mean of Q7, Q8, and Q9).

3. Results

All subjects performed the three MI tasks (grasping, flexion/extension, and random) during the test stage; flexion and extension were grouped as one MI task for this analysis owing to the similar brain response. The random MI task attempted to evaluate the subject’s ability to perform MI tasks of different nature in the same run.

3.1. Classification Performance. The mean cross-validation accuracy of both feedback groups for the grasping and flexion/extension MI tasks was above 85%, with SD lower than 8%. These results validated the SVM classifier model.

Table 2 presents the accuracy and F1-score of both feedback groups during the test stage for the grasping, flexion/extension, and random MI tasks. The mean accuracy was close to the mean F1-score for all MI tasks; i.e., there was a balance of correct classifications. The VES feedback group achieved greater mean accuracy and lower SD for the grasping (93.00% \pm 3.50%) and flexion/extension (95.00% \pm 5.27%) MI tasks than those of the visual feedback group (grasping: 87.50% \pm 4.25%, flexion/extension: 91.50% \pm 7.09%). On the other hand, the mean accuracy for the random MI task of both feedback groups was close. However, the variability of the VES feedback group was greater than that of the visual feedback group.

The S–W test verified the accuracy normal distribution; the VES feedback group did not accomplish the S–W test ($p < 0.05$) for the grasping MI task. Then, the Friedman test found overall statistical differences ($\chi^2(1) = 4.52$, $p = 0.0335$) between the accuracy of both feedback groups. Thus, the nonparametric Wilcoxon rank-sum test found statistical differences between both feedback groups for the grasping MI

TABLE 2: Classification accuracy (Acc) % and F1-score (F1) % of each subject (S) of both feedback (F) groups (VIS: visual, VES: visual-electrotactile stimulation) for all MI tasks (G: grasping, F/E: flexion/extension, R: random).

F	S	G		F/E		R	
		Acc	F1	Acc	F1	Acc	F1
VIS	1	80.00	83.33	80.00	80.00	90.00	90.91
	2	85.00	82.35	80.00	83.33	90.00	90.00
	3	85.00	85.71	100.00	100.00	85.00	86.96
	4	90.00	90.91	90.00	90.00	85.00	85.71
	5	90.00	88.89	95.00	95.24	90.00	90.91
	6	95.00	94.74	95.00	94.74	90.00	90.00
	7	85.00	86.96	90.00	88.89	95.00	94.74
	8	85.00	86.96	100.00	100.00	85.00	86.96
	9	90.00	90.00	95.00	94.74	75.00	76.19
	10	90.00	88.89	90.00	90.00	80.00	75.00
	Mean	87.50	87.87	91.50	91.69	86.50	86.74
	SD	4.25	3.66	7.09	6.58	5.80	6.41
VES	11	90.00	88.89	90.00	90.91	90.00	90.91
	12	100.00	100.00	100.00	100.00	100.00	100.00
	13	95.00	95.24	100.00	100.00	95.00	95.24
	14	90.00	88.89	100.00	100.00	80.00	75.00
	15	90.00	88.89	95.00	95.24	70.00	62.50
	16	95.00	95.24	95.00	95.24	75.00	73.68
	17	95.00	95.24	90.00	88.89	80.00	80.00
	18	90.00	90.00	100.00	100.00	70.00	76.92
	19	90.00	90.00	85.00	84.21	95.00	94.74
	20	95.00	94.74	95.00	94.74	100.00	100.00
	Mean	93.00	92.71	95.00	94.92	85.50	84.90
	SD	3.50	3.87	5.27	5.48	11.89	12.95

task ($p = 0.0091$); however, there were no differences for the flexion/extension and random MI tasks ($p > 0.05$).

Additionally, Table 3 shows the overall VR-BCI performance calculated by the information transfer rate. The mean information transfer rate of the VES feedback group was higher than that of the visual feedback group for all MI tasks; however, the SD of the VES feedback group for the random MI task was higher.

3.2. Frequency Spectrum. The frequency spectrum was calculated by the spectrogram of EEG data recorded of each subject during the test stage for the grasping and flexion/extension MI tasks of both feedback groups. The PSD decreases in the μ - and central β -bands, mainly owing to movement execution or MI [33, 42]. Thereby, the spectrograms verified that the PSD decreased during both MI tasks. Also, the PSD for both MI tasks of the VES feedback group were less intense than those of the visual feedback group. Then, the VES feedback group reached a lower ERD level than that of the visual feedback.

On the other hand, the coefficient of determination r^2 [51–53] between the grand average PSD in the μ - and central β -bands of both feedback groups for both MI tasks in each channel was close to 1; thus, there was good discrimination between both feedback groups [54].

3.3. Relative Power. The mean relative power was calculated using the PSD of EEG data recorded of each subject during

TABLE 3: Mean information transfer rate (bpm) of both feedback (F) groups (VIS: visual, VES: visual-electrotactile stimulation) for all MI tasks (G: grasping, F/E: flexion/extension, R: random).

F	G	F/E	R
VIS	2.81 ± 0.74	3.77 ± 1.51	2.68 ± 0.90
VES	3.91 ± 0.92	4.56 ± 1.38	2.96 ± 2.08

the test stage for the grasping and flexion/extension MI tasks of both feedback groups. The grand average relative power in the μ - and central β -bands of both feedback groups in premotor (FC3 and FC4 channels), primary motor (C3 and C4 channels), and somatosensory (CP3 and CP4 channels) cortices is shown in Figures 3 and 4, without considering the negative sign. The premotor cortex is related to movement preparation, the primary motor cortex is related to motor execution and motor imagery [58, 59], and the somatosensory cortex is related to sensory perception [60].

The VES feedback group had a grand average relative power in the μ -band (approximately 72.71%) for the premotor cortex greater than that of the visual feedback group for both MI tasks. Thereby, the ERD over the movement preparation region of the VES feedback group was more intense. The grand average relative power of both bands (approximately 75.45%) for the primary motor cortex was similar for both MI tasks. Thus, the MI performance was also similar for both feedback groups, whereas the visual feedback group had a grand average relative power of both bands (approximately 77.89%) for the somatosensory cortex greater than those of the VES feedback group. Thereby, the ERD over the sensory perception region of the VES feedback group was weaker, verifying the results of [61]. Also, both feedback groups achieved relative powers higher than those of similar approaches (approximately 40%) [34, 35] in the μ - and central β -bands.

The mean relative power in each channel approached of both feedback groups did not accomplish the S–W test of normal distribution ($p < 0.05$). The Friedman test found overall statistical differences ($p < 0.05$) between both feedback groups for both MI tasks and both bands. Thus, the Wilcoxon rank-sum test found statistical differences ($p < 0.05$) between both feedback groups in the channel CP3 for the grasping (μ -band: $p = 0.0207$, central β -band: $p = 0.0077$) and flexion/extension (μ -band: $p = 0.0026$, central β -band: $p = 0.0036$) MI tasks. Also, there were statistical differences in channel CP4 of the central β -band ($p = 0.0499$) for the grasping MI task. The sensory perception region was affected by the type of feedback, as mentioned previously.

3.4. Hemispheric Asymmetry. The mean hemispheric asymmetry was calculated using the mean PSD of EEG data recorded over the left and right motor brain regions of each subject during the calibration and test stages for the grasping and flexion/extension MI tasks of both feedback groups. Figures 5 and 6 show the grand average hemispheric asymmetry in both bands and both feedback groups. The increase of hemispheric asymmetry in

sessions with feedback (test stage) was verified and compared with sessions without feedback (calibration stage) [8, 9]. Also, the hemispheric asymmetry of the VES feedback group was greater than that of the visual feedback group.

The mean hemispheric asymmetry in both bands of both stages and feedback groups did not accomplish the S–W test of normal distribution ($p < 0.05$). Thus, the Friedman test did not find overall statistical differences ($p > 0.05$) between both feedback groups.

3.5. System Perception. The subjects of both feedback groups answered the questionnaire about system perception; these answers on the Likert scale are shown in Figure 7. Also, Table 4 shows the mean perception levels of both feedback groups. The mean immersion and ownership perception levels of the visual feedback group were higher than those of the VES feedback group; besides, the VES feedback group had a mean attention level higher and a mean difficulty level lower than those of the visual feedback group. Most of the subjects of both feedback groups felt very high levels of immersion perception and attention.

The attention level did not accomplish the S–W test of normal distribution ($p < 0.05$). Then, the Friedman test did not find overall statistical differences ($\chi^2(1) = 0.93$, $p = 0.3338$) between both feedback groups.

On the other hand, the Spearman correlation found significant correlations between the perception levels and the channel's relative power in both bands and for both MI tasks, as shown in Table 5. Regarding the grasping MI task, the ownership perception level was correlated with the premotor cortex, and the attention level was correlated with the somatosensory and prefrontal cortices. The difficulty level was correlated with the somatosensory, prefrontal, and visual cortices, while, for the flexion/extension MI task, the attention level was correlated with the somatosensory, and the difficulty level was correlated with the premotor, somatosensory, prefrontal, and visual perception regions. Additionally, attention and difficulty levels were correlated inversely ($\rho = -0.45$, $p = 0.0459$).

4. Discussion

This work investigated the feasibility of applying electro-tactile stimulation along with visual feedback by assessing VES feedback compared to visual feedback.

Regarding the classification accuracy, the VES feedback group had the best results for the grasping and flexion/extension MI tasks; however, there were only statistical differences between the classification accuracy of both feedback groups for the grasping MI task. The response to the electro-tactile stimulation feedback could be owing to the muscles involved with the movements. Grasping is a movement more complex than flexion/extension. It activates brain regions related to the finger's movement proximate or overlapped to those of the flexion/extension, which are related to wrist movement [62, 63]. Thus, performing the flexion/extension MI was easier than the grasping MI, and

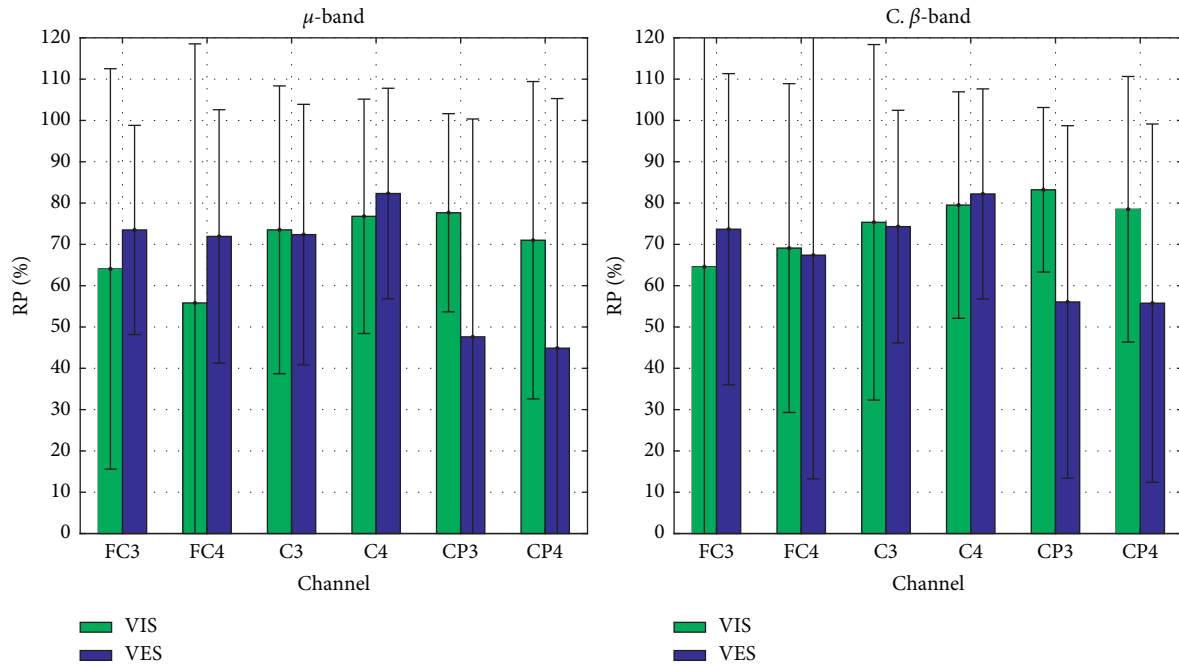


FIGURE 3: Grand average relative power (RP) in the μ - and central (C) β -band, without considering the negative sign, in the channels FC3, FC4, C3, C4, CP3, and CP4 for the grasping MI task of both feedback groups (VIS: visual, VES: visual-electrotactile stimulation).

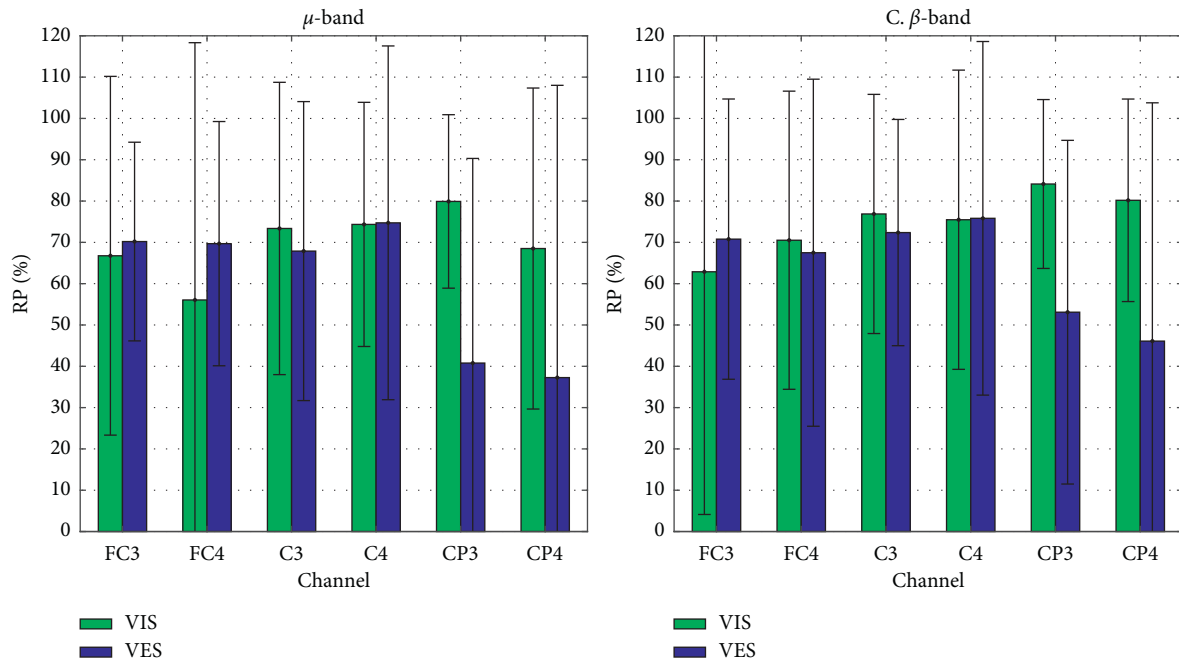


FIGURE 4: Grand average relative power (RP) in the μ - and central (C) β -band, without considering the negative sign, in the channels FC3, FC4, C3, C4, CP3, and CP4 for the flexion/extension MI task of both feedback groups (VIS: visual, VES: visual-electrotactile stimulation).

they could need no additional stimulation during feedback. On the other hand, both feedback groups had similar mean classification accuracy for the random MI task; however, the VES feedback group had a dispersion greater than that of the visual feedback group. Performing two MI tasks in a random order required more concentration. However, the electro-tactile stimulation could distract the subject. Moreover, most of the subjects had significant accuracy (above 80%) for the

random MI task. It showed the feasibility of increasing the BCI control options by combining different MI tasks for the left and right limbs in an immersive environment, such as similar motor rehabilitation BCI [37, 38] and cognitive training BCI systems [64, 65].

In the frequency spectrum, there were differences between the PSD of both feedback groups. The channels' PSD of the VES feedback group were lower than those of the

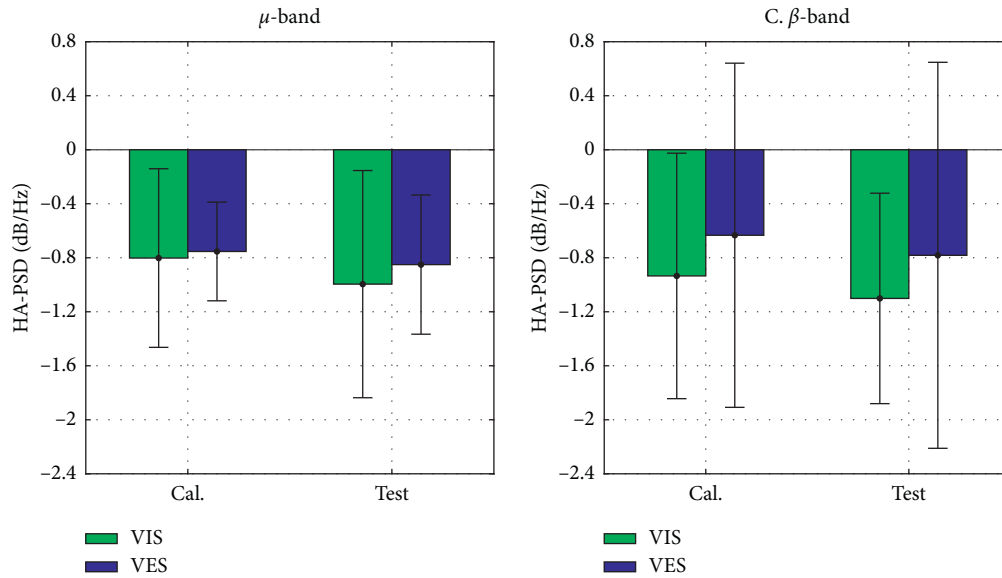


FIGURE 5: Grand average hemispheric asymmetry (HA) in the μ - and central (C) β -bands of the calibration (Cal.) and test stages for the grasping MI task of both feedback groups (VIS: visual, VES: visual-electrotactile stimulation).

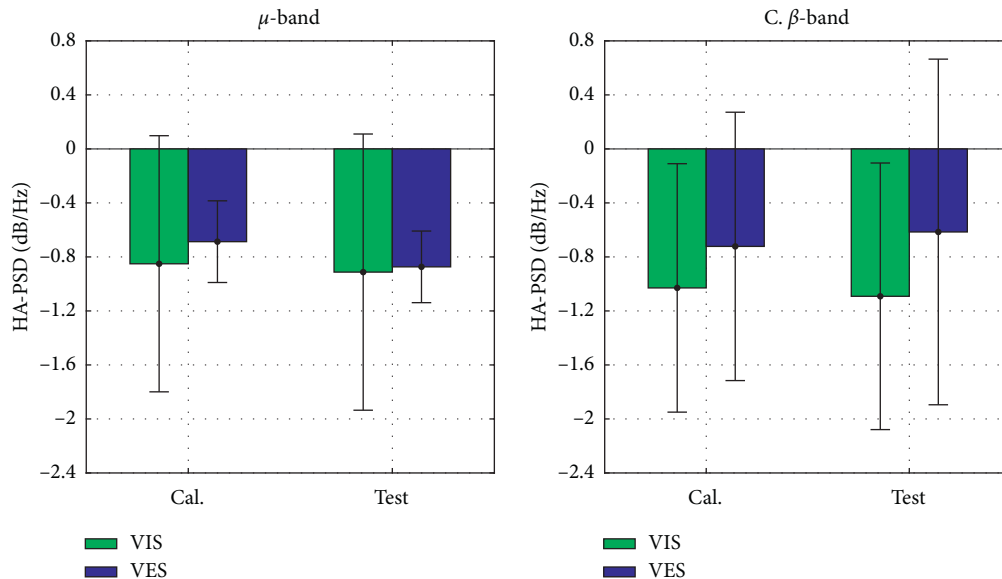


FIGURE 6: Grand average hemispheric asymmetry (HA) in the μ - and central (C) β -bands of the calibration (Cal.) and test stages for the flexion/extension MI task of both feedback groups (VIS: visual, VES: visual-electrotactile stimulation).

visual feedback group; the lower PSD for the occipital α -band (8–12 Hz) for the VES feedback group indicated a higher attention level during test trials [66]. Thus, subjects experiencing proprioceptive feedback paid more attention to the VR-BCI system than those with visual feedback [11]. Also, there were statistical differences between the somatosensory cortex relative powers of both feedback groups. The VES feedback group had a relative power lower than that of the visual feedback group, verifying that the β -band trends to keep the current sensorimotor state. Then, the electrical stimulation produced a change of the status quo by decreasing the β -band activity [67]. On the other hand, the hemispheric asymmetry of PSD can be modulated and

increased during feedback sessions [8], improving the performance of fine motor tasks and triggering motor learning changes [56]. Thereby, our system could promote inter-hemispheric interaction in patients with affected hemispheric differences [38]. It could also contribute to motor learning transfer by using a healthy hand to improve the paretic hand movements [9]. Therefore, the reached relative power and hemispheric asymmetry can contribute to different learning processes [68] and restore motor and cognitive functions [64, 69].

The questionnaire answers confirmed that subjects of the VES feedback group paid more attention. It was related to the decrease in difficulty level to perform MI tasks. The

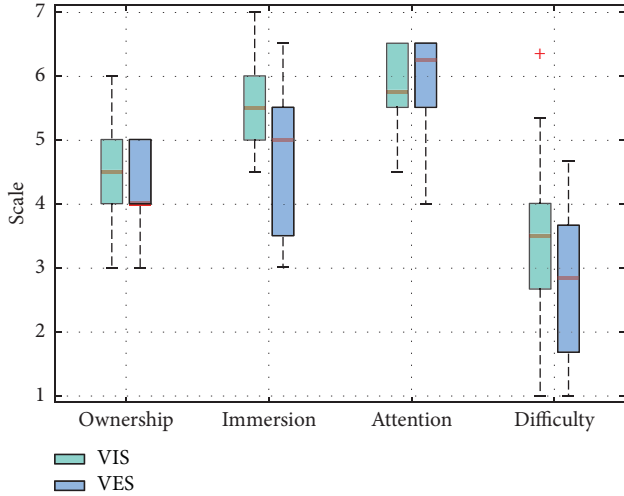


FIGURE 7: System perception levels on the Likert scale from 1 to 7 of both feedback groups (VIS: visual, VES: visual-electrotactile stimulation).

TABLE 4: Mean system perception levels on the Likert Scale from 1 to 7 of both feedback (F) groups (VIS: visual, VES: visual-electrotactile stimulation).

F	Ownership	Immersion	Attention	Difficulty
VIS	4.45 ± 0.98	5.50 ± 0.75	5.75 ± 0.68	3.37 ± 1.59
VES	4.15 ± 0.75	4.80 ± 1.30	5.90 ± 0.84	2.80 ± 1.20

TABLE 5: Spearman correlations (ρ) between the system perception levels (O: ownership, A: attention, D: difficulty) and the channel's relative power in the μ - and central (C) β -bands for the grasping (G) and flexion/extension (F/E) MI tasks.

MI task	Band	Channel	Level	ρ	p
G	μ	FC3	O	-0.46	0.0419
		AF3	A	0.52	0.0193
		CP3	A	0.45	0.0493
		AF3	D	-0.49	0.0272
	C. β	CP3	D	-0.61	0.0044
		O1	D	-0.47	0.0388
		AF3	A	0.58	0.0077
		AF3	D	-0.48	0.0309
F/E	μ	CP3	D	-0.62	0.0033
		AF3	A	0.51	0.0221
		AF3	D	-0.54	0.0135
		FCz	D	-0.47	0.0350
	C. β	CP3	D	-0.67	0.0011
		O1	D	-0.46	0.0433
		AF3	A	0.57	0.0082
		CP3	A	0.49	0.0278
		AF3	D	-0.50	0.0246
		CP3	D	-0.64	0.0023

attention and difficulty levels were correlated with the relative power of the somatosensory channels, verifying the electrotactile stimulation effect for decreasing the relative power in this brain region [67]. On the other hand, the body ownership illusion results from the interaction between

sensory inputs and internal body models; however, the immersion and ownership perception levels influenced by the VR, as mentioned in [37, 38], were higher without proprioceptive feedback. Then, realistic visual feedback generated an ownership perception higher than that of cutaneous perception. It could attenuate proprioceptive signals from the skin, altering the subject's somatosensory perception [70].

Our VR-BCI system with realistic visual feedback provided richer and more explanatory feedback, which could reduce illiteracy and deficiency in naive subjects, than that of conventional BCI systems during BCI training [71]. Also, the sensorimotor rhythms' modulation was influenced by realistic visual feedback, positively biased feedback, and sense of embodiment. They reinforced MI learning in the short term to improve the BCI performance [14]. In addition, the electrotactile stimulation and positively biased feedback contributed to enhancing the VR environment interaction by their influence on the subject's motivation and confidence; thus, they improved MI learning. Then, the VES feedback enhanced the VR-BCI with visual feedback in some features, such as classification accuracy of MI tasks, subject's attention during MI, and MI preparation.

This work was limited by no pre-training sessions, few test stage sessions, and the number of subjects. Subjects can feel difficulty practicing MI learning skills in pre-training sessions; then, they explore strategies and learn better in the subsequent calibration sessions [14, 71]. Also, they can improve MI performance with feedback during more test sessions. Thus, the differences between visual and VES feedbacks could increase. Moreover, the results will be more reliable by increasing the number of subjects. However, other works evaluated BCI systems with a similar number of subjects [11, 15, 20, 21, 57].

The proposed immersive system will be assessed with poststroke patients in future research, considering the limitations mentioned above. The VR-BCI would be updated according to the patients' constraints. In addition, cognitive background and spatial abilities should be considered to predict the subject's response to the feedback and the BCI performance [72, 73].

5. Conclusions

The visual-electrotactile feedback was assessed and compared to the visual feedback to discriminate MI tasks between both limbs; the MI tasks were grasping, flexion/extension, and random combination of them. Visual-electrotactile feedback improved the mean classification accuracy for the grasping (93.00% ± 3.50%) and flexion/extension (95.00% ± 5.27%) MI tasks and reached higher information transfer rates for the three MI tasks (maximum of 4.56 ± 1.38 bpm). In addition, subjects achieved a significant mean classification accuracy (maximum of 86.5% ± 5.80%) for the random MI task; however, it was lower than that of the other MI tasks. Since the random MI task required more subject's concentration, electrotactile stimulation could distract the subject during MI performing, generating greater dispersion of classification accuracy. There were only statistical differences for the grasping

MI task between the classification accuracies of both feedback groups.

The proprioceptive feedback kept lower mean PSD in all channels and higher attention levels than those of the visual feedback during test trials for the grasping and flexion/extension MI tasks. This feedback also generated a relative power in the μ -band greater for the premotor cortex, which indicated a better MI preparation. On the other hand, the hemispheric asymmetry was lower for the visual-electrotactile feedback; however, there were no statistical differences between both feedback groups. Then, both feedback types can contribute to the motor and cognitive learning processes. Also, the questionnaire confirmed attention level higher and difficulty level lower for the visual-electrotactile feedback, whereas the immersive and ownership perception levels were higher for visual feedback. However, there were also no statistical differences between the system perception levels of both feedback groups.

Therefore, the use of electrotactile stimulation along with visual feedback enhanced the immersive VR-BCI classification performance. It also retained the subject's attention and eased motor imagery better than visual feedback alone.

Data Availability

The datasets recorded and used to support the findings of this study are available from the corresponding author upon request.

Conflicts of Interest

The authors declare that there are no conflicts of interest regarding the publication of this paper.

Acknowledgments

This work was supported in part by FONDECYT from CONCYTEC, Peru, under Contract 112-2017, and in part by the Japan Society for the Promotion of Science Grant-in-Aid for Scientific Research (B) under Project 18H01399.

References

- [1] J. R. Wolpaw, N. Birbaumer, D. J. McFarland, G. Pfurtscheller, and T. M. Vaughan, "Brain-computer interfaces for communication and control," *Clinical Neurophysiology*, vol. 113, no. 6, pp. 767–791, 2002.
- [2] E. J. Benjamin, S. S. Virani, C. W. Callaway et al., "Heart disease and stroke statistics-2018 update: a report from the american heart association," *Circulation*, vol. 137, no. 12, pp. e67–e492, 2018.
- [3] WHO, *Global Health Estimates 2016: Deaths by Cause, Age, Sex, by Country and by Region, 2000–2016*, World Health Organization, Geneva, Switzerland, 2018.
- [4] I. Faria-Fortini, S. M. Michaelsen, J. G. Cassiano, and L. F. Teixeira-Salmela, "Upper extremity function in stroke subjects: relationships between the international classification of functioning, disability, and health domains," *Journal of Hand Therapy*, vol. 24, no. 3, pp. 257–265, 2011.
- [5] U. Chaudhary, N. Birbaumer, and M. R. Curado, "Brain-machine interface (bmi) in paralysis," *Annals of Physical and Rehabilitation Medicine*, vol. 58, no. 1, pp. 9–13, 2015.
- [6] G. Pfurtscheller and C. Neuper, "Motor imagery and direct brain-computer communication," *Proceedings of the IEEE*, vol. 89, no. 7, pp. 1123–1134, 2001.
- [7] A. N. Belkacem, N. Jamil, and J. A. Palmer, "Brain computer interfaces for improving the quality of life of older adults and elderly patients," *Frontiers in Neuroscience*, vol. 14, p. 692, 2020.
- [8] C. Neuper, A. Schlögl, and G. Pfurtscheller, "Enhancement of left-right sensorimotor eeg differences during feedback-regulated motor imagery," *Journal of Clinical Neurophysiology*, vol. 16, no. 4, pp. 373–382, 1999.
- [9] N. Takeuchi, Y. Oouchida, and S.-I. Izumi, "Motor control and neural plasticity through interhemispheric interactions," *Neural Plasticity*, vol. 2012, Article ID 823285, 2012.
- [10] I. N. Angulo-Sherman and D. Gutiérrez, "Effect of different feedback modalities in the performance of brain-computer interfaces," in *Proceedings of the 2014 International Conference on Electronics, Communications and Computers (CON-IELECOMP)*, pp. 14–21, Cholula, Mexico, February 2014.
- [11] S. Bhattacharyya, M. Clerc, and M. Hayashibe, "Augmenting motor imagery learning for brain-computer interfacing using electrical stimulation as feedback," *IEEE Transactions on Medical Robotics and Bionics*, vol. 1, no. 4, pp. 247–255, 2019.
- [12] P. D. Ganzer, S. C. Colachis, and M. A. Schwemmer, "Restoring the sense of touch using a sensorimotor demultiplexing neural interface," *Cell*, vol. 181, no. 4, pp. 763–773, 2020, <http://www.sciencedirect.com/science/article/pii/S0092867420303470>.
- [13] R. Foong, K. K. Ang, C. Quek et al., "Assessment of the efficacy of eeg-based mi-bci with visual feedback and eeg correlates of mental fatigue for upper-limb stroke rehabilitation," *IEEE Transactions on Biomedical Engineering*, vol. 67, no. 3, pp. 786–795, 2020.
- [14] M. Alimardani, S. Nishio, and H. Ishiguro, "Brain-computer interface and motor imagery training: the role of visual feedback and embodiment," in *Evolving BCI Therapy*, D. Larrivee, Ed., IntechOpen, London, UK, 2018.
- [15] R. Ron-Angevin and A. Diaz-Estrella, "Brain-computer interface: changes in performance using virtual reality techniques," *Neuroscience Letters*, vol. 449, no. 2, pp. 123–127, 2009.
- [16] M. A. Bockbrader, G. Francisco, R. Lee, J. Olson, R. Solinsky, and M. L. Boninger, "Brain computer interfaces in rehabilitation medicine," *PM&R*, vol. 10, no. 9, pp. S233–S243, 2018.
- [17] M. Tani, Y. Ono, M. Matsubara et al., "Action observation facilitates motor cortical activity in patients with stroke and hemiplegia," *Neuroscience Research*, vol. 133, pp. 7–14, 2018.
- [18] S. P. Tipper, "Eps mid-career award 2009: from observation to action simulation: the role of attention, eye-gaze, emotion, and body state," *Quarterly Journal of Experimental Psychology*, vol. 63, no. 11, pp. 2081–2105, 2010.
- [19] J. Kim, B. Lee, H. S. Lee, K. H. Shin, M. J. Kim, and E. Son, "Differences in brain waves of normal persons and stroke patients during action observation and motor imagery," *Journal of Physical Therapy Science*, vol. 26, no. 2, pp. 215–218, 2014.
- [20] T. Ono, A. Kimura, and J. Ushiba, "Daily training with realistic visual feedback improves reproducibility of event-related desynchronisation following hand motor imagery," *Clinical Neurophysiology*, vol. 124, no. 9, pp. 1779–1786, 2013.
- [21] Y. Ono, K. Wada, M. Kurata, and N. Seki, "Enhancement of motor-imagery ability via combined action observation and

- motor-imagery training with proprioceptive neurofeedback,” *Neuropsychologia*, vol. 114, pp. 134–142, 2018.
- [22] D. B. Popovic, “Advances in functional electrical stimulation (fes),” *Journal of Electromyography and Kinesiology*, vol. 24, no. 6, pp. 795–802, 2014.
- [23] K. Li, *Electrotactile Feedback for Sensory Restoration: Modelling and Application*, University of Portsmouth, Portsmouth, UK, 2018.
- [24] R. Johansson and J. Flanagan, “Coding and use of tactile signals from the fingertips in object manipulation tasks,” *Nature reviews, Neuroscience*, vol. 10, pp. 345–359, 2009.
- [25] M. R. Mulvey, H. J. Fawcner, H. E. Radford, and M. I. Johnson, “Perceptual embodiment of prosthetic limbs by transcutaneous electrical nerve stimulation,” *Neuromodulation: Technology at the Neural Interface*, vol. 15, no. 1, pp. 42–47, 2012.
- [26] M. Isaković, M. Belić, and M. Štrbac, “Electrotactile feedback improves performance and facilitates learning in the routine grasping task,” *European Journal of Translational Myology*, vol. 26, p. 6, 2016.
- [27] J. A. Wilson, L. M. Walton, M. Tyler, and J. Williams, “Lingual electrotactile stimulation as an alternative sensory feedback pathway for brain-computer interface applications,” *Journal of Neural Engineering*, vol. 9, no. 4, p. 45007, 2012.
- [28] Z. Wang, Y. Zhou, L. Chen et al., “A BCI based visual-haptic neurofeedback training improves cortical activations and classification performance during motor imagery,” *Journal of Neural Engineering*, vol. 16, no. 6, p. 66012, 2019.
- [29] K. Li, P. Boyd, Y. Zhou, Z. Ju, and H. Liu, “Electrotactile feedback in a virtual hand rehabilitation platform: evaluation and implementation,” *IEEE Transactions on Automation Science and Engineering*, vol. 16, no. 4, pp. 1556–1565, 2019.
- [30] F. Trincado-Alonso, E. López-Larraz, and F. Resquin, “A pilot study of brain-triggered electrical stimulation with visual feedback in patients with incomplete spinal cord injury,” *Journal of Medical and Biological Engineering*, vol. 38, pp. 790–803, 2017.
- [31] A. Moldoveanu, O.-M. Ferche, F. Moldoveanu et al., “The travee system for a multimodal neuromotor rehabilitation,” *IEEE Access*, vol. 7, pp. 8151–8171, 2019.
- [32] G. Onose, C. Grozea, and A. Anghelescu, “On the feasibility of using motor imagery eeg-based brain-computer interface in chronic tetraplegics for assistive robotic arm control: a clinical test and long-term post-trial follow-up,” *Spinal Cord*, vol. 50, pp. 599–608, 03 2012.
- [33] G. Pfurtscheller and F. H. Lopes da Silva, “Event-related eeg/meg synchronization and desynchronization: basic principles,” *Clinical Neurophysiology*, vol. 110, no. 11, pp. 1842–1857, 1999.
- [34] Z. Wang, L. Chen, and W. Yi, “Enhancement of cortical activation for motor imagery during bci-fes training*,” in *Proceedings of the 2018 40th Annual International Conference of the IEEE Engineering in Medicine and Biology Society (EMBC)*, pp. 2527–2530, Honolulu, Hawaii, July 2018.
- [35] I. Choi, K. Bond, and C. S. Nam, “A hybrid bci-controlled fes system for hand-wrist motor function,” in *Proceedings of the 2016 IEEE International Conference on Systems, Man, and Cybernetics (SMC)*, pp. 2324–2328, Budapest, Hungary, October 2016.
- [36] C. Nam, A. Nijholt, and F. Lotte, *Brain-Computer Interfaces Handbook: Technological and Theoretical Advances*, CRC Press, Boca Raton, FL, USA, 2018.
- [37] F. Škola, S. Tinková, and F. Liarokapis, “Progressive training for motor imagery brain-computer interfaces using gamification and virtual reality embodiment,” *Frontiers in Human Neuroscience*, vol. 13, p. 329, 2019.
- [38] A. Vourvopoulos and S. Bermúdez i Badia, “Motor priming in virtual reality can augment motor-imagery training efficacy in restorative brain-computer interaction: a within-subject analysis,” *Journal of NeuroEngineering and Rehabilitation*, vol. 13, no. 1, p. 69, 2016.
- [39] J. Kalcher, D. Flotzinger, C. Neuper, S. Göllly, and G. Pfurtscheller, “Graz brain-computer interface ii: towards communication between humans and computers based on online classification of three different eeg patterns,” *Medical & Biological Engineering & Computing*, vol. 34, no. 5, pp. 382–388, 1996.
- [40] M. Clerc, L. Bougrain, and F. Lotte, *Brain-Computer Interfaces 1 : Foundations and Methods*, ISTE Ltd, London, UK, 2016.
- [41] J. Müller-Gerking, G. Pfurtscheller, and H. Flyvbjerg, “Designing optimal spatial filters for single-trial eeg classification in a movement task,” *Clinical Neurophysiology*, vol. 110, no. 5, pp. 787–798, 1999.
- [42] B. Blankertz, R. Tomioka, S. Lemm, M. Kawanabe, and K.-R. Muller, “Optimizing spatial filters for robust eeg single-trial analysis,” *IEEE Signal Processing Magazine*, vol. 25, no. 1, pp. 41–56, 2008.
- [43] D. Achancaray and M. Hayashibe, “Decoding hand motor imagery tasks within the same limb from eeg signals using deep learning,” *IEEE Transactions on Medical Robotics and Bionics*, vol. 2, no. 4, pp. 692–699, 2020.
- [44] C. M. Bishop, *Pattern Recognition and Machine Learning*, Springer, New York, NY, USA, 2006.
- [45] P. B. Junior, W. R. B. M. Nunes, and A. E. Lazzaretti, “Classifier for motor imagery during parametric functional electrical stimulation frequencies on the quadriceps muscle*,” in *Proceedings of the 2019 9th International IEEE/EMBS Conference on Neural Engineering (NER)*, pp. 526–529, San Francisco, CA, USA, March 2019.
- [46] C.-C. Chang and C.-J. Lin, “Libsvm,” *ACM Transactions on Intelligent Systems and Technology*, vol. 2, no. 3, pp. 1–27, 2011.
- [47] A. I. Sburlea, L. Montesano, and J. Minguez, “Continuous detection of the self-initiated walking pre-movement state from EEG correlates without session-to-session recalibration,” *Journal of Neural Engineering*, vol. 12, no. 3, p. 36007, 2015.
- [48] S. Ren, W. Wang, Z.-G. Hou, X. Liang, J. Wang, and W. Shi, “Enhanced motor imagery based brain-computer interface via fes and vr for lower limbs,” *IEEE Transactions on Neural Systems and Rehabilitation Engineering*, vol. 28, no. 8, pp. 1846–1855, 2020.
- [49] M. A. Romero-Laiseca, D. Delisle-Rodriguez, V. Cardoso et al., “A low-cost lower-limb brain-machine interface triggered by pedaling motor imagery for post-stroke patients rehabilitation,” *IEEE Transactions on Neural Systems and Rehabilitation Engineering*, vol. 28, no. 4, pp. 988–996, 2020.
- [50] D. J. McFarland, W. A. Sarnacki, and J. R. Wolpaw, “Brain-computer interface (BCI) operation: optimizing information transfer rates,” *Biological Psychology*, vol. 63, no. 3, pp. 237–251, 2003.
- [51] X. Yong and C. Menon, “Eeg classification of different imaginary movements within the same limb,” *PLoS One*, vol. 10, no. 4, pp. 1–24, 2015.
- [52] M. Tavakolan, Z. Frehlick, X. Yong, and C. Menon, “Classifying three imaginary states of the same upper extremity using time-domain features,” *PLoS One*, vol. 12, no. 3, pp. 1–18, 2017.
- [53] C. B. Tabernig, C. A. Lopez, and L. C. Carrere, “Neuro-rehabilitation therapy of patients with severe stroke based

- on functional electrical stimulation commanded by a brain computer interface,” *Journal of Rehabilitation and Assistive Technologies Engineering*, vol. 5, 2018.
- [54] R. Aldea and O. Eva, “Detecting sensorimotor rhythms from the eeg signals using the independent component analysis and the coefficient of determination,” in *Proceedings of the International Symposium on Signals, Circuits and Systems ISSCS2013*, pp. 1–4, Iasi, Romania, July 2013.
- [55] J. Devore, *Probability and Statistics for Engineering and the Sciences*, Cengage Learning, Boston, MA, USA, 2015.
- [56] M. I. Garry, G. Kamen, and M. A. Nordstrom, “Hemispheric differences in the relationship between corticomotor excitability changes following a fine-motor task and motor learning,” *Journal of Neurophysiology*, vol. 91, no. 4, pp. 1570–1578, 2004.
- [57] S. Kishore, M. González-Franco, C. Hintemüller et al., “Comparison of ssvpe bci and eye tracking for controlling a humanoid robot in a social environment,” *Presence: Teleoperators and Virtual Environments*, vol. 23, no. 3, pp. 242–252, 2014.
- [58] M. Jeannerod and V. Frak, “Mental imaging of motor activity in humans,” *Current Opinion in Neurobiology*, vol. 9, no. 6, pp. 735–739, 1999.
- [59] K. J. Miller, G. Schalk, E. E. Fetz, M. den Nijs, J. G. Ojemann, and R. P. N. Rao, “Cortical activity during motor execution, motor imagery, and imagery-based online feedback,” *Proceedings of the National Academy of Sciences*, vol. 107, no. 9, pp. 4430–4435, 2010.
- [60] G. Pfurtscheller and A. Berghold, “Patterns of cortical activation during planning of voluntary movement,” *Electroencephalography and Clinical Neurophysiology*, vol. 72, no. 3, pp. 250–258, 1989.
- [61] C. Reynolds, B. A. Osuagwu, and A. Vuckovic, “Influence of motor imagination on cortical activation during functional electrical stimulation,” *Clinical Neurophysiology*, vol. 126, no. 7, pp. 1360–1369, 2015.
- [62] J. Sanes, J. Donoghue, V. Thangaraj, R. Edelman, and S. Warach, “Shared neural substrates controlling hand movements in human motor cortex,” *Science*, vol. 268, no. 5218, pp. 1775–1777, 1995.
- [63] E. B. Plow, P. Arora, M. A. Pline, M. T. Binstock, and J. R. Carey, “Within-limb somatotopy in primary motor cortex-revealed using fMRI,” *Cortex*, vol. 46, no. 3, pp. 310–321, 2010.
- [64] J. Gomez-Pilar, R. Corralejo, L. F. Nicolas-Alonso, D. Álvarez, and R. Hornero, “Neurofeedback training with a motor imagery-based bci: neurocognitive improvements and eeg changes in the elderly,” *Medical & Biological Engineering & Computing*, vol. 54, no. 11, pp. 1655–1666, 2016.
- [65] S. Jirayucharoensak, P. Israsena, S. Pan-Ngum, S. Hemrungronj, and M. Maes, “A game-based neurofeedback training system to enhance cognitive performance in healthy elderly subjects and in patients with amnesic mild cognitive impairment,” *Clinical Interventions in Aging*, vol. 14, pp. 347–360, 2019.
- [66] J. Frey, C. Mühl, F. Lotte, and M. Hachet, “Review of the use of electroencephalography as an evaluation method for human-computer interaction,” in *Proceedings of the PhyCS-International Conference on Physiological Computing Systems*, Scitepress, Lisbonne, Portugal, January 2014.
- [67] A. K. Engel and P. Fries, “Beta-band oscillations-signalling the status quo?” *Current Opinion in Neurobiology*, vol. 20, no. 2, pp. 156–165, 2010.
- [68] J. A. Pineda, D. S. Silverman, A. Vankov, and J. Hestenes, “Learning to control brain rhythms: making a brain-computer interface possible,” *IEEE Transactions on Neural Systems and Rehabilitation Engineering*, vol. 11, no. 2, pp. 181–184, 2003.
- [69] T.-S. Lee, S. J. A. Goh, and S. Y. Quek, “A brain-computer interface based cognitive training system for healthy elderly: a randomized control pilot study for usability and preliminary efficacy,” *PLoS One*, vol. 8, no. 11, pp. 1–8, 2013.
- [70] M. Alimardani, S. Nishio, and H. Ishiguro, “Removal of proprioception by bci raises a stronger body ownership illusion in control of a humanlike robot,” *Scientific Reports*, vol. 6, p. 33514, 2016.
- [71] C. Jeunet, E. Jahanpour, and F. Lotte, “Why standard brain-computer interface (BCI) training protocols should be changed: an experimental study,” *Journal of Neural Engineering*, vol. 13, no. 3, p. 36024, 2016.
- [72] K. Pacheco, K. Acuña, E. Carranza, D. Achancaray, and J. Andreu-Perez, “Performance predictors of motor 2017, imagery brain-computer interface based on spatial abilities for upper limb rehabilitation,” in *Proceedings of the 2017 39th Annual International Conference of the IEEE Engineering in Medicine and Biology Society (EMBC)*, pp. 1014–1017, Jeju Island, Korea, July 2017.
- [73] N. Leeuwis and M. Alimardani, “High aptitude motor-imagery bci users have better visuospatial memory,” in *Proceedings of the 2020 IEEE International Conference on Systems, Man, and Cybernetics (SMC)*, pp. 1518–1523, Toronto, Canada, October 2020.

Research Article

EEG Assessment in a 2-Year-Old Child with Prolonged Disorders of Consciousness: 3 Years' Follow-up

Gang Xu ¹, Qianqian Sheng ¹, Qinggang Xin ¹, Yanxin Song ², Gaoyan Zhang ³,
Lin Yuan ¹, Peng Zhao ¹, and Jun Liang ^{4,5}

¹Rehabilitation Branch, Tianjin Children' Hospital, Tianjin 300400, China

²Tianjin Tianshi University Medical College, Tianjin 301700, China

³School of Artificial Intelligence, College of Intelligence and Computing, Tianjin University, Tianjin 300354, China

⁴Department of Rehabilitation, Tianjin Medical University General Hospital, Tianjin 300041, China

⁵Lab of Neural Engineering & Rehabilitation, Department of Biomedical Engineering,

College of Precision Instruments and Optoelectronics Engineering, Tianjin University, Tianjin 300354, China

Correspondence should be addressed to Peng Zhao; patrickzhao@163.com and Jun Liang; 15122878711@163.com

Received 7 August 2020; Revised 21 October 2020; Accepted 31 October 2020; Published 27 November 2020

Academic Editor: Abdelkader Nasreddine Belkacem

Copyright © 2020 Gang Xu et al. This is an open access article distributed under the Creative Commons Attribution License, which permits unrestricted use, distribution, and reproduction in any medium, provided the original work is properly cited.

A 2-year-old girl, diagnosed with traumatic brain injury and epilepsy following car trauma, was followed up for 3 years (a total of 15 recordings taken at 0, 2, 3, 4, 5, 6, 7, 9, 10, 11, 12, 14, 19, 26, and 35 months). There is still no clear guidance on the diagnosis, treatment, and prognosis of children with disorders of consciousness. At each appointment, recordings included the child's height, weight, pediatric Glasgow Coma Scale (pGCS), Coma Recovery Scale-Revised (CRS-R), Gesell Developmental Schedule, computed tomography or magnetic resonance imaging, electroencephalogram, frequency of seizures, oral antiepileptic drugs, stimulation with subject's own name (SON), and median nerve electrical stimulation (MNS). Growth and development were deemed appropriate for the age of the child. The pGCS and Gesell Developmental Schedule provided a comprehensive assessment of consciousness and mental development; the weighted Phase Lag Index (wPLI) in the β -band (13–25 Hz) can distinguish unresponsive wakefulness syndrome from minimally conscious state and confirm that the SON and MNS were effective. The continuous increase of delta-band power indicates a poor prognosis. Interictal epileptiform discharges (IEDs) have a cumulative effect and seizures seriously affect the prognosis.

1. Introduction

The development of emergency and critical care medicine is changing rapidly. After severe brain damage caused by trauma, patients may experience coma, unresponsive wakefulness syndrome (UWS), minimally conscious state (MCS) [1, 2], and long-term motor and cognitive impairment. The prevalence of UWS is between 0.2 and 3.4 per 100,000 [3, 4]. 10 to 15% of patients (including adults and children) who survived the acute coma stage entered a state of prolonged disorders of consciousness (PDOC) [5, 6]. The incidence in children is particularly prominent due to a lack of self-protection awareness and the errors of parents or caregivers [7]. In the U.S., between 4,000 and 10,000 children

each year suffer from a persistent vegetative state (now termed UWS). 24% of children in a persistent vegetative state after traumatic brain injury (TBI) regained consciousness after 3 months, while after 12 months, this proportion rose to 62% [8, 9]. 63% of UWS patients survived for more than 8 years [10]. This undoubtedly reduces the patient's quality of life and increases the burden on the family and society.

At present, the diagnosis and treatment of disorders of consciousness caused by severe brain injury are still very difficult, especially in children [11]. Further, there is no clear guidance regarding diagnosis, treatment, or prognosis. Multisensory stimulation is widely recommended because of an extremely low adverse reaction rate and the presence of

observable immediate reactions and because it facilitates active family participation. However, the technique lacks any evidence of efficacy [12, 13]. Electroencephalogram (EEG) is the only electrophysiological recording technique available in most primary hospitals. EEG can be used to provide periodic and repeated evaluations at the bedside to track the patient's rehabilitation trajectory [14]. EEG analysis can give information related to a child's consciousness level and epilepsy activity and complements brain imaging research. EEG analysis has been widely used in research in the field of disorders of consciousness [15–19]. In this paper, EEG analysis is used to longitudinally observe the diagnosis and treatment process in a severe brain injury case, which may provide a reference for clinical research.

2. Materials and Methods

2.1. Case. A 2-year-old girl presented having suffered from prolonged disorders of consciousness (PDOC) for 2 months and was diagnosed with traumatic brain injury and epilepsy. The girl's development before the injury was normal.

On attending the emergency department after the car accident, a pediatric Glasgow Coma Scale (pGCS) of 3 was recorded. CT (computed tomography) showed a high-density shadow in the right temporal lobe representing a small amount of cerebral parenchymal hematoma. Also observed were subarachnoid hemorrhage and bilateral traumatic wet lung, but no abnormalities in the abdominal pelvis. Neurosurgery provided ventilator-assisted breathing, a blood transfusion was given to increase blood volume, in addition to mannitol and dexamethasone, and other non-surgical protective treatments to reduce cerebral edema. After the vital signs had become stable, the patient was transferred to the rehabilitation department to continue treatment. At this point, a pGCS of 8 was recorded (E4-V2-M2) in addition to quadriplegia.

Head magnetic resonance imaging (MRI) showed bilateral frontotemporal apical subdural effusion, white matter areas with high signal intensity in the bilateral parietal lobe, low signal shadows in the bilateral cerebellar hemispheres, brainstem, and cistern of the foot signified contusion and laceration and possible subarachnoid hemorrhage, and long T_1 and long T_2 signals in the right lateral basal ganglia area signified hemorrhagic absorption, and there was a notable widening of the ventricle and extraventricular space.

The treatment regime comprised (1) maintaining stable vital signs and nutritional support to prevent complications; (2) the administration of various benign stimuli (namely, subject's own name, SON; electrical median nerve stimulation, MNS; and proprioceptive stimulation) and physiotherapy; (3) hyperbaric oxygen cabin treatment; and (4) oral antiepileptic medication as shown in Figure 1.

2.2. Assessments. pGCS, CRS-R, Gesell Developmental Schedule, height, weight, seizure frequency, oral antiepileptic medication, CT, and MRI are shown in Figure 1. The same researchers (comprising 3 rehabilitation physicians and 1 psychological counselor) performed EEG acquisition and observations via video recordings taken in the EEG

room or at the bedside. The processed EEG recordings are shown in Figure 2. CRS-R and pGCS were evaluated by three rehabilitation physicians at different times within the same day. The results were based on the same score being given by more than two physicians. Clinical examination, pGCS, and CRS-R assessment (accounting for fluctuations in the functional status of the child) began immediately before the EEG recording. The Gesell test was evaluated by a psychological counselor.

2.3. Resting-State EEG. Resting-state EEG was recorded using 16-channel silver chloride single disc electrodes, placed according to the international 10/20 system. The placement of each channel on the head is shown in Figure 3. Data were collected at a sampling rate of 500 Hz or 512 Hz and were later downsampled to 128 Hz offline. The patient's behaviors and EEG data were monitored online to ensure recordings were free from seizure activity. The test paradigm is shown in Figure 2. SON stimulation was recorded by the child's mother, with 2 seconds between adjacent stimulus repeats, edited by Format Factory, and presented using the EDIFIER K800 headset. MNS was administered using a Shanghai NuoCheng stimulator. A skin electrode (2.5 cm × 2.5 cm) was applied to the patient's right forearm 2 cm above the wrist striate. MNS was administered using direct current in the form of a 300 ms-wide asymmetric square wave, with 13 mA stimulation intensity (with reference to thumb or finger jitter), and 40 Hz frequency. The test was repeated twice [20].

Data were filtered between 1 and 25 Hz and then epoched to 2-second epochs. Epochs containing excessive eye movement or muscular artifacts were rejected using a quasidautomated procedure whereby abnormally noisy channels and epochs were identified by calculating their normalized variance. Further noisy channels and epochs were manually rejected or retained by visual inspection. Data with continuous epilepsy-like activity were excluded (e.g., periodic interictal epileptiform discharges, IEDs). Data were rereferenced to compute the average across all channels. Then use independent component analysis (ICA), which is implemented by the RUNICA tool within EEGLAB [21]. Once relatively artifact-free EEG data had been obtained, functions in MATLAB (version 7.6) were used to conduct the power spectrum and functional connection analyses.

EEG data covering the known frequency bands, δ_1 (1–2 Hz), δ_2 (3–4 Hz), θ_1 (5–6 Hz), θ_2 (7–8 Hz), α_1 (9–10 Hz), α_2 (11–12 Hz), and β (13–25 Hz), were analyzed. The selected EEG epochs were processed using a fast Fourier transform (FFT). The weighted Phase Lag Index (wPLI) was used to measure connectivity between each pair of electrodes. wPLI minimizes the effects of volume conduction on the estimation of brain connectivity. The wPLI values across all channel pairs were used to construct symmetric 16 × 16 wPLI connectivity matrices for the β -band, as shown in Figure 3.

3. Results and Discussion

There is limited literature on the diagnosis and treatment of disorders of consciousness in children [11, 22]. The research

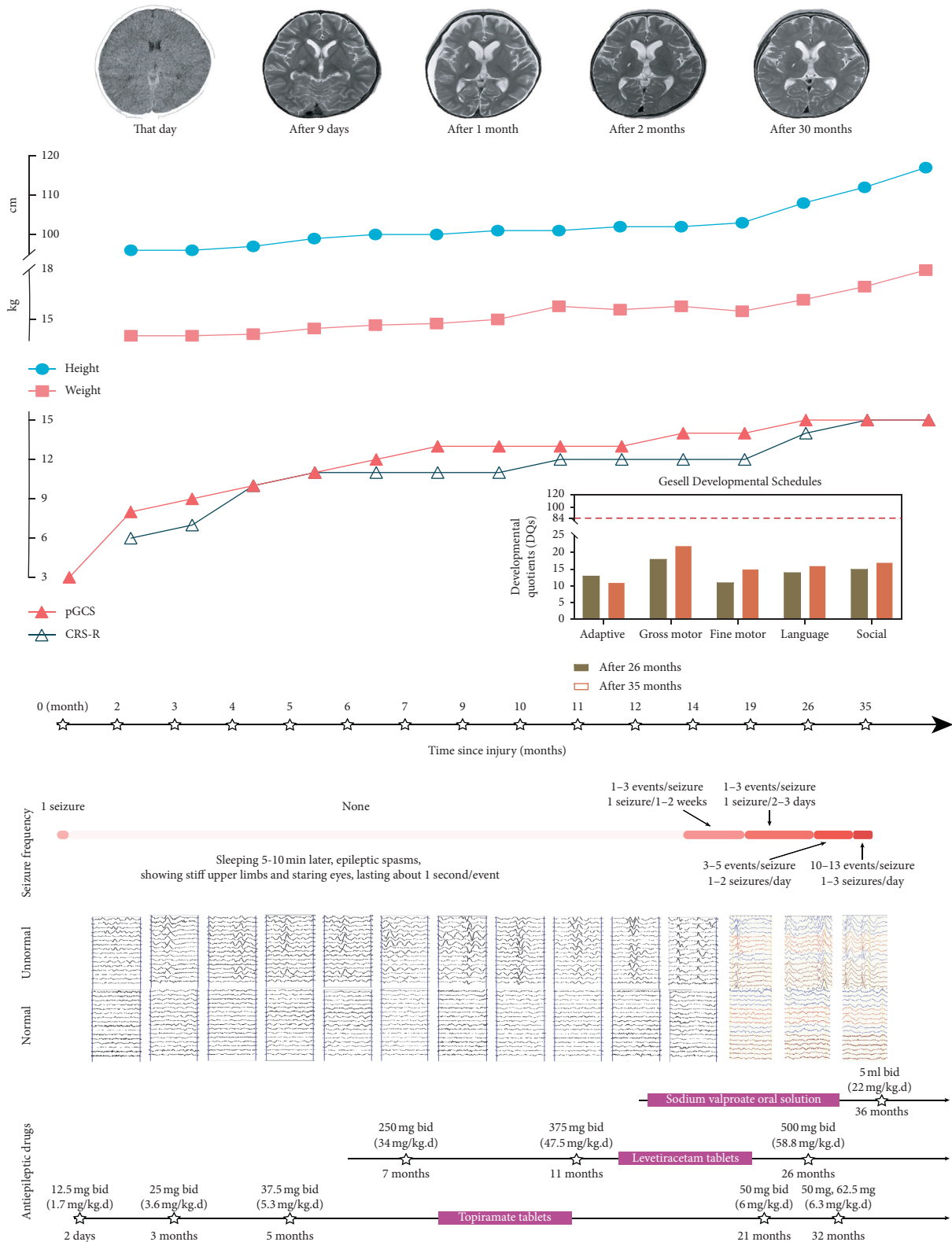


FIGURE 1: 14 consecutive assessments after the onset: pGCS, CRS-R, Gesell, height, weight, seizure frequency, oral antiepileptic medications, CT, and MRI.

methods are mostly cross-sectional. Due to the instability of the consciousness state of patients with prolonged disorders of consciousness, the repeatability (especially during UWS

and MCS) is poor. The process of recovery comprises two components: development and plasticity. Longitudinal research is of great significance.

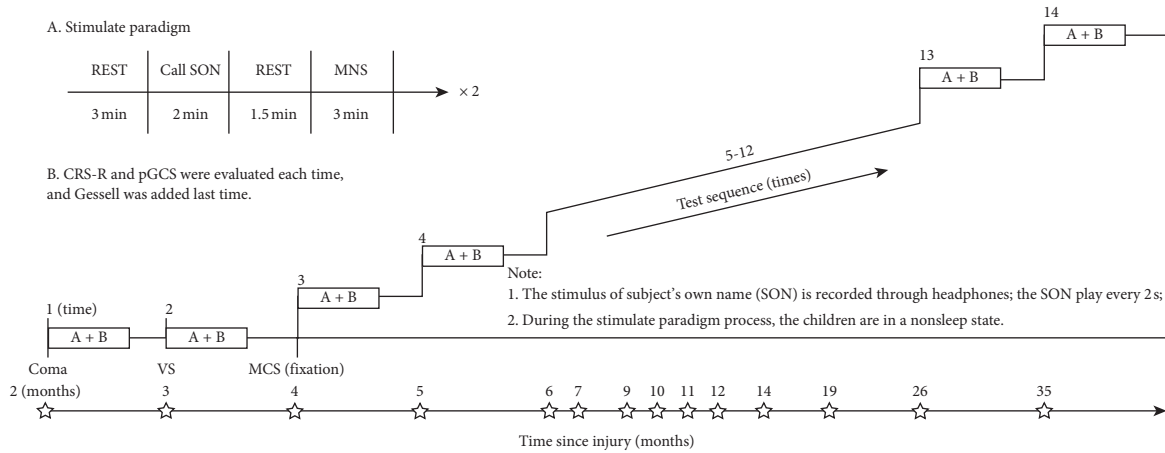


FIGURE 2: Experimental design.

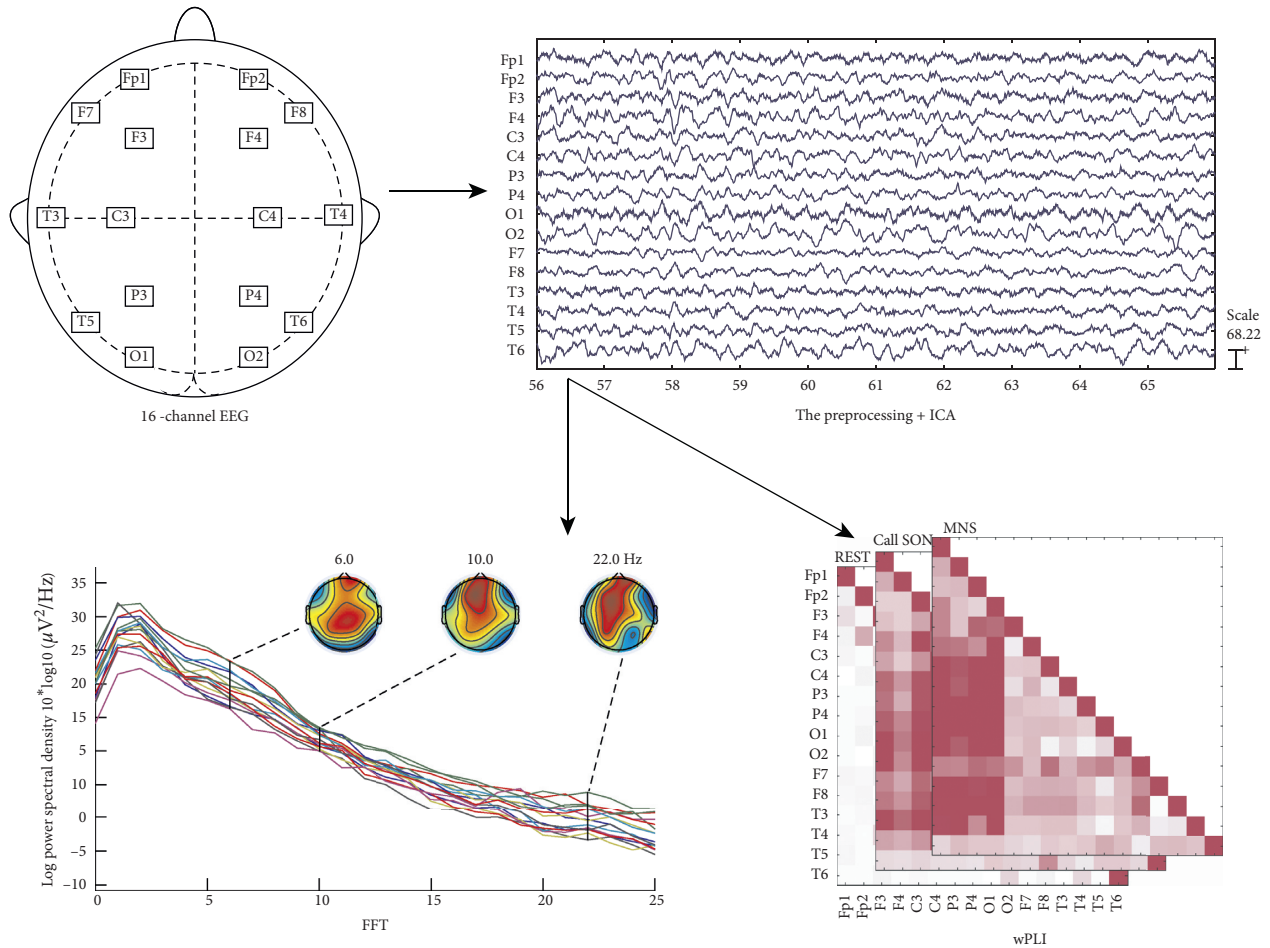


FIGURE 3: Data processing: after preprocessing and independent component analysis (ICA), the selected EEG epochs were analyzed using fast Fourier transform (FFT) and weighted Phase Lag Index (wPLI).

In terms of the child's growth and development, her height and weight were seen to develop at the correct rate. With regards to behavior evaluation (Figure 1), her pGCS gradually increased as disease recovery progressed, until it reached 15 points (the maximum score) after 19 months of onset. Her CRS-R appeared to plateau three times during

disease recovery (at 5–9 months, 10–14 months, and 26–35 months). The Gesell assessment showed that all 5 areas were extremely underdeveloped at 26 and 35 months. The mother of the child believes that the child has continued to progress. At 19 months after injury, she has been able to understand and execute simple instructions (such as “sit,” “do not

shout,” and “wave goodbye”). Further, the frequency of execution has increased slowly.

EEG spectral analysis showed the δ -band power spectrum continued to increase over the 3 years (Figure 4). At the end of the 3 years, the Gesell assessment showed that all 5 areas were still extremely underdeveloped. This indicated that the continued rapid increase of slow waves may be related to a poor prognosis. It is suggested that the continuous increase of slow waves may be a manifestation of brain dysfunction. The Gesell assessment is more generally used to monitor late neurodevelopment in preterm infants [23], bilirubin encephalopathy [24], and hypoglycemic encephalopathy [25]. Therefore, this study attempts to use the Gesell assessment to monitor the level of neurodevelopment during later follow-up of a child with traumatic brain injury. In follow-up studies related to the prognosis of adult disorders of consciousness, the increase in slow waves has been associated with a poor prognosis [26–29], in agreement with our findings. The decrease of $\alpha + \beta/\delta + \theta$ is also a common indicator of poor prognosis [18]; however, it was not found during continuous follow-up in this case. One reason for this may be that a case study, being a study of a single individual, is biased. Alternatively, during the rapid development of a 2-year-old child, each frequency band has been shown to change significantly with age [30, 31].

Stimulation using SON and MNS had a positive role in the functional connectivity in the β (13–25 Hz) frequency band, as shown in Figure 4. In the UWS period, SON and MNS increased the functional connectivity to a level above that of the resting state. However, there was no obvious difference between long-range functional connectivity and short-range functional connectivity. Counterintuitively, short-range functional connectivity sometimes even exceeded long-range functional connectivity. Over the same period, pGCS and CRS-R scores increased. Therefore, on the one hand, stimulation using SON and MNS may increase cortical functional connectivity in children and improve the state of consciousness, but conversely, short-range functional connectivity still accounts for a large proportion of stimulus responses. This suggests that SON and MNS effectively activate the brain, but that activation is largely concentrated in local brain regions. From the diagnosis of MCS to 19 months after the onset, SON and MNS induced increases in both long-range and short-range functional connectivity to a level above that of the resting state, while pGCS and CRS-R scores also increased. This finding suggests that SON and MNS can significantly increase cortical functional connectivity in children in an MCS and improve the state of consciousness. Between 19 and 35 months following onset, functional connectivity in response to SON and MNS suddenly decreased. This is in agreement with a previous study that demonstrated no significant difference in the short- and long-range functional connectivity in response to stimulation in UWS and MCS. Observations have shown that multisensory stimulation therapy had a more positive effect in unconscious children than in a control group. The early manifestations are reduced agitation and decreased muscle tone, while longer-term manifestations are improved cognitive and self-care abilities [32]. However, no

evidence has been provided on the mechanism of action. This study suggests that SON and MNS can increase the short- and long-range cortical functional connectivity in children and provide a partial basis for the mechanism behind the effectiveness of multisensory stimulation.

Epilepsy (including IEDs) was found to play a negative role. IEDs persisted and increased in the first 13 months after injury; however, there were no clinical seizures. Cognitive function significantly improved over this period. Between 13 and 35 months after the injury, spastic seizures appeared and gradually increased while cognitive function stagnated, as shown in Figure 1. Although the dosage and types of antiepileptic drugs had been increased since onset, they did not effectively control the progress of epilepsy. Taking this evidence in combination with the change in β -band functional connectivity, it suggests that IEDs have little effect on functional connectivity. However, there may be a cumulative effect that has gone undetected. Seizures had a greater impact on functional connectivity, suggesting that abnormal discharge may be detrimental to brain function. Sometimes, antiepileptic drugs have no obvious effect. The effect of epilepsy on the prognosis of children with disorders of consciousness has not attracted enough attention [22], potentially due to the relatively low incidence of epilepsy in the early stages of these disorders. The incidence of epilepsy within the 5 days following brain trauma is 7%, of which 6% go on to an epilepsy diagnosis [33]. However, after 59 months of follow-up, the incidence of epilepsy reached 20% [34]. It is suggested that children with IEDs or normal EEG in the early stages of brain injury may be likely to develop epilepsy in the long term. The cognitive impairment associated with IEDs is transient or slight, but the cognitive impairment of persistent IEDs can be cumulative [35]. Some studies have shown that the presence of IEDs is an independent risk factor for cognitive impairment in children and may even affect cognitive development through pathological damage to the brain [36, 37]. Controlling IEDs has also been shown to improve cognition and behavior [38]. This serves as a reminder that it is important to pay attention to the management of abnormal discharge. For children with a severe head injury and prolonged increased abnormal discharge, although early identification and diagnosis continue to improve, there is still a possibility of a poor long-term prognosis.

In the entire life cycle of human development, from infants to young children, adolescents, adults, and old age, there are different patterns underlying changes in cognitive and motor abilities [39]. These patterns are affected by the plasticity of the central nervous system. For example, a study found that correct rejection rates (CRRs) improved, and reaction times (RTs) became longer (got worse). Performance increased between a cohort of children to a cohort of young adults but decreased again in the older adult cohort [40]. Observing 586 healthy subjects aged between 2 and 73 years old, it was found that plasticity of the auditory brainstem persisted, especially between 5 and 8 years old [41]. The excitability and plasticity of cells in the cerebral cortex, neural pathways, and neural networks are the key to our exploration of age-related changes in brain structure and

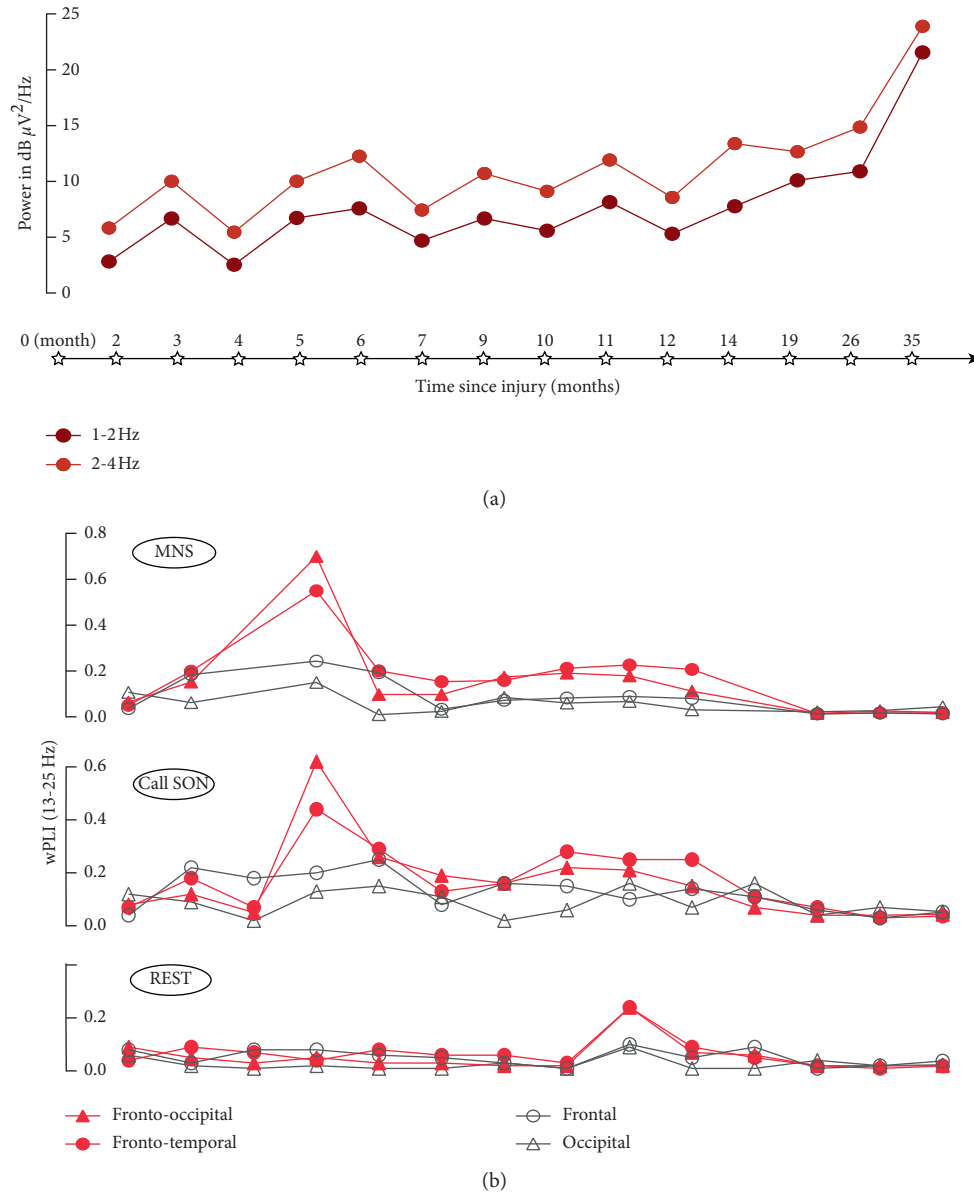


FIGURE 4: 14 consecutive EEG assessments following the injury: (a) FFT and (b) wPLI.

function [42]. As a method of electrophysiological monitoring, EEG is one of the most important methods in cognitive neuroscience research [43, 44]. Children with severe neurological diseases may not be able to communicate or interact with their surroundings. Brain-computer interfaces (BCI) provide new opportunities for such children to participate in interactions to improve their quality of life. One study showed that children can quickly achieve control and execute multiple tasks using simple EEG-based BCI systems [45]. This has been demonstrated in autism [46] and cerebral palsy [47]. Therefore, the longitudinal study of pediatric EEG provides a reference for the development of BCI for children. At the same time, it also has important

guiding significance for the study of BCI technology for the elderly.

4. Limitations

This is a case report. It is challenging to design and conduct a controlled study in this area. The scope of the behavior scale used (the pediatric GCS) is restricted to young children. The Rappaport Coma/Near Coma Scale (CNCS) and Level of Cognitive Functioning Assessment Scale (LOCFAS) [48] may be considered in future studies; however, both these scales are currently used less often and it will take time for clinicians to become familiar with their use. Multimodality

assessments, combined with brain imaging, may provide a more advantageous measure.

5. Conclusions

In the follow-up of this case, it was found that the continuous increase in the δ -band power spectrum indicated a poor prognosis. wPLI in the β -band was used to identify the effect stimulation using SON and MNS on cortical functional connectivity. Spectral analyses and wPLI can be used as auxiliary tools for the diagnosis and follow-up of prolonged disorders of consciousness. Interepileptic seizures seriously affect long-term prognosis and need to be actively managed. Long-term continuous follow-up of children with prolonged disorders of consciousness is of great significance in understanding the occurrence and development of these diseases.

Data Availability

Part of the data used to support the findings of this study may be released upon application to the first author (Gang Xu), who can be contacted via e-mail, xugangrehab@163.com.

Ethical Approval

This study was carried out in accordance with the recommendations of the Tianjin Children's Hospital Ethics Committee for Cambridgeshire.

Consent

The patient's parents gave written informed consent before enrolment in the study in accordance with the UK Mental Capacity Act 2005 and Declaration of Helsinki.

Conflicts of Interest

All authors declare that they have no conflicts of interest.

Authors' Contributions

Peng Zhao and Jun Liang are co-authors.

Acknowledgments

This work was supported in part by the National Natural Science Foundation of China (no. 61876126).

References

- [1] J. T. Giacino, J. J. Fins, S. Laureys, and N. D. Schiff, "Disorders of consciousness after acquired brain injury: the state of the science," *Nature Reviews Neurology*, vol. 10, no. 2, pp. 99–114, 2014.
- [2] O. Gosseries, A. Vanhauwenhuysse, M. A. Bruno et al., "Disorders of consciousness: coma, vegetative and minimally conscious states," *States of Consciousness*, pp. 29–55, 2011.
- [3] J. C. M. Lavrijsen, J. S. van den Bosch, R. T. Koopmans, and C. van Weel, "Prevalence and characteristics of patients in a vegetative state in Dutch nursing homes," *Journal of Neurology, Neurosurgery & Psychiatry*, vol. 76, no. 10, pp. 1420–1424, 2005.
- [4] J. Donis and B. Kräftner, "The prevalence of patients in a vegetative state and minimally conscious state in nursing homes in Austria," *Brain Injury*, vol. 25, no. 11, pp. 1101–1107, 2011.
- [5] X. Wang, X. Sun, and H. Liu, "Clinical analysis and misdiagnosis of cerebral venous thrombosis," *Experimental and Therapeutic Medicine*, vol. 4, no. 5, pp. 923–927, 2012.
- [6] H. S. Levin, C. Saydjari, H. M. Eisenberg et al., "Vegetative state after closed-head injury," *Archives of Neurology*, vol. 48, no. 6, pp. 580–585, 1991.
- [7] K. Chaitanya, A. Addanki, R. Karambelkar, and R. Ranjan, "Traumatic brain injury in indian children," *Child s Nervous System*, vol. 34, 2018.
- [8] Multi-Society Task Force on PVS, "Medical aspects of the persistent vegetative state (1)," *The New England Journal of Medicine*, vol. 330, pp. 1499–1508, 1994.
- [9] N. Listed, "Medical aspects of the persistent vegetative state (1)," *The Multi-Society Task Force on PVS*, vol. 330, pp. 1572–1579, 1994.
- [10] D. J. Strauss, S. Ashwal, S. M. Day, and R. M. Shavelle, "Life expectancy of children in vegetative and minimally conscious states," *Pediatric Neurology*, vol. 23, no. 4, pp. 312–319, 2000.
- [11] J. T. Giacino, D. I. Katz, N. D. Schiff et al., "Comprehensive systematic review update summary: disorders of consciousness," *Archives of Physical Medicine & Rehabilitation*, vol. 91, 2018.
- [12] L. Turner-Stokes, "Prolonged disorders of consciousness: new national clinical guidelines from the royal college of physicians, London," *Clinical Medicine*, vol. 14, no. 1, pp. 4–5, 2014.
- [13] A. L. Houston, N. S. Wilson, M. C. Morrall, R. Lodh, and J. R. Oddy, "Interventions to improve outcomes in children and young people with unresponsive wakefulness syndrome following acquired brain injury: a systematic review," *European Journal of Paediatric Neurology*, vol. 25, pp. 40–51, 2020.
- [14] A. M. Goldfine, J. D. Victor, M. M. Conte, J. C. Bardin, and N. D. Schiff, "Determination of awareness in patients with severe brain injury using EEG power spectral analysis," *Clinical Neurophysiology*, vol. 122, no. 11, pp. 2157–2168, 2011.
- [15] N. André-Obadia, J. Zyss, M. Gavaret, J. P. Lefaucheur, and A. Delval, "Recommendations for the use of electroencephalography and evoked potentials in comatose patients," *Neurophysiologie Clinique/Clinical Neurophysiology*, vol. 48, 2018.
- [16] D. Kondziella, A. Bender, K. Diserens et al., "European academy of neurology guideline on the diagnosis of coma and other disorders of consciousness," *European Journal of Neurology*, vol. 27, 2020.
- [17] S. Corchs, G. Chioma, R. Dondi et al., "Computational methods for resting-state EEG of patients with disorders of consciousness," *Frontiers in Neuroscience*, vol. 13, p. 807, 2019.
- [18] Y. Bai, X. Xia, and X. Li, "A review of resting-state electroencephalography analysis in disorders of consciousness," *Frontiers of Neurology*, vol. 8, p. 471, 2017.
- [19] C. A. Bareham, J. Allanson, N. Roberts et al., "Longitudinal bedside assessments of brain networks in disorders of consciousness: case reports from the field," *Frontiers of Neurology*, vol. 9, p. 676, 2018.
- [20] M. Dovgialo, A. Chabuda, A. Duszyk et al., "Assessment of statistically significant command-following in pediatric patients with disorders of consciousness, based on visual,

- auditory and tactile event-related potentials,” *International Journal of Neural Systems*, vol. 29, no. 3, p. 1850048, 2019.
- [21] A. Delorme and S. Makeig, “EEGLAB: an open source toolbox for analysis of single-trial EEG dynamics including independent component analysis,” *Journal of Neuroscience Methods*, vol. 134, no. 1, pp. 9–21, 2004.
- [22] M. Pozzi, S. Galbiati, F. Locatelli et al., “Severe acquired brain injury aetiologies, early clinical factors, and rehabilitation outcomes: a retrospective study on pediatric patients in rehabilitation,” *Brain Injury*, vol. 33, no. 12, pp. 1522–1528, 2019.
- [23] X. G. Qian, B. X. Jin, Y. B. Zhang et al., “Effects of scalp acupuncture on brain injury in premature infants with different months of age,” *Zhongguo Zhen Jiu*, vol. 38, pp. 723–726, 2018.
- [24] H. G. Wu, Z. J. Li, J. F. Liu, G. Liu, and X. Yang, “Clinical study on amplitude integrated electroencephalogram in cerebral injury caused by severe neonatal hyperbilirubinemia,” *Minerva Pediatr*, vol. 70, pp. 539–544, 2018.
- [25] L. X. Qiao, J. Wang, J. H. Yan et al., “Follow-up study of neurodevelopment in 2-year-old infants who had suffered from neonatal hypoglycemia,” *BMC Pediatr*, vol. 19, p. 133, 2019.
- [26] J. Leon-Carrion, J. F. Martin-Rodriguez, J. Damas-Lopez, Y. Barroso, J. M. Martin, and M. R. Dominguez-Morales, “Brain function in the minimally conscious state: a quantitative neurophysiological study,” *Clinical Neurophysiology*, vol. 119, no. 7, pp. 1506–1514, 2008.
- [27] A. A. Fingelkurts, A. A. Fingelkurts, S. Bagnato, C. Boccagni, and G. Galardi, “DMN operational synchrony relates to self-consciousness: evidence from patients in vegetative and minimally conscious states,” *The Open Neuroimaging Journal*, vol. 6, pp. 55–68, 2012.
- [28] M. Cavinato, C. Genna, P. Manganotti et al., “Coherence and consciousness: study of fronto-parietal gamma synchrony in patients with disorders of consciousness,” *Brain Topography*, vol. 28, no. 4, pp. 570–579, 2015.
- [29] R. Lehembre, B. Marie-Aur lie, A. Vanhauzenhuysse et al., “Resting-state EEG study of comatose patients: a connectivity and frequency analysis to find differences between vegetative and minimally conscious states,” *Functional Neurology*, vol. 27, pp. 41–47, 2012.
- [30] M. Eisermann, A. Kaminska, M.-L. Moutard, C. Soufflet, and P. Plouin, “Normal EEG in childhood: from neonates to adolescents,” *Neurophysiologie Clinique/Clinical Neurophysiology*, vol. 43, no. 1, pp. 35–65, 2013.
- [31] A. Kaminska, M. Eisermann, and P. Plouin, “Child EEG (and maturation),” *Handbook of Clinical Neurology*, vol. 160, 2019.
- [32] G. A. Hotz, A. Castelblanco, I. M. Lara, A. D. Weiss, R. Duncan, and J. W. Kuluz, “Snoezelen: a controlled multi-sensory stimulation therapy for children recovering from severe brain injury,” *Brain Injury*, vol. 20, no. 8, pp. 879–888, 2006.
- [33] A. Shahwan, C. Bailey, L. Shekardemian, and A. S. Harvey, “The prevalence of seizures in comatose children in the pediatric intensive care unit: a prospective video-EEG study,” *Epilepsia*, vol. 51, no. 7, pp. 1198–1204, 2010.
- [34] K. M. Barlow, E. Thomson, D. Johnson, and R. A. Minns, “Late neurologic and cognitive sequelae of inflicted traumatic brain injury in infancy,” *Pediatrics*, vol. 116, no. 2, pp. e174–e185, 2005.
- [35] A. P. Aldenkamp and J. Arends, “Effects of epileptiform EEG discharges on cognitive function: is the concept of “transient cognitive impairment” still valid,” *Epilepsy Behav*, vol. 5, no. Suppl 1, pp. S25–S34, 2004.
- [36] S. Ebus, J. Arends, J. Hendriksen et al., “Cognitive effects of interictal epileptiform discharges in children,” *European Journal of Paediatric Neurology*, vol. 16, no. 6, pp. 697–706, 2012.
- [37] J. M. Glennon, L. Weiss-Croft, S. Harrison, J. H. Cross, S. G. Boyd, and T. Baldeweg, “Interictal epileptiform discharges have an independent association with cognitive impairment in children with lesional epilepsy,” *Epilepsia*, vol. 57, no. 9, pp. 1436–1442, 2016.
- [38] K. P. J. Braun, “Preventing cognitive impairment in children with epilepsy,” *Current Opinion in Neurology*, vol. 30, no. 2, pp. 140–147, 2017.
- [39] A. N. Belkacem, N. Jamil, J. A. Palmer, S. Ouhbi, and C. Chen, “Brain computer interfaces for improving the quality of life of older adults and elderly patients,” *Frontiers in Neuroscience*, vol. 14, p. 692, 2020.
- [40] M. A. Motes, J. S. Spence, M. R. Brier et al., “Conjoint differences in inhibitory control and processing speed in childhood to older adult cohorts: discriminant functions from a Go/No-Go task,” *Psychology and Aging*, vol. 33, no. 7, pp. 1070–1078, 2018.
- [41] E. Skoe, J. Krizman, S. Anderson, and N. Kraus, “Stability and plasticity of auditory brainstem function across the lifespan,” *Cerebral Cortex*, vol. 25, no. 6, pp. 1415–1426, 2015.
- [42] X. Tang, P. Huang, Y. Li et al., “Age-related changes in the plasticity of neural networks assessed by transcranial magnetic stimulation with electromyography: a systematic review and meta-analysis,” *Frontiers in Cellular Neuroscience*, vol. 13, p. 469, 2019.
- [43] V. Noreika, S. Georgieva, S. Wass, and V. Leong, “14 challenges and their solutions for conducting social neuroscience and longitudinal EEG research with infants,” *Infant Behavior and Development*, vol. 58, p. 101393, 2020.
- [44] C. Babiloni, R. J. Barry, E. Bařar et al., “International Federation of Clinical Neurophysiology (IFCN)-EEG research workgroup: recommendations on frequency and topographic analysis of resting state EEG rhythms. Part 1: applications in clinical research studies,” *Clinical Neurophysiology*, vol. 131, no. 1, pp. 285–307, 2020.
- [45] J. Zhang, Z. Jadavji, E. Zewdie, and A. Kirton, “Evaluating if children can use simple brain computer interfaces,” *Frontiers in Human Neuroscience*, vol. 13, p. 24, 2019.
- [46] E. Kinney-Lang, B. Auyeung, and J. Escudero, “Expanding the (kaleido)scope: exploring current literature trends for translating electroencephalography (EEG) based brain-computer interfaces for motor rehabilitation in children,” *Journal of Neural Engineering*, vol. 13, no. 6, Article ID 061002, 2016.
- [47] M. Jochumsen, M. Shafique, A. Hassan, and I. K. Niazi, “Movement intention detection in adolescents with cerebral palsy from single-trial EEG,” *Journal of Neural Engineering*, vol. 15, no. 6, Article ID 066030, 2018.
- [48] E. Molteni, K. Colombo, V. Pastore et al., “Joint neuropsychological assessment through coma/near coma and level of cognitive functioning assessment scales reduces negative findings in pediatric disorders of consciousness,” *Brain Science*, vol. 10, 2020.

Research Article

The Time Course of Perceptual Closure of Incomplete Visual Objects: An Event-Related Potential Study

Chenyang Liu,¹ Sha Sha,² Xiujun Zhang ¹, Zhiming Bian,¹ Lin Lu,³ Bin Hao,³ Lina Li,¹ Hongge Luo,¹ Xiaotian Wang,⁴ Changming Wang,^{1,2} and Chao Chen ^{5,6}

¹North China University of Science and Technology, Tangshan, Hebei 063000, China

²Depression Treatment Center, Beijing Anqing Hospital, Capital Medical University, Beijing 100088, China

³Zhonghuan Information College Tianjin University of Technology, Tianjin 300380, China

⁴School of Artificial Intelligence, Xidian University, Xi'an 710071, China

⁵Key Laboratory of Complex System Control Theory and Application, Tianjin University of Technology, Tianjin 300384, China

⁶Academy of Medical Engineering and Translational Medicine, Tianjin University, Tianjin 300072, China

Correspondence should be addressed to Xiujun Zhang; zhangxiujun66@163.com and Chao Chen; cccovb@hotmail.com

Received 9 May 2020; Revised 30 July 2020; Accepted 2 September 2020; Published 6 October 2020

Academic Editor: Abdelkader Nasreddine Belkacem

Copyright © 2020 Chenyang Liu et al. This is an open access article distributed under the Creative Commons Attribution License, which permits unrestricted use, distribution, and reproduction in any medium, provided the original work is properly cited.

Perceptual organization is an important part of visual and auditory information processing. In the case of visual occlusion, whether the loss of information in images could be recovered and thus perceptually closed affects object recognition. In particular, many elderly subjects have defects in object recognition ability, which may be closely related to the abnormalities of perceptual functions. This phenomenon even can be observed in the early stage of dementia. Therefore, studying the neural mechanism of perceptual closure and its relationship with sensory and cognitive processing is important for understanding how the human brain recognizes objects, inspiring the development of neuromorphic intelligent algorithms of object recognition. In this study, a new experiment was designed to explore the realistic process of perceptual closure under occlusion and intact conditions of faces and building. The analysis of the differences in ERP components P1, N1, and Ncl indicated that the subjective awareness of perceptual closure mainly occurs in Ncl, but incomplete information has been processed and showed different manners compared to complete stimuli in N170 for facial materials. Although occluded, faces, but not buildings, still maintain the specificity of perceptual processing. The Ncl by faces and buildings did not show significant differences in both amplitude and latency, suggesting a “completing” process regardless of categorical features.

1. Introduction

In everyday life, visual objects are usually shaded and even occluded, making visual content inputs to human visual systems incomplete. We have to be accustomed to complementing views blocked by leaves, perceiving visual scenes in dust and recognizing a friend with a face mask.

Loss of information in early visual processing stage has to be completed following some rules in order to form a stable and holistic perception prior to cognitive stage, which facilitates recognizing objects quickly and accurately. This completion stage between sensory and cognitive process is described as perceptual organization according to the theory

of Gestalt psychology [1]. Specifically, the process to deal with incomplete, incoherent, and intermittent visual content is considered as perceptual closure against lack of physical closure [2], which may start several subprocesses to make perception complete, such as element integration, contour detection and formation, feature binding, and template matching. Deficits in perceptual closure results in failure in object recognition, misidentification of emotion, and even hallucination, which is popular in elder people and patients with neuropsychiatric disorders [3]. Actually, perceptual closure is not only a processing stage but also reflects the completion result of incomplete information. It not only plays very important roles in processing visual information

in human brains, but also crucial in inspiring developing intelligent algorithms and artificial neural networks. However, the time course and the neural mechanisms of how occluded objects are processed in our brains are still not fully understood.

When we see incomplete visual images, brain areas in the occipital, temporal, and parietal lobes participate in the completing processes. In functional magnetic resonance imaging (fMRI) studies, lateral occipital complex (LOC) and posterior intraparietal region was found to be more activated by incomplete stimuli than complete stimuli in the perceptual closure task [4, 5]. Early visual cortex and fusiform areas in inferior temporal cortex are activated rapidly, and then incomplete information in visual content is predicted which is conducive to subsequent target recognition [6, 7]. The bottom-up processing starting from low-level visual features is also regulated by top-down processing, as subjective perception is usually affected instructions and visual experiences because of the involvement of frontal networks [8]. In addition, intraparietal sulcus (IPS) and inferior parietal cortex (IPC) in dorsal visual stream also interact with temporal and occipital cortexes in ventral stream when dealing with stimulus degradation by noise [9]. However, the time course of perceptual closure is still worth for further investigation.

EEG has higher time resolution than fMRI, so this technology can provide fine description of the time course of sensory and perceptual processes of incomplete visual information. The EEG signal evoked by visual or auditory stimuli is categorized to event-related potential (ERP). In ERP studies, P1 and N1 are two typical components related to visual sensory and perceptual processing [10]. P1 starts at about 60–90 ms after visual stimulation and peaks at 100–130 ms, which can be observed at electrodes around bilateral occipital regions. It is believed to reflect the early sensory process of low-level visual information [10]. N1 is a component that begins at 130 ms after the presentation of facial and other visual objects and peaks at 160–180 ms [11, 12]. N1 can be evoked by many visual stimuli such as cars and houses and that by human faces is specifically named N170 [11]. N1/N170 is sensitive to object categories, and the amplitude of N170 by faces is much larger than N1 by nonface objects [10]. Given that faces usually contains more elements and involves integrating more complex features than other objects, the differences in N1 and N170 may be ascribed to the organization manners of visual features, and N170 corresponds to the processes of structural encoding of global visual features of faces [13, 14]. This implies that the neural activities producing N1/N170 is more likely to be responsible for perceptual organization of various features rather than the initial sensation of low-level information.

In the case incomplete visual objects, a subsequent component named negativity of closure (Ncl) could be evoked except for the two earlier components above. Previous studies indicated that when people are viewing incomplete line drawings, a negative wave that starts at 220–230 ms and reaches a peak at 290–300 ms can be found mainly in the occipital or occipito-temporal lobe [15–17] and

can be localized to the electrophysiological activities in LOC [18]. This Ncl component is believed to reflect the process of visual completion instead of visual representation, but it needs extensive exploration on different styles of stimulus before wide acceptance [19, 20].

To sum up, the time course of neural activities for incomplete objects is still unclear. Although the characteristics of P1 and N1/N170 have been repeated by many studies, they are mostly evoked by complete visual objects and the conclusions cannot be automatically generalized to incomplete objects. There is still lack of evidence about whether N1/N170 or Ncl is more important for perceptual closure. And even whether incomplete information has been complemented or at least detected in the temporal stage around P1 is worth experimental studies. In addition, incomplete objects express with several styles, including occluded objects, virtual contour consisting of discrete elements, and noisy images with different visibility. Occluded faces and familiar nonliving objects have seldom been studied since they are better examples of perceptual closure than contours.

To answer the above questions, a new experiment paradigm and new visual stimuli consisting of a series of occluded faces and buildings were designed to explore the differences in three different ERP components. The stimuli contains two exemplars of visual objects, and by comparing the occluded edition of them with the intact edition, ERP under occlusion conditions and intact conditions could be evoked and thus enable systematic comparison. The sequential change of differences in ERP amplitude and latency also helps reveal the time course of perceptual closure. All the efforts above could provide solid support when we are trying to reconstruct object recognition ability for elder people and to construct neural networks with human-like intelligence following the neural mechanisms of human visual systems.

2. Methods

2.1. Participants. A total of 22 healthy subjects were included in this study (Table 1). All subjects had normal vision or corrected visual acuity. They fully understood the experimental task and signed the informed consent. This study was approved by the Ethics Committee of Beijing Anding Hospital affiliated to Capital Medical University.

2.2. Stimuli. The facial materials used in this study were quoted from the Chinese Standard Emotional Face Picture Library. Natural neutral facial pictures were selected as stimulating materials in this experiment. 40 Male and 40 female faces were used. 40 building pictures were collected from the Internet and edited by the authors of this study. Adobe Photoshop was used to randomly occlude the whole experimental material, and the average occlusion ratio was 41.5% of the whole picture (Figure 1).

2.3. Experimental Paradigm. In this experiment, the experimental stimulus was presented by E-Prime 2.0, faces and

TABLE 1: Information of subjects ($\bar{x} \pm s$).

	$N = 24$
Age	26.54 ± 5.469
Education years	14.33 ± 3.088
Gender (male/female)	12/12

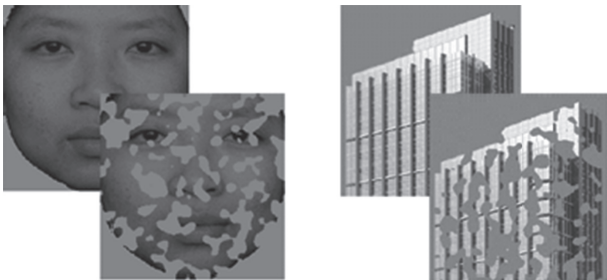


FIGURE 1: ERP waveforms of occluded and intact faces.

buildings were presented on a LCD monitor in two separate sessions, and each session consists of 140 trials. In each trial, the subjects were presented with two pictures (one complete picture and one occluded picture) in random order. Each stimulus picture lasts 500 ms in screen and was followed by a blank screen with a “+” in the center. The task of the experiment for the subjects was to judge whether the two pictures (occluded and complete) presented can be recognized as the same picture and to feedback the judgment by pressing “F” or “J” on the keyboard. When the second picture is presented, subjects press the keyboard to feedback. The ISI (interstimulus interval) was 1000 ms, and ITI was 2000 ms (Figure 2). Before the experiment was officially started, there were 10 practice trials to ensure that the subjects were clear about the task of the experiment.

During the experiment, EEG data were recorded by EGI 128-channel EEG system (Electrical Geodesic Instrument, USA). The sampling rate was 1000 Hz, and Cz was selected as the reference channel. During the experiment, the scalp resistance of each subject was guaranteed to drop below 50 k Ω .

2.4. Data Analysis. The EEG data were analyzed using EEGLAB 13.5.4b (<http://scn.ucsd.edu/eeglab/>), an open-source signal processing toolbox on Matlab platform and programs developed by the authors to preprocess the EEG data including remove eye movement noise. The sampling rate of the EEG data was downsampled to 250 Hz, filtered by 0.1–40 Hz by a bandpass filter, and the average of EEG from all channels were used as reference. Principal component analysis (PCA) and independent component analysis (ICA) were used to decompose EEG signals into 20 components in usual, and those related to eyeblinks and eye movement noise were identified visually by the author and removed manually. Then EEG data of all trials were epoched into segments of -200 to 500 ms relative to the stimulus presentation onset. Segments corresponding to four stimuli types (complete\occluded faces and buildings) were

averaged, and ERP waveform was finally extracted. The amplitude and latency of peaks in three ERP components P1, N170, and Ncl were selected for statistical analysis in SPSS 19.0.

3. Results

In this study, P1 and N170 could be elicited by both complete and occluded faces in commonly accepted visual areas, i.e., right occipital lobe (corresponding to O₂ in 10–20 EEG electrode systems) (Figure 3). For buildings, P1 and a smaller component N1 (which is thus not named as N170 for nonface objects) could also be observed in Figure 4. The differences of amplitude and latency in ERP components between complete and occluded visual stimuli were further analyzed.

In the case of face condition, the amplitude and latency of P1 component were not significantly different (Table 2) between complete and occluded conditions according to the results of paired-sample *T*-test ($p > 0.05$). In addition to faces, significant differences could be found in neither latency nor amplitude in P1 component between occluded and complete buildings. One possible explanation is that P1 component corresponds to the early stage of initial processing of low-level visual information, and object category and even object completeness detection have not started at P1 stage.

Then the amplitude and latency of N170 component between complete and occluded faces were both significantly different ($p < 0.05$, Table 2). The peak latency of N170 for occluded faces was 4 ms early than that for complete faces, and the amplitude of N170 for occluded faces was significantly more positive than that for complete faces, suggesting occluded objects may be processed more quickly because of smaller amount/loss of visual information and resulting in a less sufficient structural encoding process ($1.57 \mu\text{V}$ smaller in N170 peak amplitude). However, the effect in N170 for occluded stimuli could not be observed in N1 by occluded buildings. According to the results in Table 3, the peak amplitude values of N1 by occluded buildings were not significantly more positive than those by complete buildings ($p > 0.05$). N1 by occluded buildings occurred later in peak latency, but the differences were not statistically significant.

The ERP component Ncl could be evoked by both occluded faces and occluded buildings, not by complete visual stimuli. The findings in this study support that Ncl is specific to incomplete visual object and thus named negativity of “closure” in early studies. Unlike the abstract object made by line drawings used in previous studies (the unoccluded object by line drawings still look “incomplete”), real face and buildings were selected and occluded in this study. Hence, further evidences were provided supporting a common “complete” progress for all visual objects including faces and nonface objects happening around 200–300 ms after visual presentation.

4. Discussion

How incomplete objects are retrieved, complemented, and processed remain a challenge in both cognitive neuroscience

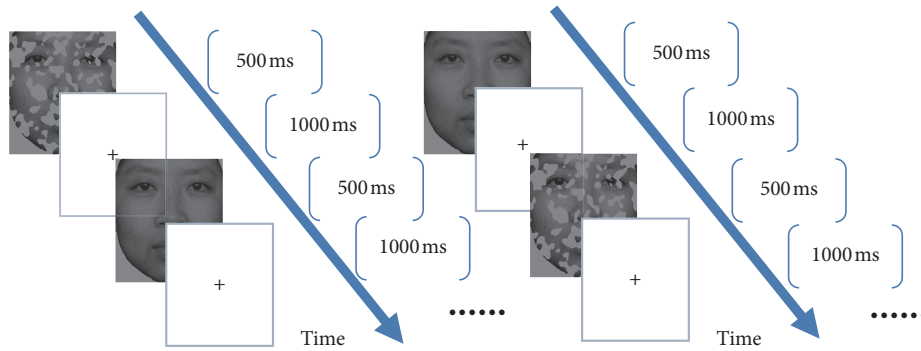


FIGURE 2: The experiment procedure of the complete-occluded object comparison task.

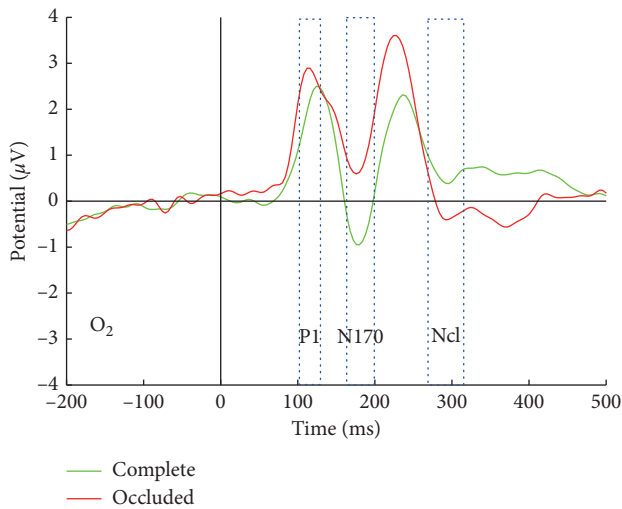


FIGURE 3: ERP waveforms of complete and occluded faces.

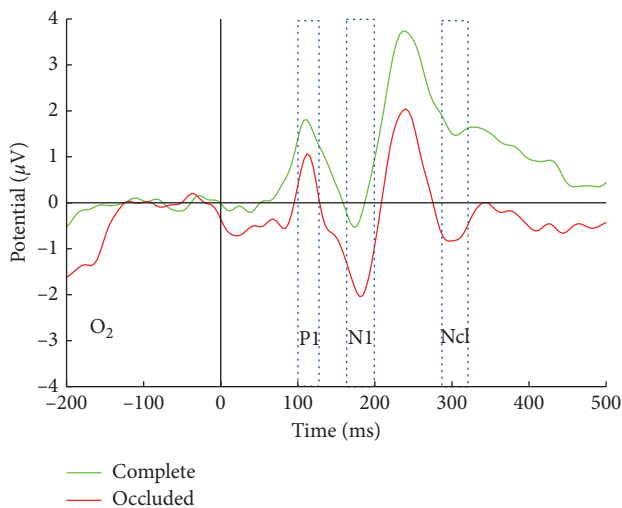


FIGURE 4: ERP waveform of occluded building and complete building.

and artificial intelligence. Intact and occluded visual objects may activate different neural mechanisms in initial representation stage, perceptual organization stage, or relatively late stage.

This study designed a new paradigm and new stimuli to investigate the process of perceptual closure by comparing the ERP differences between occluded and complete conditions. The visual materials were from the same collection of face and building images, and thus they had the same size and the same content, except for the degree of occlusion. All of them were presented to subjects in random order, and all the evoked EEG responses were used to generate ERP by grand average. Hence, differences in ERP could be ascribed by different experimental conditions, i.e., occlusion or completeness. Another advantage of ERP lies in the high temporal resolution which could separate different stages of object completion and thus help exploit which stage contribute more to the visual completion of multiple categories of objects. All the investigation above empirical information guide scientists and engineers to design more intelligent and efficient hardware or algorithms for visual information processing.

When does perceptual closure occur, at the very early stage or at a relatively late stage of visual information? This question has not been fully answered, leaving much confusion when experts majored in computational intelligence are trying to design an artificial network to identify or recognize visual objects inspired by the human brains. According to previous studies, occluded objects are believed to have been processed in the stage corresponding to Ncl component [15, 18]. In this study, similar conclusions could be drawn since an ERP component Ncl specific to perceptual closure could only be evoked by incomplete stimuli; moreover, the stimuli categories were expanded from abstract line drawings to real faces and buildings.

When tracing back to an earlier stage corresponding to N1/N170 component, that is, around 80 ms earlier than Ncl, we found that incomplete visual information had been processed at least for faces. Incompleteness may be detected first because of earlier latency in N170 component for faces and then starts a subsequent complementation process around 170 ms which is believed to correspond to the structural coding process in Bruce-Young model and newly revised model [14, 19, 21]. Insignificant differences in either peak latency or amplitude in P1 component indicated that occluded and complete images were not distinguished at this stage because it is a too early stage that may only participate in initial low-level representation of visual information to encode the global wholeness [22].

TABLE 2: Comparison of the amplitudes and latencies of each component of incomplete and complete faces ($\bar{x} \pm s$).

		Occluded	Complete	<i>t</i>	<i>p</i>
Amplitude (μV)	P1	2.914 \pm 2.285	2.529 \pm 2.259	1.009	0.326
	N170	0.551 \pm 2.986	-1.019 \pm 3.092	2.225	0.039
	Ncl	-0.562 \pm 2.694	0.399 \pm 2.554	-2.567	0.017
Latency (ms)	P1	116 \pm 7.438	117 \pm 9.418	-0.944	0.358
	N170	176 \pm 6.591	180 \pm 7.342	-2.418	0.026
	Ncl	299 \pm 10.557	298 \pm 12.681	0.266	0.793

TABLE 3: Comparisons of the amplitudes and latencies of each component of incomplete and complete buildings ($\bar{x} \pm s$).

		Occluded	Complete	<i>t</i>	<i>p</i>
Amplitude (μV)	P1	1.004 \pm 1.365	1.836 \pm 1.243	-0.543	0.242
	N1	-2.135 \pm 1.867	-0.683 \pm 2.687	-0.856	0.365
	Ncl	-0.886 \pm 2.330	1.445 \pm 2.426	-3.293	0.003
Latency (ms)	P1	108 \pm 8.355	106 \pm 5.454	0.134	0.891
	N1	179 \pm 5.856	175 \pm 7.693	0.644	0.453
	Ncl	301 \pm 7.503	304 \pm 12.067	-0.816	0.423

In addition, in the processing stage corresponding to N1/N170, occluded objects of different categories may be processed and complemented in different manners. For face images, the perceptual closure may occur earlier than buildings as larger and significant differences could be observed in the N170 by faces, not in the N1 by buildings. The results in this study also showed that the process of perceptual closure is highly dependent on the underlying “template” or visual experiences [23, 24]. We are all experts in recognizing faces but not in buildings, so specific neural networks or modules to faces in visual cortex may have been evolved billions of years ago. As it has been shown in many literature studies, the N170 by faces is so distinct that its peak amplitude is usually much larger than the N1 and thus named by a new component [10, 11]. Even for occluded face pictures, the specificity in faces is still maintained.

Then a common process may occur subsequently regardless of the category of visual objects. Following N1/N170, Ncl component could be evoked by both incomplete faces and incomplete buildings, the waveform by both stimuli appeared similar, and both the amplitude and latency values of Ncl were not significantly different between faces and buildings. All the findings above indicate that there is a common “complete” process for all visual objects. Prior to this stage, visual objects from different categories are represented by neural activities distinctly, and low-level features are extracted, integrated, and organized according to the visual template of each category. It is thus prone to find category-specific perceptual closure ERP features in N1/N170 when processing occluded objects. When higher-level visual information resulting from perceptual organization is transmitted hierarchically to superior stage corresponding to Ncl compared to P1 and N1, it normally involves a pure processing stage irrelevant of visual content input here. Thus Ncl may reflect a subjective awareness of incompleteness and recover it consciously.

In future studies, more categories of visual objects will be used to support and to expand the neural mechanisms of

perceptual closure found in this study. In related works, P300 ERP component was used for brain computer interface study [25–27], the ERP components in this study also can be used to build an affective brain computer interface. BCI also can be very useful for the elder people [28–31]. To improve BCI performance for daily-life use, advanced classification methods are required [32, 33].

Furthermore, the ability of perceptual organization in elder people and in patients with neuropsychiatric disorders, such as schizophrenia, ADHD, and ASD, could be systematically investigated to help exploit how the neural network in their brain should still work in spite of impairment in neural oscillation and neural plasticity and thus help build a more robust artificial neural network to all kinds of noise.

Data Availability

The experiment data are not available online for further research but available on reasonable request according to the policy of North China University of Science and Technology, Capital Medical University, and Tianjin University of Technology.

Ethical Approval

All procedures performed in studies involving human participants were in accordance with the ethical standards of ethics committee of Beijing Anding hospital, Capital Medical University (ZYLX201607). This ethics committee’s responsibilities, composition, function, operations, and records are fully compliant with ICH-GCP and related to regulation and law of China.

Conflicts of Interest

The authors declare that there are no conflicts of interest regarding the publication of this paper.

Authors' Contributions

Chenyang Liu and Sha Sha contributed equally in the study. Chenyang Liu, Zhiming Bian, and Xiaotian Wang recorded the original experiment data, analyzed the experiment data, and wrote the manuscript. Sha Sha and Xiaotian Wang completed the ethic files of this experiment. Lin Lu, Bin Hao, Lina Li, and Hongge Luo wrote parts of the manuscript. Xiujun Zhang, Changming Wang, and Chao Chen designed the experiment and revised the manuscript.

Acknowledgments

This work was financially supported by the National Natural Science Foundation of China (61806146), National Key R&D Program of China (2018YFC1314500), Anti Coronavirus Project of Tianjin City (20ZXGBSY00060), the Fundamental Research Funds for the Central Universities (JBF201903), Beijing Municipal Administration of Hospitals Incubating Program (PX2018063), Belt and Road International Scientific and Technological Cooperation Demonstration Project (17PTYPHZ20060), and Young and Middle-Aged Innovation Talents Cultivation Plan of Higher Institutions in Tianjin.

References

- [1] J. Wagemans, J. H. Elder, M. Kubovy et al., "A century of Gestalt psychology in visual perception: I. Perceptual grouping and figure-ground organization," *Psychological Bulletin*, vol. 138, no. 6, p. 1172, 2012.
- [2] J. G. Snodgrass and K. Feenan, "Priming effects in picture fragment completion: support for the perceptual closure hypothesis," *Journal of Experimental Psychology: General*, vol. 119, no. 3, p. 276, 1990.
- [3] D. D. Kurylo, R. Pasternak, G. Silipo et al., "Perceptual organization by proximity and similarity in schizophrenia," *Schizophrenia Research*, vol. 95, no. 1–3, pp. 205–214, 2007.
- [4] E. Freud, A. K. Robinson, and M. Behrmann, "More than action: the dorsal pathway contributes to the perception of 3-D structure," *Journal of Cognitive Neuroscience*, vol. 30, no. 7, pp. 1047–1058, 2018.
- [5] J. Hegdé, F. Fang, S. O. Murray, and D. Kersten, "Preferential responses to occluded objects in the human visual cortex," *Journal of Vision*, vol. 8, no. 4, p. 16, 2008.
- [6] R. Laycock, D. P. Crewther, and D. P. Crewther, "A role for the "magnocellular advantage" in visual impairments in neurodevelopmental and psychiatric disorders," *Neuroscience & Biobehavioral Reviews*, vol. 31, no. 3, pp. 363–376, 2007.
- [7] G. M. Doniger, J. J. Foxe, C. E. Schroeder, M. M. Murray, B. A. Higgins, and D. C. Javitt, "Visual perceptual learning in human object recognition areas: a repetition priming study using high-density electrical mapping," *NeuroImage*, vol. 13, no. 2, pp. 305–313, 2001.
- [8] S. Yantis, "Objects, attention, and perceptual experience," *Visual Attention*, vol. 8, pp. 187–214, 1998.
- [9] N. Darcy, P. Sterzer, and G. Hesselmann, "Category-selective processing in the two visual pathways as a function of stimulus degradation by noise," *Neuroimage*, vol. 188, pp. 785–793, 2018.
- [10] E. S. Kappenman and S. J. Luck, *The Oxford Handbook of Event-Related Potential Components*, Oxford University Press, Oxford, UK, 2011.
- [11] R. J. Itier and M. J. Taylor, "N170 or N1? Spatiotemporal differences between object and face processing using ERPs," *Cerebral Cortex*, vol. 14, no. 2, pp. 132–142, 2004.
- [12] C. Wang, J. Zhang, Z. Li, Li Yao, and X. Hu, "Combining features from ERP components in single-trial EEG for discriminating four-category visual objects," *Journal of Neural Engineering*, vol. 9, no. 5, Article ID 056013, 2012.
- [13] M. Eimer, "The face-specific N170 component reflects late stages in the structural encoding of faces," *Neuroreport*, vol. 11, no. 10, pp. 2319–2324, 2000.
- [14] J. Liu, A. Harris, and N. Kanwisher, "Stages of processing in face perception: an MEG study," *Nature Neuroscience*, vol. 5, no. 9, pp. 910–916, 2002.
- [15] C. Grützner, P. J. Uhlhaas, E. Genc, A. Kohler, W. Singer, and M. Wibral, "Neuroelectromagnetic correlates of perceptual closure processes," *Journal of Neuroscience*, vol. 30, no. 24, pp. 8342–8352, 2010.
- [16] D. T. Stuss, T. W. Picton, A. M. Cerri, E. E. Leech, and L. L. Stethem, "Perceptual closure and object identification: electrophysiological responses to incomplete pictures," *Brain and Cognition*, vol. 19, no. 2, pp. 253–266, 1992.
- [17] G. M. Doniger, J. J. Foxe, M. M. Murray et al., "Activation timecourse of ventral visual stream object-recognition areas: high density electrical mapping of perceptual closure processes," *Journal of Cognitive Neuroscience*, vol. 12, no. 4, pp. 615–621, 2000.
- [18] P. Sehatpour, S. Molholm, D. C. Javitt, and J. J. Foxe, "Spatiotemporal dynamics of human object recognition processing: an integrated high-density electrical mapping and functional imaging study of "closure" processes," *Neuroimage*, vol. 29, no. 2, pp. 605–618, 2005.
- [19] P. Zhao, S. Li, J. Zhao, C. M. Gaspar, and X. Weng, "Training by visual identification and writing leads to different visual word expertise N170 effects in preliterate Chinese children," *Developmental Cognitive Neuroscience*, vol. 15, pp. 106–116, 2015.
- [20] B. Jemel, M. Pisani, M. Calabria, M. Crommelinck, and R. Bruyer, "Is the N170 for faces cognitively penetrable? Evidence from repetition priming of Mooney faces of familiar and unfamiliar persons," *Cognitive Brain Research*, vol. 17, no. 2, p. 431, 2003.
- [21] R. Campbell, "Speechreading and the Bruce-Young model of face recognition: early findings and recent developments," *British Journal of Psychology*, vol. 102, no. 4, pp. 704–710, 2011.
- [22] G. Ganis, D. Smith, and H. E. Schendan, "The N170, not the P1, indexes the earliest time for categorical perception of faces, regardless of interstimulus variance," *Neuroimage*, vol. 62, no. 3, pp. 1563–1574, 2012.
- [23] J. J. Koenderink, "Gestalts as ecological templates," *Handbook of Perceptual Organization*, pp. 1046–1062, Oxford University Press, Oxford, UK, 2015.
- [24] R. Kimchi and B.-S. Hadad, "Influence of past experience on perceptual grouping," *Psychological Science*, vol. 13, no. 1, pp. 41–47, 2002.
- [25] J. Jin, Z. Chen, R. Xu, Y. Miao, X. Y. Wang, and T. P. Jung, "Developing a novel tactile P300 brain-computer interface with a cheeks-stim paradigm," *IEEE Transactions on Biomedical Engineering*, vol. 67, no. 9, pp. 2585–2593, 2020.
- [26] J. Jin, S. Li, I. Daly et al., "The study of generic model set for reducing calibration time in P300-based brain-computer interface," *IEEE Transactions on Neural Systems and Rehabilitation Engineering*, vol. 28, no. 1, pp. 3–12, 2020.
- [27] J. Yoon, J. Lee, and M. Whang, "Spatial and time domain feature of ERP speller system extracted via convolutional

- neural network,” *Computational Intelligence and Neuroscience*, vol. 2018, Article ID 6058065, 11 pages, 2018.
- [28] A. N. Belkacem, N. Jamil, J. A. Palmer, S. Ouhbi, and C. Chen, “Brain computer interfaces for improving the quality of life of older adults and elderly patients,” *Frontiers in Neuroscience*, vol. 14, 2020.
- [29] L. Shao, L. Zhang, A. N. Belkacem et al., “EEG-controlled wall-crawling cleaning robot using SSVEP-based brain-computer interface,” *Journal of Healthcare Engineering*, vol. 2020, Article ID 6968713, 11 pages, 2020.
- [30] C. Chen, P. Zhou, A. N. Belkacem et al., “Quadcopter robot control based on hybrid brain-computer interface system,” *Sensors and Materials*, vol. 32, no. 3, p. 991, 2020.
- [31] C. Chen, J. Zhang, A. N. Belkacem et al., “G-causality brain connectivity differences of finger movements between motor execution and motor imagery,” *Journal of Healthcare Engineering*, vol. 2019, Article ID 5068283, 12 pages, 2019.
- [32] C. Chen, X. Li, A. N. Belkacem et al., “The mixed Kernel function SVM-based point cloud classification,” *International Journal of Precision Engineering and Manufacturing*, vol. 20, no. 5, pp. 737–747, 2019.
- [33] C. Chen, P. Chen, A. N. Belkacem et al., “Neural activities classification of left and right finger gestures during motor execution and motor imagery,” *Brain-Computer Interfaces*, pp. 1–11, 2020.

Research Article

Effect of Emotion on Prospective Memory in Those of Different Age Groups

Jinhua Xian,^{1,2,3} Yan Wang ^{1,3} and Buxin Han ^{1,3}

¹Center on Aging Psychology, CAS Key Laboratory of Mental Health, Institute of Psychology, Beijing, China

²School of Education Science, Jiangsu Second Normal University, Nanjing, China

³Department of Psychology, University of Chinese Academy of Sciences, Beijing, China

Correspondence should be addressed to Yan Wang; wangyan@psych.ac.cn and Buxin Han; hanbx@psych.ac.cn

Received 12 May 2020; Revised 12 August 2020; Accepted 14 August 2020; Published 21 September 2020

Academic Editor: Abdelkader Nasreddine Belkacem

Copyright © 2020 Jinhua Xian et al. This is an open access article distributed under the Creative Commons Attribution License, which permits unrestricted use, distribution, and reproduction in any medium, provided the original work is properly cited.

The effect of emotion on prospective memory on those of different age groups and its neural mechanism in Chinese adults are still unclear. The present study investigated the effect of emotion on prospective memory during the encoding and retrieval phases in younger and older adults by using event-related potentials (ERPs). In the behavioral results, a shorter response time was found for positive prospective memory cues only in older group. In the ERP results, during the encoding phase, an increased late positive potential (LPP) was found for negative prospective memory cues in younger adults, while the amplitude of the LPP was marginally greater for positive prospective memory cues than for negative prospective memory cues in older adults. Correspondingly, younger adults showed an increased parietal positivity for negative prospective memory cues, while an elevated parietal positivity for positive prospective memory cues was found in older adults during the retrieval phase. This finding reflects the increased attentional processing of encoding and the more cognitive resources recruited to carry out a set of processes that are associated with the realization of delayed intentions when the prospective memory cues are emotional. The results reveal the effect of emotion on prospective memory during the encoding and retrieval phases in Chinese adults, modulated by aging, as shown by a positivity effect on older adults and a negativity bias in younger adults.

1. Introduction

Prospective memory (PM) refers to remembering to execute delayed intentions in the future [1, 2]. Difficulties in prospective memory adversely impact the quality of life of older adults who experience problems independently managing their instrumental activities of daily living, for example, forgetting to take medications [3].

In laboratory-based prospective memory tasks, participants need to perform an intended action after the recognition of an external cue in the environment [4]. Regarding the age-related decrease in executive functions and episodic memory [5], some studies have revealed a decline in prospective memory with increasing age [6–8]. However, when more salient cues are presented to participants, older adults perform better prospective memory [9, 10]. Additionally,

this age-related decline has not been found in naturalistic PM tasks, which has been labeled the “age-PM paradox” [11]. Regarding the reason for this paradox, the stimuli in naturalistic tasks usually seem to be emotional and may contain personal or social meanings. Therefore, emotional PM cues may enhance prospective memory performance in older adults through their emotional valence.

Considering the ecological validity of studies, researchers have been interested in the influence of emotional PM cues on prospective memory in younger and older adults, obtaining inconsistent results. Some studies have shown better prospective memory performance for positive and negative PM cues in both age groups [12]. However, other studies have shown that positive and negative PM cues improve prospective memory performance only for older adults [4, 13]. Moreover, in still other research, compared

with neutral PM cues, better prospective memory performance was found only for positive PM cues and not for negative PM cues in both younger and older adults [14]. Therefore, the effects of emotion on prospective memory among those of different age groups are still unclear.

Similarly, a growing body of the literature has revealed that emotion affects attention and retrospective memory [15–17]. Furthermore, different effects of emotion have been found in younger and older adults. According to socioemotional selectivity theory, older adults tend to remember more positive stimuli than negative stimuli, which is called the positivity effect. Because the future is limited for older adults, positive stimuli are considered more emotionally meaningful [18]. However, a negativity preference has been found in younger adults [19, 20]. Such effects of emotion on retrospective memory can be found not only in Western adults but also in Eastern adults (Korea and China) [21, 22]. Another research has compared visual attention to emotional and neutral facial expressions in Chinese adults by using eye-tracking techniques. The results revealed no attentional preferences for positive stimuli in older adults [23]. Therefore, the emotional enhancement effect between Western and Eastern adults is inconsistent. According to our current search of the literature, studies on the effects of emotion on prospective memory were all conducted in Western adults [4, 12, 13]. The effect of emotion on prospective memory in Chinese adults needs to be clarified.

To explain the mechanism of age-related effects of emotion on prospective memory, a few studies have used event-related potentials (ERPs) to demonstrate the different effects of emotion on prospective memory in younger and older adults. For example, one study examined the influence of emotional PM cues on prospective memory only in younger adults [24]. Another study further examined it in younger and older adults [25]. During encoding, the late positive potential (LPP), which is located in the central and parietal regions, begins approximately 300 ms after stimulus onset and lasts for 1000–2000 ms. It has been shown to reflect attentional processes [26]. Hering et al. [25] found an elevated LPP for emotional PM cues for both age groups, indicating an increased attentional processing of encoding emotional PM cues. Moreover, the elevated activity for unpleasant PM cues was found in younger adults. During retrieval, the N300, which appears between 300 and 500 ms after the onset of a prospective memory cue, is located in the occipital-parietal region. It is associated with the detection of PM cues [27]. Parietal positivity, which appears between 400 and 1200 ms after the onset of a prospective memory cue, is located in the parietal region. It reflects three components related to the detection of low probability targets (P3b), the recognition of prospective memory cues (parietal old-new effect), and the configuration of the prospective memory task set (prospective positivity). Parietal positivity represents a set of processes that are associated with the realization of delayed intentions [27]. Some studies have revealed that emotional materials modulate parietal positivity [24, 25]. Furthermore, Hering et al. [25] found increased activity of ERP components for pleasant PM cues in older adults.

The aim of this study is to investigate the effect of emotion on prospective memory among those of different age groups and its neural mechanism in Chinese adults. Following previous studies [22, 25], we expect that, given their general deficits in cognition, older adults' prospective memory performance will benefit from emotional PM cues. Moreover, we expect younger adults to have better prospective memory performance than older adults. Regarding the ERP results, we expect to find an effect of emotion on prospective memory during the encoding and retrieval phases, with a positivity effect on older adults and a negativity bias in younger adults. We expect elevated ERP activities (LPP and parietal positivity) for positive PM cues relative to negative and neutral PM cues in older adults, while we expect increased amplitudes of the LPP and parietal positivity for negative PM cues relative to positive and neutral PM cues in younger adults.

2. Methods

2.1. Participants. The experiment was conducted in accordance with the Declaration of Helsinki and was approved by the Ethics Committee of the Institute of Psychology, Chinese Academy of Sciences. All participants signed an informed consent form and received monetary compensation for their participation.

A total of 24 young adults from local universities (age $M = 20.9$, $SD = 1.9$; 18–24 years; 13 female) and 23 community-dwelling older adults were included in the experiment (age $M = 72.2$, $SD = 5.4$; 65–83 years; 10 female). All participants had normal or corrected-to-normal vision and no neurological or psychiatric pathologies. None of the participants reported having phobic fears (e.g., ophidiophobia) related to our study materials. Moreover, the Mini-Mental State Examination (MMSE) test for general cognitive status was used for all older adults. Only those with scores above 27 were allowed to participate in our test ($M = 28.61$, $SD = 1.03$) [28, 29].

The two groups were matched by the educational level, $t(45) = 0.07$, $p > 0.05$; self-rated general health, $t(45) = 1.74$, $p > 0.05$; self-rated mental health, $t(45) = 0.53$, $p > 0.05$; and initial mood (as measured before the experiment), $t(45) = 0.44$, $p > 0.05$ (Table 1). Their health, mental health, and initial mood were all measured on a 5-point rating scale, with 1 as very bad and 5 as very good.

2.2. Materials. This study used the paradigm of Cona et al. [24], the prospective memory task comprised an ongoing task with a prospective memory instruction, to remember to make a key-press when specific stimulus occurred [25]. All 213 pictures were selected from the International Affective Pictures System [30, 31]. The 1-back visual working memory paradigm was used as the ongoing task which included 51 positive ($M = 6.58$, $SD = 1.29$), 51 negative ($M = 3.63$, $SD = 1.31$), and 51 neutral pictures ($M = 5.00$, $SD = 1.34$). There were 20 positive PM cues ($M = 6.91$, $SD = 1.33$), 20 negative PM cues ($M = 3.08$, $SD = 1.26$), and 20 neutral PM cues ($M = 5.01$, $SD = 1.32$). The emotional arousal levels of

TABLE 1: Demographic data for younger and older adults.

Demographic data	Younger adults ($n = 24$)		Older adults ($n = 23$)	
	M	SD	M	SD
Age	20.9	1.9	72.2	5.4
Years of education	14.0	1.5	14.0	2.5
Self-rated health	4.1	0.6	3.8	0.6
Self-rated mental health	4.0	0.6	4.0	0.6
Initial mood	3.4	0.6	3.4	0.5

pictures were kept at the middle of the arousal scale (ongoing task stimuli: $M = 4.73$, $SD = 1.72$; prospective memory cues: $M = 4.73$, $SD = 1.83$) [4]. The emotional valence and arousal ratings were taken from the ratings that were natively assessed by Huang and Luo [31]. Each picture ($4.7^\circ \times 6.3^\circ$) was displayed in the center of a black screen.

2.3. Procedure. The whole experiment included three sessions, which varied based on the emotional valence of the PM cue (positive, negative, and neutral) [24]. Each session contained 5 blocks, and each block contained 73 ongoing stimuli and 8 PM cues (four PM cues were repeated) for a total of 405 stimuli with equal proportions of positive, negative, and neutral pictures. In each trial, a fixation cross randomly lasted 1200, 1400, or 1600 ms [24, 25], followed by the stimulus, which was displayed for a maximum of 3000 ms or until a response was made. All stimuli were presented in a fixed pseudorandomized order. In the course of the ongoing task, in each session, 96 one-back hits (24% of 405 stimuli) were presented. The PM cues were never one-back hits. The order of the three sessions was counter-balanced across participants [4, 24].

During the test, the participants were asked to carry out the 1-back visual working memory task, which involved deciding whether the picture occurring on the screen was the same (by pressing the “N” key) or different (by pressing the “M” key) from the picture occurring one trial before. After finishing 39 1-back visual working memory practice trials, the participants were informed that later in the session, they needed to complete two equally important tasks simultaneously. Then, the 1-back visual working memory instructions and prospective memory instructions were shown. The participants needed to remember to press the “V” key whenever predefined PM cues were displayed. They were asked to explain the task in their own words before they studied these PM cues. Before each block, four PM cues were displayed randomly one by one on the screen. When one session was finished, the participants were asked to identify the 20 PM cues among 20 distractors as a recognition task. E-Prime (V2; Psychology Software Tools, Inc., Pittsburgh, PA) was used to implement the experiment.

2.4. Electrophysiological Recording. EEG data were recorded from 64 Ag/AgCl electrodes mounted in an elastic cap (Neuroscan Inc.). The physical reference electrode was

approximately 2 cm posterior to the CZ, and the EEG data were rereferenced to the average of the left and right mastoids. Vertical and horizontal eye movements were recorded from electrodes placed below and beside the eyes. Electrode impedance was kept below 5 k Ω . Data were digitized at a sampling rate of 500 Hz, applying a filter bandwidth of 0.05–100 Hz.

2.5. Data Analysis. Data were analyzed with SPSS (SPSS, Inc., Chicago) for Windows. $p < 0.05$ was considered statistically significant. The prospective memory accuracy and response time for correct PM cue responses were analyzed by a mixed 2×3 ANOVA, with the age group (younger and older) as the between-subject factor and emotional valence of PM cues (positive, neutral, and negative) as the within-subject factor.

ERP epochs were extracted offline and included 200 ms of prestimulus activity and 1400 ms of poststimulus activity. The ERP data were digitally filtered with a 30 Hz low pass, and baseline correction was made using the prestimulus 200 ms interval. Epoch rejection was performed with a criterion of $\pm 100 \mu V$. ERPs were averaged for correct PM cue trials.

The selection of epochs and electrodes for the analyses was guided by previous studies [24, 32, 33]. The amplitude of the LPP was measured as the mean activity between 400 and 650 ms and included data from six electrodes: PO3, PO4, PO5, PO6, PO7, and PO8. For the analyses, the electrodes within one hemisphere were collapsed to obtain a mean activity. The amplitude of the N300 was measured as the mean activity between 270 and 350 ms and included six electrodes: PO3, PO4, PO5, PO6, PO7, and PO8. The amplitude of the parietal positivity was measured as the mean activity between 500 and 800 ms and included six electrodes: P1, P2, P3, P4, P5, and P6. The ANOVA factors included age group (younger and older), emotional valence of PM cues (positive, neutral, and negative) and hemisphere (left and right). Greenhouse–Geisser correction was used to compensate for sphericity violations. Simple effect analyses were conducted to explore the interaction effects.

3. Results

3.1. Behavioral Results. The prospective memory performance for younger and older adults is presented in Table 2. The analysis of prospective memory accuracy revealed significant main effects of emotional valence of PM cues and age group [$F(2, 90) = 4.89$, $p < 0.05$, $\eta^2 = 0.10$; $F(1, 45) = 13.79$, $p < 0.01$, $\eta^2 = 0.23$]. The interaction between age group and emotional valence of PM cues was significant [$F(2, 90) = 3.93$, $p < 0.05$, $\eta^2 = 0.08$], revealing higher accuracy for both positive and negative PM cues relative to neutral PM cues for older adults ($ps < 0.01$), but not for younger adults. The accuracy in prospective memory performance was lower for older adults than for younger adults in all conditions [$F(1, 45) = 6.49$, $p < 0.05$, $\eta^2 = 0.13$; $F(1, 45) = 12.81$, $p < 0.01$, $\eta^2 = 0.22$; $F(1, 45) = 4.52$, $p < 0.05$, $\eta^2 = 0.09$].

TABLE 2: Prospective memory performance for younger and older adults.

Age group	Emotional valence of PM cues		
	Positive	Neutral	Negative
<i>Accuracy (SD)</i>			
Younger adults ($n = 24$)	0.98 (0.04)	0.97 (0.06)	0.97 (0.05)
Older adults ($n = 23$)	0.94 (0.07)	0.88 (0.10)	0.94 (0.05)
<i>Response time (SD)</i>			
Younger adults ($n = 24$)	896.83 (111.41)	886.57 (108.02)	882.62 (99.49)
Older adults ($n = 23$)	1057.18 (158.64)	1123.66 (136.36)	1157.04 (216.14)

The analysis of prospective memory response time revealed the significant main effects of emotional valence of PM cues and age group [$F(2, 90) = 3.38, p < 0.05, \eta^2 = 0.07$; $F(1, 45) = 36.47, p < 0.001, \eta^2 = 0.45$]. The interaction between age group and emotional valence of PM cues was significant [$F(2, 90) = 6.04, p < 0.01, \eta^2 = 0.12$], revealing shorter response times for positive PM cues than for negative and neutral PM cues for older adults ($ps < 0.05$), but not for younger adults. The response times in prospective memory were longer for older adults than for younger adults in the three conditions [$F(1, 45) = 16.19, p < 0.001, \eta^2 = 0.27$; $F(1, 45) = 43.85, p < 0.001, \eta^2 = 0.49$; $F(1, 45) = 31.70, p < 0.001, \eta^2 = 0.41$].

3.2. ERP Results

3.2.1. Encoding Phase. LPP: the main effect of age group was significant [$F(1, 45) = 6.80, p < 0.05, \eta^2 = 0.13$], reflecting the increased amplitude for younger adults compared to older adults. The interaction between emotional valence of PM cues and age group was significant [$F(2, 90) = 4.44, p < 0.05, \eta^2 = 0.09$], reflecting the greater amplitude for negative PM cues than for neutral and positive PM cues in younger adults ($ps < 0.05$), and the marginally greater amplitude for positive PM cues than for negative PM cues in older adults ($p = 0.067$). The interaction between emotional valence of PM cues and hemisphere was significant [$F(2, 90) = 4.48, p < 0.05, \eta^2 = 0.09$], reflecting a greater amplitude for negative PM cues than for neutral PM cues in the left hemisphere ($p < 0.05$) (Figure 1, Table 3).

3.2.2. Retrieval Phase. N300: the main effect of emotional valence of PM cues was significant [$F(2, 90) = 7.27, p < 0.01, \eta^2 = 0.14$], reflecting the attenuated amplitude for positive and negative PM cues compared to neutral PM cues ($ps < 0.05$). The main effect of age group was significant [$F(1, 45) = 10.28, p < 0.01, \eta^2 = 0.19$], reflecting more expressed amplitude in older adults than in younger adults. The interaction between emotional valence of PM cues and hemisphere was significant [$F(2, 90) = 5.27, p < 0.01, \eta^2 = 0.11$], reflecting more expressed amplitude for neutral PM cues than for positive and negative PM cues in the left hemisphere ($ps < 0.01$), and more expressed amplitude for neutral PM cues than for positive PM cues in the right hemisphere ($p < 0.01$) (Figure 2, Table 3).

Parietal Positivity: the main effect of emotional valence of PM cues was significant [$F(2, 90) = 9.28, p < 0.001,$

$\eta^2 = 0.17$], reflecting an elevated parietal positivity for negative PM cues than for neutral PM cues ($p < 0.001$). The main effect of age group was significant [$F(1, 45) = 12.63, p < 0.01, \eta^2 = 0.22$], reflecting an elevated parietal positivity for younger adults than for older adults. The interaction between emotional valence of PM cues and age group was significant [$F(2, 90) = 10.32, p < 0.001, \eta^2 = 0.19$], reflecting an elevated parietal positivity for negative PM cues compared to neutral and positive PM cues in younger adults ($ps < 0.001$) and an elevated parietal positivity for positive PM cues compared to neutral PM cues in older adults ($p < 0.05$). The interaction between age group and hemisphere was significant [$F(1, 45) = 5.15, p < 0.05, \eta^2 = 0.10$], reflecting an elevated parietal positivity in the left hemisphere than in the right hemisphere in older adults ($p < 0.05$). The interaction between emotional valence of PM cues and hemisphere was significant [$F(2, 90) = 4.15, p < 0.05, \eta^2 = 0.08$], reflecting an elevated parietal positivity for negative PM cues compared to neutral and positive PM cues in the left hemisphere ($ps < 0.05$), and an elevated parietal positivity for negative and positive PM cues compared to neutral PM cues in the right hemisphere ($ps < 0.05$) (Figure 2, Table 3).

4. Discussion

The aim of our study was to investigate the effect of emotion on prospective memory in younger and older Chinese adults by using ERPs. Higher accuracy of prospective memory was found for positive/negative PM cues than for neutral PM cues in older adults, which was in line with previous studies showing that emotional PM cues could improve older adults' prospective memory performance through high salience [4, 13]. However, the accuracy of prospective memory in younger adults was generally high, and no effect of emotion was found, which is consistent with previous studies [4, 13, 24]. This may be because the task we used was easy. Due to the ERP approach of our study, we decided to use the easy prospective memory task to avoid having to reject too many epochs, especially for older adults [25]. Furthermore, the response times of prospective memory were significantly different only for older adults, with shorter response times for positive PM cues than for negative and neutral PM cues. This finding seems to indicate a positivity effect on prospective memory in older adults [18].

The ERP data also showed this effect of emotion on prospective memory in younger and older adults during the encoding and retrieval phases. As hypothesized, the emotional manipulation started from the encoding phase of

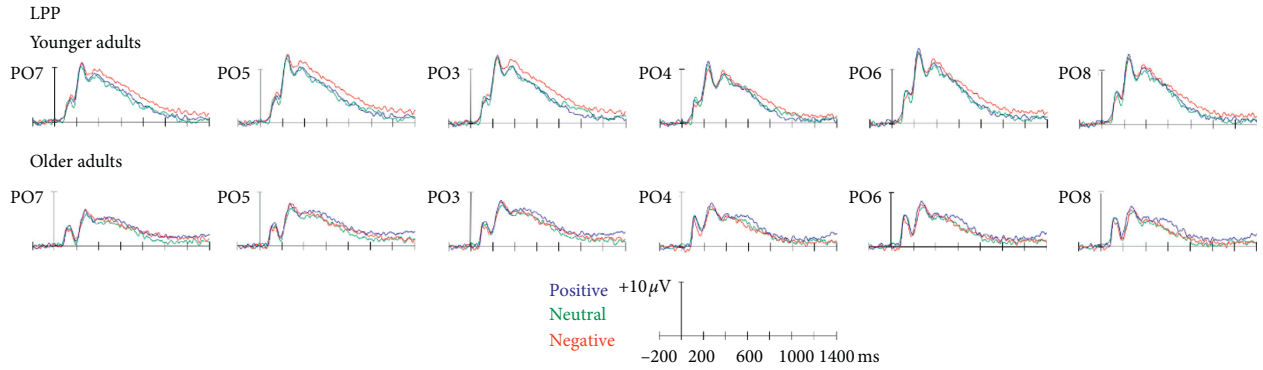


FIGURE 1: Encoding phase. Grand average event-related potentials at 6 electrodes used in the ANOVA, demonstrating the LPP (400–650 ms, PO3, PO4, PO5, PO6, PO7, and PO8) elicited by positive, neutral, and negative PM cues in younger and older adults.

TABLE 3: Grand average of LPP, N300, and parietal positivity.

Age group	Emotional valence of PM cues					
	Positive (L)	Neutral (L)	Negative (L)	Positive (R)	Neutral (R)	Negative (R)
<i>LPP (µV)</i>						
Younger adults (<i>n</i> = 24)	7.51 (4.06)	7.15 (3.35)	8.75 (3.83)	7.59 (5.29)	7.45 (4.27)	8.14 (5.84)
Older adults (<i>n</i> = 23)	5.84 (3.75)	4.92 (3.80)	5.15 (3.32)	5.28 (3.84)	4.33 (3.53)	4.33 (3.50)
<i>N300 (µV)</i>						
Younger adults (<i>n</i> = 24)	8.58 (4.20)	7.91 (4.29)	8.58 (4.61)	8.74 (4.70)	7.67 (5.11)	8.02 (5.07)
Older adults (<i>n</i> = 23)	5.15 (3.41)	4.41 (3.27)	5.35 (3.41)	4.70 (3.62)	4.38 (3.42)	4.61 (3.83)
<i>Parietal positivity (µV)</i>						
Younger adults (<i>n</i> = 24)	10.94 (4.25)	11.23 (4.54)	12.90 (3.98)	11.79 (5.09)	11.35 (5.45)	13.28 (5.16)
Older adults (<i>n</i> = 23)	8.81 (3.55)	7.73 (3.29)	8.37 (3.39)	8.14 (3.57)	6.97 (3.33)	7.26 (3.25)

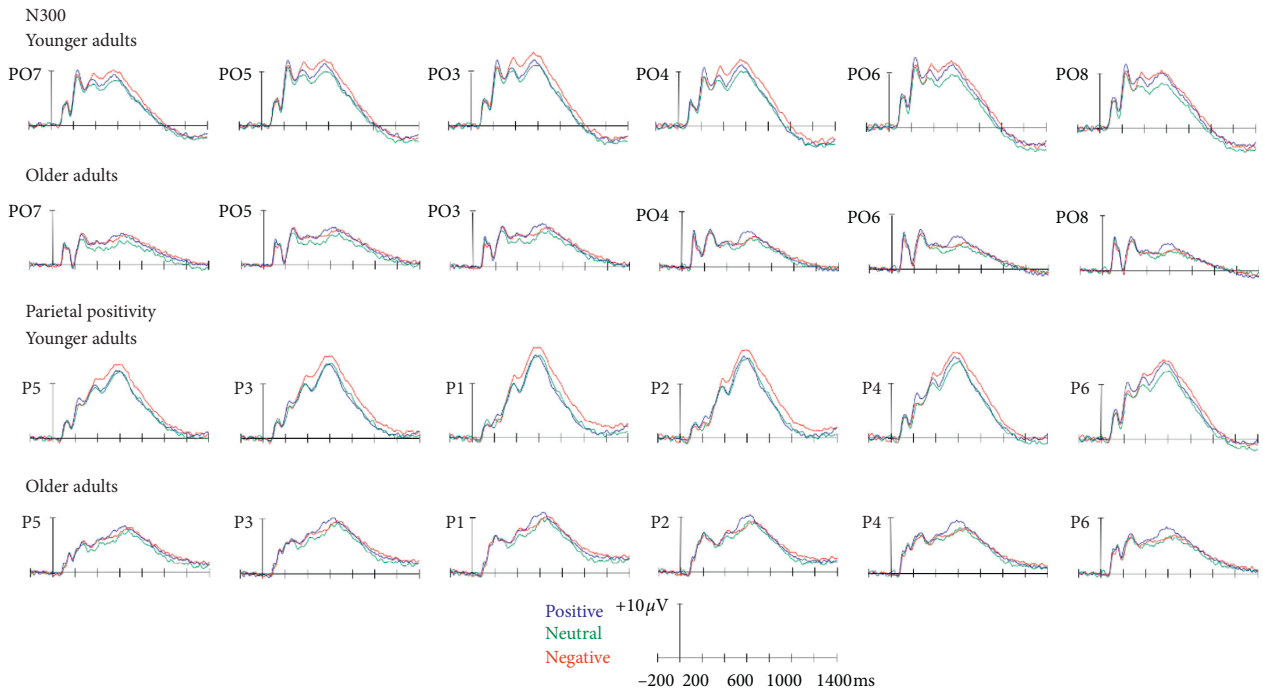


FIGURE 2: Retrieval phase. Grand average event-related potentials at 12 electrodes used in the ANOVA, demonstrating the N300 (270–350 ms, PO3, PO4, PO5, PO6, PO7, PO8) and parietal positivity (500–800 ms, P1, P2, P3, P4, P5, P6) elicited by positive, neutral, and negative PM cues in younger and older adults.

prospective memory. The interaction effect between aging and emotion was found, as evidenced by the increased LPP for negative PM cues compared to neutral and positive PM cues in younger adults, while the amplitude of the LPP was marginally greater for positive PM cues than for negative PM cues in older adults. Moreover, the results revealed a greater LPP for negative PM cues over left occipital-parietal regions. This finding may indicate that the emotional valence of PM cues affects the encoding of intention differently in the hemispheres. Given that the LPP is related to attention to emotional information [26, 34], our findings indicate that both age groups had increased attentional processing of encoding the emotional PM cues. Furthermore, the emotional materials differently affected younger and older adults' prospective memory, with a negativity bias in younger adults and a positivity effect on older adults.

Regarding the retrieval phase, attenuated amplitudes of the N300 were found for emotional PM cues compared to neutral PM cues in both age groups. As mentioned before, the N300 is associated with the detection of PM cues [27]. This finding reflects that emotional materials affected cue detection in both age groups. Moreover, consistent with a previous study [25], N300 was more expressed in older adults than in younger adults. However, another study revealed attenuated activity in older adults compared to younger adults [35]. Others did not find any age-related differences in the amplitude of the N300 [32, 36]. This may be because the stimuli in our study were emotional.

In addition, an interaction effect between aging and emotion on prospective memory was also found during the retrieval phase, as evidenced by an elevated parietal positivity for negative PM cues compared to neutral and positive PM cues in younger adults, while there was an increased parietal positivity for positive PM cues compared to neutral PM cues in older adults. The results also revealed an elevated parietal positivity for negative PM cues over left parietal regions, and an elevated parietal positivity for negative and positive PM cues over right parietal regions. This finding seems to indicate the effect of emotion on prospective memory across hemispheres during the retrieval phase. As mentioned before, parietal positivity reflects three components related to the detection of low probability targets (P3b), the recognition of prospective memory cues (parietal old-new effect), and the configuration of the prospective memory task set (prospective positivity) [27]. Our results demonstrated an increased allocation of resources to carry out a set of processes that are associated with the realization of delayed intentions when the PM cues were emotional [24]. This may be because emotional information receives increased processing due to motivational factors [26, 37].

Taken together, our study revealed an effect of emotion on prospective memory in Chinese adults, showing a positivity effect on older adults and a negativity bias in younger adults. Furthermore, this effect of emotion on prospective memory started from the encoding phase, increased the attentional processing of encoding emotional PM cues and then recruited more resources to accomplish the realization of delayed intentions during the retrieval phase. These findings in Chinese adults are similar to those of a study

based on Western participants [25], showing the similar effect of emotion on the encoding and retrieval phases of prospective memory in Chinese adults. According to socioemotional selectivity theory [18, 20], our results suggest that older adults serve the positivity effect as an emotion regulatory strategy. Following previous studies [19, 38], a preference for negativity was found in younger adults, which may be because they are prone to show the stronger evolutionary demands of negative (e.g., death) stimuli [39]. Moreover, our findings were inconsistent with those of Fung et al. [23], who found no attentional preferences for positive stimuli in older Chinese adults by comparing visual attention to emotional and neutral facial expressions. This may be because performing a prospective memory task requires several cognitive processes, not just attention. Therefore, an emotional enhancement effect on prospective memory could be found in Western and Eastern adults.

As stated before, the prospective memory task is critical for independent living, which is a particularly important issue for older adults. Our study investigated the effect of emotion on prospective memory in different age groups by using ERPs, showing older adults' prospective memory performance could be enhanced by manipulating the emotional valence of PM cues. Moreover, the emotional valence of PM cues affects prospective memory during the encoding and retrieval phases. These results could be useful to improve the quality of life by carrying out prospective memory training in older adults. Recently, brain computer interface is being one of the most popular technologies to improve the quality of life among older adults by enhancing or repairing their cognitive function and motor function [40]. Some studies have revealed the brain computer interface training system could improve memory and attention in older adults [41, 42]. Therefore, future research could use a brain computer interface application to train older adults to add personally positive emotions to PM cues when performing the prospective memory task, and the intervention should start from the encoding phase of prospective memory.

In terms of possible limitations, compared with ongoing task stimuli, the number of PM cues is relatively small, and the results need further verification. This is, however, limited by the characteristics of prospective memory and the more experimental conditions. Second, because the overall potential of the N300 in older adults was quite small, the age difference in the N300 also needs further verification. Future studies should use neuroimaging methods to discuss spatial sources for the effect of emotion on prospective memory in younger and older adults.

5. Conclusions

The present results suggest that the mechanism of prospective memory is affected by emotional materials in Chinese adults, as evidenced by an increased LPP and parietal positivity for emotional PM cues. This finding reflects the increased attentional processing of encoding and the more cognitive resources recruited to carry out a set of processes that are associated with the realization of delayed

intentions when the PM cues are emotional. Moreover, this effect of emotion on prospective memory during the encoding and retrieval phases in Chinese adults is modulated by aging, as shown by a positivity effect on older adults and a negativity bias in younger adults. These findings will be helpful in enhancing older adults' quality of life by improving their prospective memory performance.

Data Availability

The data used to support the findings of this study are available from the corresponding author upon request.

Conflicts of Interest

The authors declare that there are no conflicts of interest regarding the publication of this paper.

Authors' Contributions

Jinhua Xian and Yan Wang contributed equally to this work.

Acknowledgments

This research was supported by the National Natural Science Foundation of China (nos. 31771247 and 31100810) and Beijing Municipal Science and Tech Commission (Grant/Award nos. Z171100000117004 and Z161100002616013).

References

- [1] G. O. Einstein, M. A. McDaniel, R. E. Smith, and P. Shaw, "Habitual prospective memory and aging: remembering intentions and forgetting actions," *Psychological Science*, vol. 9, no. 4, pp. 284–288, 1998.
- [2] M. A. McDaniel and G. O. Einstein, "Strategic and automatic processes in prospective memory retrieval: a multiprocess framework," *Applied Cognitive Psychology*, vol. 14, no. 7, pp. S127–S144, 2000.
- [3] S. P. Woods, M. Weinborn, A. Velnoweth, A. Rooney, and R. S. Bucks, "Memory for intentions is uniquely associated with instrumental activities of daily living in healthy older adults," *Journal of the International Neuropsychological Society*, vol. 18, no. 1, pp. 134–138, 2012.
- [4] M. Altgassen, L. H. Phillips, J. D. Henry, P. G. Rendell, and M. Kliegel, "Emotional target cues eliminate age differences in prospective memory," *Quarterly Journal of Experimental Psychology*, vol. 63, no. 6, pp. 1057–1064, 2010.
- [5] D. C. Park and P. Reuter-Lorenz, "The adaptive brain: aging and neurocognitive scaffolding," *Annual Review of Psychology*, vol. 60, no. 1, p. 173, 2009.
- [6] R. West and F. I. M. Craik, "Age-related decline in prospective memory: the roles of cue accessibility and cue sensitivity," *Psychology and Aging*, vol. 14, no. 2, p. 264, 1999.
- [7] P. S. Bisiacchi, V. Tarantino, and A. Ciccola, "Aging and prospective memory: the role of working memory and monitoring processes," *Aging Clinical and Experimental Research*, vol. 20, no. 6, pp. 569–577, 2008.
- [8] E. A. Maylor and R. H. Logie, "A large-scale comparison of prospective and retrospective memory development from childhood to middle age," *Quarterly Journal of Experimental Psychology*, vol. 63, no. 3, pp. 442–451, 2010.
- [9] G. O. Einstein, M. A. McDaniel, M. Manzi, B. Cochran, and M. Baker, "Prospective memory and aging: forgetting intentions over short delays," *Psychology and Aging*, vol. 15, no. 4, pp. 671–683, 2000.
- [10] K. E. Cherry, R. C. Martin, S. S. Simmons-D'Gerolamo, J. B. Pinkston, A. Griffing, and W. Drew Gouvier, "Prospective remembering in younger and older adults: role of the prospective cue," *Memory*, vol. 9, no. 3, pp. 177–193, 2001.
- [11] P. G. Rendell and F. I. M. Craik, "Virtual week and actual week: age-related differences in prospective memory," *Applied Cognitive Psychology*, vol. 14, no. 7, pp. S43–S62, 2000.
- [12] C. P. May, M. Manning, G. O. Einstein, L. Becker, and M. Owens, "The best of both worlds: emotional cues improve prospective memory execution and reduce repetition errors," *Aging, Neuropsychology, and Cognition*, vol. 22, no. 3, pp. 357–375, 2015.
- [13] K. M. Schnitzspahn, S. S. Horn, U. J. Bayen, and M. Kliegel, "Age effects in emotional prospective memory: cue valence differentially affects the prospective and retrospective component," *Psychology and Aging*, vol. 27, no. 2, pp. 498–509, 2012.
- [14] P. G. Rendell, L. H. Phillips, J. D. Henry et al., "Prospective memory, emotional valence and ageing," *Cognition & Emotion*, vol. 25, no. 5, pp. 916–925, 2011.
- [15] E. A. Phelps, S. Ling, and M. Carrasco, "Emotion facilitates perception and potentiates the perceptual benefits of attention," *Psychological Science*, vol. 17, no. 4, pp. 292–299, 2006.
- [16] E. A. Kensinger, "Negative emotion enhances memory accuracy: behavioral and neuroimaging evidence," *Current Directions in Psychological Science*, vol. 16, no. 4, pp. 213–218, 2007.
- [17] D. Talmi, U. Schimack, T. Paterson, and M. Moscovitch, "The role of attention and relatedness in emotionally enhanced memory," *Emotion*, vol. 7, no. 1, pp. 89–102, 2007.
- [18] M. Mather and L. L. Carstensen, "Aging and motivated cognition: the positivity effect in attention and memory," *Trends in Cognitive Sciences*, vol. 9, no. 10, pp. 496–502, 2005.
- [19] S. J. E. Langeslag and J. W. van Strien, "Aging and emotional memory: the co-occurrence of neurophysiological and behavioral positivity effects," *Emotion*, vol. 9, no. 3, pp. 369–377, 2009.
- [20] D. M. Isaacowitz and F. Blanchard-Fields, "Linking process and outcome in the study of emotion and aging," *Perspectives on Psychological Science*, vol. 7, no. 1, p. 3, 2012.
- [21] Y. Kwon, S. Scheibe, G. R. Samanez-Larkin, J. L. Tsai, and L. L. Carstensen, "Replicating the positivity effect in picture memory in Koreans: evidence for cross-cultural generalizability," *Psychology and Aging*, vol. 24, no. 3, pp. 748–754, 2009.
- [22] C. Chung and Z. Lin, "A cross-cultural examination of the positivity effect in memory: United States vs. China," *The International Journal of Aging and Human Development*, vol. 75, no. 1, pp. 31–44, 2012.
- [23] H. H. Fung, D. M. Isaacowitz, A. Y. Lu, H. A. Wadlinger, D. Goren, and H. R. Wilson, "Age-related positivity enhancement is not universal: older Chinese look away from positive stimuli," *Psychology and Aging*, vol. 23, no. 2, pp. 440–446, 2008.
- [24] G. Cona, M. Kliegel, and P. S. Bisiacchi, "Differential effects of emotional cues on components of prospective memory: an ERP study," *Frontiers in Human Neuroscience*, vol. 9, p. 10, 2015.
- [25] A. Hering, M. Kliegel, P. S. Bisiacchi, and G. Cona, "The influence of emotional material on encoding and retrieving

- intentions: an ERP study in younger and older adults,” *Frontiers in Psychology*, vol. 9, p. 114, 2018.
- [26] A. Weinberg and G. Hajcak, “Beyond good and evil: the time-course of neural activity elicited by specific picture content,” *Emotion*, vol. 10, no. 6, pp. 767–782, 2010.
- [27] R. West, “The temporal dynamics of prospective memory: a review of the ERP and prospective memory literature,” *Neuropsychologia*, vol. 49, no. 8, pp. 2233–2245, 2011.
- [28] Z. S. Nasreddine, N. A. Phillips, V. R. Bédirian et al., “The montreal cognitive assessment, MoCA: a brief screening tool for mild cognitive impairment,” *Journal of the American Geriatrics Society*, vol. 53, no. 4, pp. 695–699, 2005.
- [29] J. A. Lonie, K. M. Tierney, and K. P. Ebmeier, “Screening for mild cognitive impairment: a systematic review,” *International Journal of Geriatric Psychiatry*, vol. 24, no. 9, pp. 902–915, 2009.
- [30] P. J. Lang, M. M. Bradley, and B. N. Cuthbert, “International affective picture system (IAPS): instruction manual and affective ratings,” Technical report A5, University of Florida, Gainesville, FL, USA, 2001.
- [31] Y. X. Huang and Y. J. Luo, “Native assessment of international affective picture system,” *International Journal of Psychology*, vol. 39, no. 5-6, p. 131, 2004.
- [32] F. Mattli, J. Zöllig, and R. West, “Age-related differences in the temporal dynamics of prospective memory retrieval: a lifespan approach,” *Neuropsychologia*, vol. 49, no. 12, pp. 3494–3504, 2011.
- [33] N. S. Rose, P. G. Rendell, A. Hering, M. Kliegel, G. M. Bidelman, and F. I. M. Craik, “Cognitive and neural plasticity in older adults’ prospective memory following training with the virtual week computer game,” *Frontiers in Human Neuroscience*, vol. 9, p. 13, 2015.
- [34] D. Foti, G. Hajcak, and J. Dien, “Differentiating neural responses to emotional pictures: evidence from temporal-spatial PCA,” *Psychophysiology*, vol. 46, no. 3, pp. 521–530, 2009.
- [35] R. West, R. W. Herndon, and E. Covell, “Neural correlates of age-related declines in the formation and realization of delayed intentions,” *Psychology and Aging*, vol. 18, no. 3, pp. 461–473, 2003.
- [36] J. Zöllig, R. West, M. Martin, M. Altgassen, U. Lemke, and M. Kliegel, “Neural correlates of prospective memory across the lifespan,” *Neuropsychologia*, vol. 45, no. 14, pp. 3299–3314, 2007.
- [37] D. Sabatinelli, M. M. Bradley, J. R. Fitzsimmons, and P. J. Lang, “Parallel amygdala and inferotemporal activation reflect emotional intensity and fear relevance,” *Neuroimage*, vol. 24, no. 4, pp. 1265–1270, 2005.
- [38] E. A. Kensinger, “Age differences in memory for arousing and nonarousing emotional words,” *Journals of Gerontology Series B-Psychological Sciences and Social Sciences*, vol. 63, no. 1, pp. 13–18, 2008.
- [39] P. Rozin and E. B. Royzman, “Negativity bias, negativity dominance, and contagion,” *Personality and Social Psychology Review*, vol. 5, no. 4, pp. 296–320, 2001.
- [40] A. N. Belkacem, N. Jamil, J. A. Palmer, S. Ouhbi, and C. Chen, “Brain computer interfaces for improving the quality of life of older adults and elderly patients,” *Frontiers in Neuroence*, vol. 14, p. 692, 2020.
- [41] J. Gomez-Pilar, R. Corralejo, L. F. Nicolas-Alonso, D. Álvarez, and R. Hornero, “Neurofeedback training with a motor imagery-based BCI: neurocognitive improvements and EEG changes in the elderly,” *Medical & Biological Engineering & Computing*, vol. 54, no. 11, pp. 1655–1666, 2016.
- [42] T. S. Lee, S. J. A. Goh, S. Y. Quek et al., “A brain-computer interface based cognitive training system for healthy elderly: a randomized control pilot study for usability and preliminary efficacy,” *PLoS One*, vol. 8, no. 11, p. 8, 2013.

Research Article

Towards an Accessible Use of a Brain-Computer Interfaces-Based Home Care System through a Smartphone

Koun-Tem Sun, Kai-Lung Hsieh , and Syuan-Rong Syu

Department of Information and Learning Technology, National University of Tainan, 33, Sec. 2, Shu-Lin St., Tainan 70005, Taiwan

Correspondence should be addressed to Kai-Lung Hsieh; klhsieh@gmail.com

Received 31 January 2020; Revised 29 June 2020; Accepted 31 July 2020; Published 28 August 2020

Academic Editor: Yasuharu Koike

Copyright © 2020 Koun-Tem Sun et al. This is an open access article distributed under the Creative Commons Attribution License, which permits unrestricted use, distribution, and reproduction in any medium, provided the original work is properly cited.

This study proposes a home care system (HCS) based on a brain-computer interface (BCI) with a smartphone. The HCS provides daily help to motor-disabled people when a caregiver is not present. The aim of the study is two-fold: (1) to develop a BCI-based home care system to help end-users control their household appliances, and (2) to assess whether the architecture of the HCS is easy for motor-disabled people to use. A motion-strip is used to evoke event-related potentials (ERPs) in the brain of the user, and the system immediately processes these potentials to decode the user's intentions. The system, then, translates these intentions into application commands and sends them via Bluetooth to the user's smartphone to make an emergency call or to execute the corresponding app to emit an infrared (IR) signal to control a household appliance. Fifteen healthy and seven motor-disabled subjects (including the one with ALS) participated in the experiment. The average online accuracy was 81.8% and 78.1%, respectively. Using component N2P3 to discriminate targets from nontargets can increase the efficiency of the system. Results showed that the system allows end-users to use smartphone apps as long as they are using their brain waves. More important, only one electrode O1 is required to measure EEG signals, giving the system good practical usability. The HCS can, thus, improve the autonomy and self-reliance of its end-users.

1. Introduction

Individuals with locked-in syndrome (LIS), amyotrophic lateral sclerosis (ALS), spinal cord injury, and congenital or accidental nerve injury may experience serious obstacles in developing motor skills in their limbs, yet most of them have normal brain function [1–3]. When they cannot speak clearly, the demands they are trying to articulate cannot be understood [1, 4]. Because of the gradual loss of mobility, such individuals may need a 24-hour personal caregiver [5, 6]. A brain-computer interface (BCI) system would be practical for this population. A BCI can permit them to control external devices and enable them to perform some tasks by themselves [7–10].

Locked-in syndrome (LIS) is a condition in which a patient is aware but cannot communicate verbally or move because of complete paralysis of nearly all voluntary muscles in the body except for vertical eye

movements and blinking [11]. It is caused by damage to specific portions of the lower brain and brainstem, with no harm to the upper brain. Thus, such patients are fully awake and alert and are aware not only of their abnormal situation but also, and to a full extent, of their surroundings. There are three categories of LIS: classic LIS, incomplete LIS, and total LIS [4, 12]. In total LIS, even the eyes are paralyzed [13].

ALS is a relatively rare neurodegenerative disorder characterized by gradual loss of both upper and lower motor neurons in the brain, brainstem, and spinal cord [14]. ALS usually starts at around the age of 60 and, in inherited cases, around the age of 50 [2]. The average survival from onset to death is 3 to 5 years [15]. Most people with classic LIS, incomplete LIS, or ALS are free to move their eyeballs. If the brain activity of these people is not affected and their eyeballs are free to move, then a BCI system can help them communicate with others [7, 16–18].

A BCI system is a system that connects the human brain and its surroundings. It enables people to communicate with others using their brain waves without muscle movement [9, 17, 19–22]. There are different technologies for measuring brain activity. Among these, electroencephalographs (EEG) are the most frequently used because of their many advantages, including lower cost, better portability, and higher temporal resolution [23]. Over the past two decades, there has been a dramatic proliferation of research concerned with a noninvasive/stimulus-driven/visual BCI (vBCI) system [23–25]. Such BCI systems obtain the user's brain potentials on the surface of the cortex via an EEG [7, 21, 24].

There are four different types of EEG-based BCI modalities: event-related desynchronization/synchronization (ERD/ERS), steady-state visual evoked potentials (SSVEP), event-related potentials (ERP), and slow cortical potentials (SCP). Among these, ERP and SSVEP-based BCIs are more practical than others because they support large numbers of output commands and need little training time [7].

Table 1 shows recent studies of BCI-based systems implemented in real-world scenarios.

Table 1 shows that applications of BCI systems include speller, robot control, healthcare, environmental control, and social network use. The graphic user interface (GUI) is roughly divided into the row-column (RC) paradigm, as with the speller system, and the direction paradigm, as with robot control. There are two broad categories of stimulation for ERP: flashing LED-light and motion-onset. Most studies use more than six electrodes to collect the user's brainwaves, and their average accuracy is good. However, only healthy subjects participated in these experiments. The home care system (HCS) in this study is an environmental control system. The arrangement of the options in the GUI is derived from the row-column paradigm, but its stimulation is motion-onset [25]. Based on our previous work [8], this GUI with motion-onset stimulation can significantly improve the target detection performance to achieve higher accuracy and shorten the stimulation time, in contrast to the stimulus intensification pattern used in the conventional P300-based system.

Event-related potentials (ERP), proposed by Sutton in 1965, are a series of potentials of a user's brain waves elicited by external stimuli. These potentials are time-dependent voltage fluctuations triggered by specific physical or psychological events [27]. An ERP-based vBCI system usually flashes a specific stimulus (such as text, pictures, or a flickering strip) on the graphic user interface (GUI) many times, and the user's brain waves respond to each stimulus [7, 9, 10, 28, 29]. An ERP-based vBCI system uses an EEG to obtain the users' brain rhythm and learn the basics of their brain system [30]. The EEG device amplifies and records the potentials of the user's brain waves [31, 32] and sends these signals to the vBCI system to classify and to interpret the specific features of the ERP components. Significant ERPs may, then, be extracted from the EEG by filtering and signal averaging methods [33]. In the final step, the BCI system converts these signals into instructions and outputs them [25, 34]. In this study, we use Ag/AgCl electrodes to record

the weak potential of brain waves on the user's scalp. The system uses a 0.3~15 Hz band-pass filter to filter the signals [35]. After multiple stimulations, the EEG signals are, then, superimposed and averaged to form the results of the ERP for each trial [8].

ERP research provides an impersonal and workable discrimination method for a BCI system [36, 37]. This study adopts an ERP paradigm that combines oddball presentation and motion onset. This paradigm primarily exploits two ERP components, N200 and P300, instead of only P300 [25]. N200 (N2) and P300 (P3) are brain responses to specific cognitive tasks, as shown in Figure 1. A P300 peak in an ERP is a higher positive deflection of an event-related potential component and usually occurs around 300 ms after the target stimulus presentation [21, 28, 35, 39–42]. Conversely, an N200 trough is the lower negative deflection of event-related potential, and usually occurs nearly 200 ms after the target stimulus presentation [25, 39]. The N200 and P300 waves only occur if the subject is actively engaged in the task of detecting the targets [40, 43] and the waveform of the component P300 (N200) of the target stimulus is higher (lower) than that of the nontarget stimuli [10]. The amplitude of P300 (N200) depends on the improbability of the target stimulus. The latency of ERP components varies with the difficulty of discriminating between the target and nontarget stimuli [22, 35].

However, conventional BCIs have not become practical because they lack high accuracy and reliability and have low information transfer rate and user acceptability [44]. First, in a visual BCI system, although gaze is not a requirement [45], the presence of the gaze in a visual ERP-based BCI improves its performance. Thus, in the system, we prefer that the user stares at the GUI to select an option. If the users have lost their sight or cannot stare at the screen, it is more appropriate to use an auditory BCI [46] or the BCI system presented in the work of Thurlings et al. [45].

A flashing stimulation paradigm such as that the row-col paradigm [9, 22] easily leads to user eye fatigue. The motion-strip stimulation paradigm is more comfortable for the user's eyes because of the low luminance and low contrast required by the stimuli [25]. Furthermore, the identification rate and the accuracy of the motion-strip stimulation paradigm are better than that of the flashing stimulation paradigm [8, 25].

Second, the fewer the electrodes are, the more comfortable the user is. Based on the previous research results of our laboratory, when the user stares at the GUI of a vBCI system, the ERPs acquired from electrode O1 or O2 in the occipital area of the skull (the visual region of the human brain) can achieve a statistically significant difference between the target and nontarget stimuli [8, 26]. Thus, a system using only one electrode can obtain outstanding accuracy.

Third, the waveform and the amplitude of ERP (N200 and P300) of the target stimulus vary from person to person. Thus, the BCI system needs to use a more stable ERP component to increase its accuracy. Based on the results of our previous experiments, the accuracy from using component N2P3 is significantly higher and steadier than the accuracy obtained using any other ERP component. Herein,

TABLE 1: Recent studies of BCI-based systems implemented in real-world scenarios.

Study	Main function	Stimulation modality	Electrodes	Subjects	Accuracy (%)	Bit rate
[25]	Speller	ERP: motion-onset-P300	Fz, Cz, Pz, Oz, P7, and P8	10 CS	N2-91.5, P3-72.4	N2-15.91, P3-12.84
[8]	Chinese speller	ERP: motion-onset-N2P3	F3, F4, C3, C4, P3, P4, O1, O2, Fz, Cz, and Pz	7 CS	80% using O1 only	27.8
[9]	Speller	ERP + SSVER RC paradigm	Cz, Pz, P3, P4, O1, O2, POz, PO7, and PO8	14 CS	After 8 trials: >95	53.6
[26]	Robot control	ERP: motion-onset-N2P3	O1	12 CS	80% using O1 only	353.33 s for 26.33 comm.
[7]	Robot control	EOG + EEG: flash on eight direct	Fz, Cz, Pz, Oz, P7, P3, P4, and P8	13 CS	After 5 trials: >99.04	—
[21]	Speller	ERP + SSVER RC paradigm	Fz, Cz, Pz, P3, P4, PO7, PO8, POz, Oz, O1, and O2	13 CS	95.18 for hybrid	50.41 for hybrid
[23]	Healthcare BCI syst.	ERP + SSVER RC paradigm	Cz, Pz, O1, O2, and Oz	5 CS	ERP: 95.5SSVER: 93	—
[10]	Environmental control	ERP-P300RC paradigm	Fz, FCz, Cz, CPz, P7, P3, Pz, P4, P8, O1, Oz, and O2	6 MDS, 2 CS	89.6	734.3 s for 30 comm.
[22]	Use of social networks	ERP-P300 RC paradigm	Fz, Cz, Pz, P3, P4, PO7, PO8, and Oz	18 MDS, 10 CS	80.6 for MDS, 92.3 for CS	1.47 OCM for MDS, 2.06 for CS

RC paradigm: the row-col paradigm; “N” indicates the number of subjects; “CS” stands for control abled subjects; “N2” stands for N200 evoked potential; “P3” stands for P300 evoked potential.

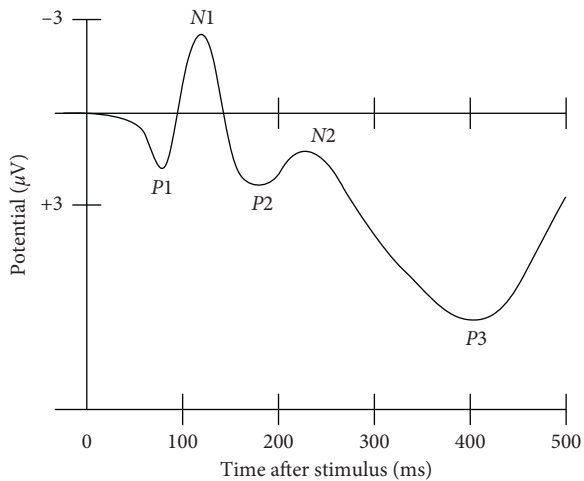


FIGURE 1: A waveform showing several ERP components, including the N200 (labelled N2) and P300 (labelled P3). Note that the ERP is plotted with negative voltages at the top, a common, but not universal, practice in ERP research [38].

the N2P3 value of one option is the potential value (μV) of its P300 minus that of its N200 [8, 26]. Thus, the system uses the N2P3 component online to expedite the experimental procedures. Moreover, users receive better real-time feedback. Yet, to test and verify that N2P3 is the most useful component for interpretation, we compared the ERP components (N200, P300, and N2P3) of the target option with those of nontarget options in an offline analysis.

According to the work of Huggins et al., if caregivers are absent, BCI users may want to perform tasks such as controlling the room temperature and lights or make emergency calls by themselves and feel more comfortable than they would using text communication [47]. However, such BCI systems are rare.

Because of the popularity of smartphones, several studies have applied BCI systems to control smartphones. Most of these studies explore merely dialing numbers [48, 49], accepting incoming calls [50], or calling contacts [49, 51]. Martínez-Cagigal et al. present a BCI system for controlling the social networking features of a smartphone [22]. Jayabhavani et al. pioneered a system which allows users to control wheelchairs, an approach that relates more closely to the topic of this paper [52].

This study develops a BCI-based home care system (HCS). The HCS allows the end-users to control their household appliances by themselves. Thus, end-users can reduce their dependence on the caregivers. In this study, there are two functions of a smartphone: to make an emergency call and to act as an adjustable infrared- (IR-) band remote controller. Thus, the user’s smartphone must have or install an IR transmitter first. The corresponding app in the user’s smartphone can, then, emit an IR signal to control the required household appliance.

Today, short-distance remote controls for devices in daily life make wide use of IR [53–55]. IR, sometimes called infrared light, is an electromagnetic radiation (EMR) with wavelengths longer than those of visible light. IR cannot pass through a wall. Thus, in the adjoining room, remote controls using the same IR wavelength do not interfere with each other. By contrast, in a chamber, the IR wavelength of all appliances should be distinct from each other. Therefore, each household appliance has a dedicated remote control.

Improving the personal autonomy and the self-reliance of end-users and giving them the ability to communicate with others are two of the primary missions of the HCS. Since the assessment of BCI systems with end-users is essential for ensuring a fair evaluation [22], we invited disabled users to test the

system to learn whether the HCS is useful for motor-disabled people. Motor-disabled people have participated in some tests of BCI systems. The BCI system allows such individuals to perform actions with their brainwave signals [10, 22, 56]. For example, these patients can now spell out words with a BCI-speller [8, 16, 25, 57]. However, if the caregiver does not immediately notice the text on the screen, it will not be possible to help the patient do what they want. If such patients can control their household appliances through a vBCI system, they can do small activities on their own and reduce their reliance on caregivers. Thus, in this study, we propose a BCI-based home care system (HCS). We hope that the HCS can help motor-disabled people improve their personal autonomy and self-reliance.

2. Materials and Methods

2.1. Subjects. The subjects used in this study were 15 healthy people (six females, aged 19–55), six motor-disabled people, and one man with ALS (SE7). Table 2 summarizes the clinical data of the motor-disabled participants. All subjects were volunteers and had normal vision or vision corrected to normal, and they were without mental illness, head injuries, or drug treatments. No subjects underwent a training phase before the experimental procedure. Only subject E3 has experience in using an ERP-based visual BCI system. All subjects signed informed consent before participation in the study, which was approved by the National Cheng Kung University Human Research Ethics Committee. If a subject decided to quit during the experiment, we ended the experiment and deleted their data.

2.2. The vBCI-Based Home Care System (HCS)

2.2.1. The Prototype of the HCS. In this study, the BCI module in the home care system is derived from the BCI module of our Chinese spelling system [8]. Figure 2 shows the design of the essential process of the vBCI-based home care system. The prototype includes three parts: signal acquisition, signal processing, and signal application.

The proposed vBCI module of the prototype, such as other human-machine interface systems for communication or control, comprises input/output processes. The BCI module requires the input of signals gained from the user's brain waves through an EEG. The EEG device in this system, which contains 32 channels, uses a typical noninvasive method [24]. The positions of electrodes accorded with the international 10–20 location system [58], and the vBCI module obtained signals from electrode O1 [8].

In all GUIs of the BCI module, there are several graphic options arranged in sequence on each GUI, as shown in Figure 3. Each option has a box, with a motion-strip as the visual stimulus, under it [25]. All motion-strips move from right to left to evoke ERPs, and the onset time of all motion-strips on the same GUI are inconsistent with each other [8]. Following the recommendations of the U.S. Department of Labor Occupational Safety and Health Administration, we let users sit 60–80 cm away from the screen to reduce fatigue and eye strain [59]. The subject has to stare at the motion-strip of their choice during each trial. At the same time, the vBCI module obtains

signals from the user's brain waves to gain the available ERPs components, including N200 and P300 [8, 60, 61]. Thus, the vBCI module can distinguish what the user wants and, then, output the control signal to the user's smartphone.

The vBCI module outputs communication signals to the user's smartphone via Arduino and the HC-5 Bluetooth module. The communication signals first execute an app on the user's smartphone designated ICAI1101, an application developed by the author. ICAI1101, then, triggers the corresponding app to make an emergency call or to send an IR signal to control a household appliance.

2.2.2. Brain-Computer Interface for Stimulation. In this study, there are four GUIs in the BCI module, including the main screen, TV control screen, air conditioner control screen, and TV channel shift screen, as shown in Figure 3. Blue strips in the white box below each option on the GUIs of Figure 3 represent the motion-strip stimuli. In a single trial, all stimulus strips on the GUI move quickly from right to left six times. The onset time of the stimulus strips on the same GUI are asynchronous with respect to each other. Thus, the vBCI module reacts more rapidly and achieves higher accuracy [8]. Moreover, there is some complexity in the interface in most vBCI systems [22, 56, 60]. In this study, except for the TV channel shift screen, there are only four or six options on the other three screens to provide a faster, more intuitive, and friendlier interface for end-users.

2.2.3. Smartphone Interface Design for Caregivers. When the BCI module identifies the option the user wants, it will send a command signal to the user's smartphone to control ICAI1101. Then, the GUI of the user's smartphone changes based on the user's selection. If there is a caregiver around the user, they can follow-up on the user's demands and help the user by using the GUI of the user's smartphone directly. Figure 4 shows the app interfaces on the user's smartphone.

2.2.4. Stimulation Trials. In this study, a stimulus is defined as the motion-strip of an option moving from right to left once, about 200 ms, as shown in Figure 3. The interval between two stimulus onsets in the same option was 200 ms. The stimulus onset asynchrony (SOA) between the two options was 50–100 ms, depending on the number of options on the same GUI. SOA prevents stimuli from interfering with each other and shortens all stimulation time. In each trial, each option performs six stimuli in a regular sequence. Figure 5 shows the stimulation sequence in a trial on the main screen. Thus, the time of 1 trial is roughly 3.0–3.8 sec (including roughly 500 ms for the system response), and the system can output the user's choice to the application immediately.

2.2.5. The ERP Features of a Trial. In Figure 3(a), there are four options on the main screen. If the user stared at the motion-strip of the TV option, then the final ERP figure of this trial resembled Figure 6. The option with the red curve (TV) has the highest event-related potential for the N2P3

TABLE 2: Clinical data of the motor-disabled participants.

Subject	Age	Gender	DD	Disease
SE1	35	M	Moderate	Spinal cord injury
SE2	37	M	Moderate	Tetraplegia
SE3	46	M	Moderate	Spinal cord injury
SE4	42	M	Mild	Spinal cord injury
SE5	39	M	Moderate	Spinal cord injury
SE6	43	M	Mild	Spinal cord injury
SE7	50	M	Marked	ALS

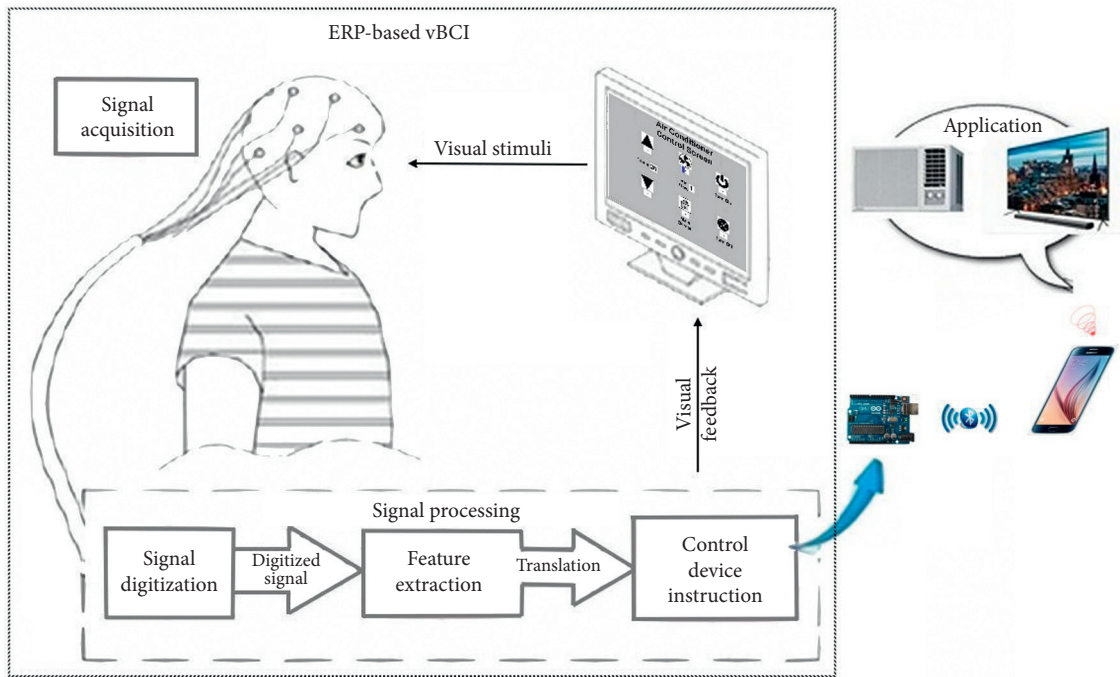


FIGURE 2: System architecture of the proposed HCS, including the ERP-based vBCI system and its applications.

component. Thus, it is the target option and is the one (TV control) that the user selected and wanted to execute.

In Figure 6, the positions marked with red circles are the N200 troughs of the waveforms, and green circles indicate the P300 peak. The N200 potential has the smallest ERP value within 150 ms~250 ms, while the P300 potential has the highest ERP value within 250 ms~350 ms. The N2P3 value of one option is its P300 potential minus its N200 potential.

2.3. Experimental Procedure

2.3.1. Overview of the Experimental Procedure. Each subject took about 0.5 to 1 hour to complete the experiment, depending on the accuracy of the trials. Figure 2 shows the experimental setup. Before the test, the subject sat in front of the computer screen at a distance of roughly 80 cm. The procedure included four steps: (1) attaching the electrodes and checking the signals- 10 mins; (2) illustrating the experimental scheme and performing two trial runs as practice- 10 mins; (3) running the experimental procedure- 5~35 mins; and (4) removing the electrodes and cleaning up- 5 mins.

The first step of the experiment was to attach electrodes to the subject's scalp and check the signals. The BCI module, then, connects with the user's smartphone via its Bluetooth module. Next, each subject performs 15 trials during the experimental procedure. In each trial, the user must choose an option from the GUI designed for the BCI module on the computer screen.

In each test, the subject had to gaze at the blue motion-strip of the option they wanted to choose. The system, then, collected the ERPs of all options available on the GUI from the EEG. After that, the BCI module identified the highest potential from the ERP components N200, P300, or N2P3. The option with the highest N2P3 potential should be the one the user was gazing at during the trial. The BCI module then sent a command signal to the user's smartphone via Bluetooth to make an emergency call or to control a household appliance via IR.

2.3.2. Flowchart of the HCS Operating Procedures. Figure 7 shows a flowchart of the BCI module operation. Each subject had to make 15 selections in the experimental procedure, representing 15 trials. In Figure 7, step 1~step 15 represent the trial sequences.

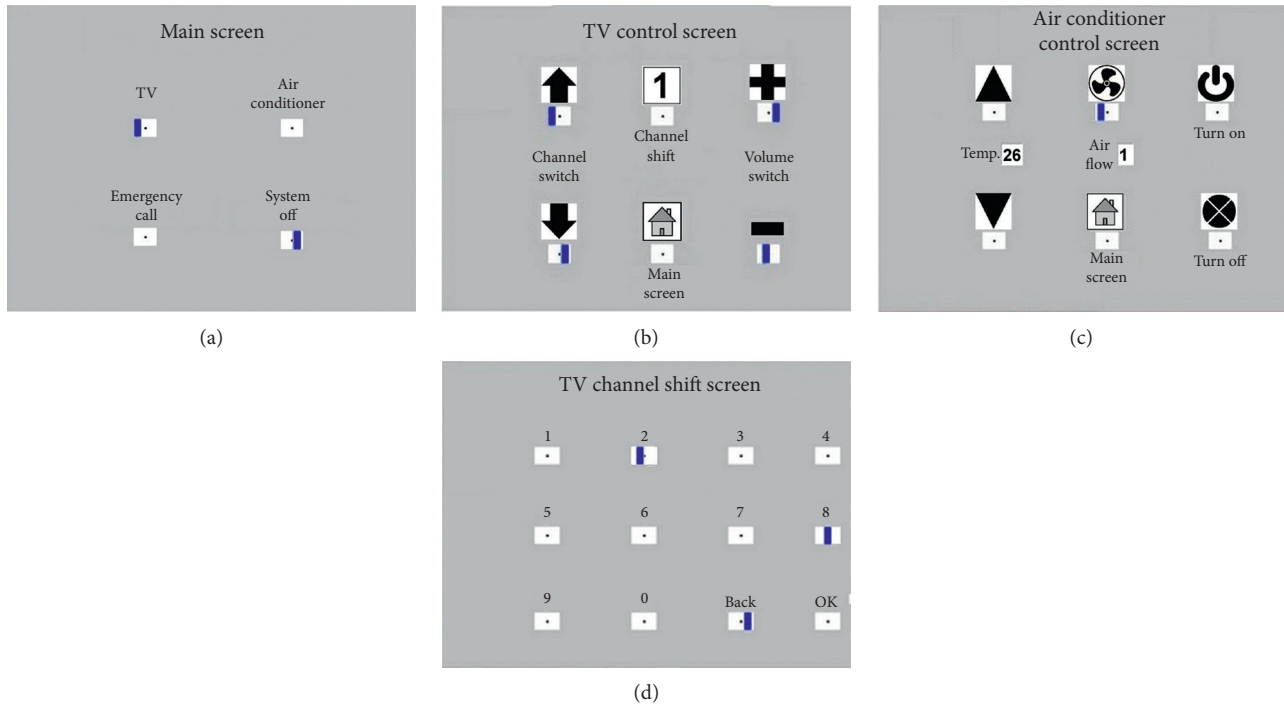


FIGURE 3: Four GUIs in the BCI module. (a) Main screen with four options; (b) TV control screen with six options; (c) air conditioner control screen with six options; and (d) TV channel shift screen with 12 options.

Each subject performed their experimental procedure using the four GUIs. The TV and the air conditioner were under control during the process. They also made an emergency call before the end of the procedure. Table 3 shows the details of the trial sequence. If the command given by the system is correct during a trial, the subject performs the following step of the procedure directly. Otherwise, the tester will discuss the cause of the error with the user and help the user return to the previous trial and try again.

2.4. Experimental Setup

2.4.1. Experiment Equipment. The equipment used to acquire the EEG data included a 32-channel EEG amplifier, an ISO-1032CE, and the control unit, CONTROL-1132, produced by Braintronics B.V. Company. The system uses PCI-1713 to convert analog data to digital data. The authors wrote the vBCI module using Borland C++ Builder and wrote the ICAI1101 smartphone app in Java. The BCI module used an Arduino Uno and HC-05 Bluetooth module to communicate with the user's mobile phone.

2.4.2. Data Acquisition. In the EEG acquisition settings, the sampling rate is 500 Hz, and the impedance remains below 10 k Ω . The EEG acquires the subject's brain waves from electrode O1 on the user's scalp. The electrodes for eye movement detection are FP1 and FP2. The reference electrodes are A1 and A2. The ground electrode is FPz [8]. All electrodes are wet Ag/AgCl electrodes. The EEG amplifier (ISO-1032CE) amplifies and records the potentials of the

user's brain waves. The data are filtered with a 0.3~15 Hz band-pass filter in the control unit, CONTROL-1132. Then, PCI-1713 converts the analog data to digital data and sends the data to the vBCI module for interpretation.

2.4.3. Data Processing. (1). ERPs acquisition: in each trial, each motion-strip moves from right to left six times, as shown in Figure 5. The system records the time of onset for each motion-strip and obtains the brain waves of the subjects. The system, then, segments the EEG into ERPs within intervals ranging from -100 ms to 800 ms of the onset time. Thus, there are six segments for each option. The system, then, sums the six ERP segments of each option and averages them to obtain the final ERPs for each option.

(2). ERPs analysis: the system saves and analyses the final ERPs for each option in each trial. The system, thus, finds the N200 value and the P300 value of each option and, then, determines the N2P3 value. Next, the system compares the N2P3 value of all options to each other to identify which option the user selected.

(3). Instruction output: the system translates the ERP analysis results into a BCI instruction and sends it to the user's smartphone via Bluetooth. When the smartphone receives a BCI instruction, it runs the application to make an emergency call or to control an appliance via IR.

2.5. System Assessment with Bit Rate. In addition to the accuracy rate, the rate at which information per unit of time is obtained is particularly important for evaluating a BCI system. To calculate the number of bits available per minute,

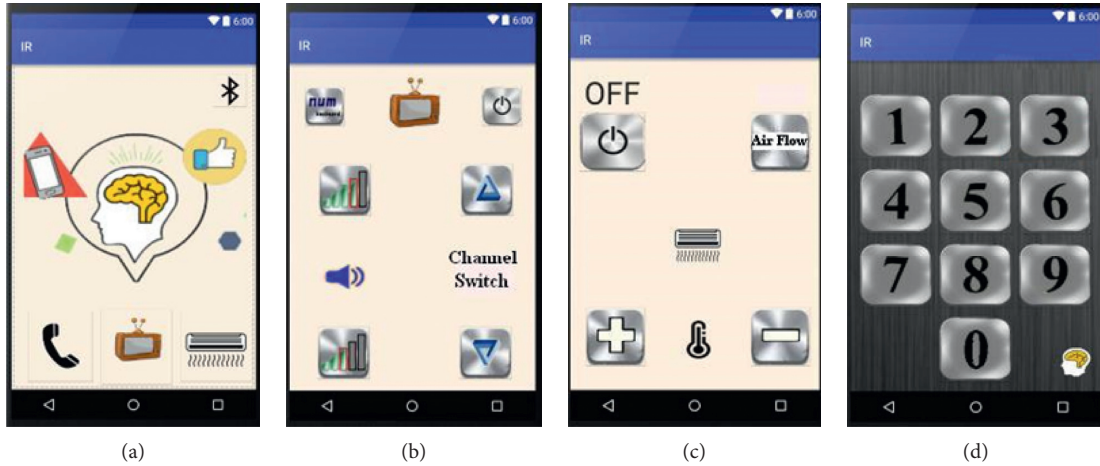


FIGURE 4: The caregiver GUIs of the ICAI1101 smartphone app: (a) main app screen on the smartphone; (b) TV remote controller; (c) air conditioner remote controller; and (d) TV channel shift screen.

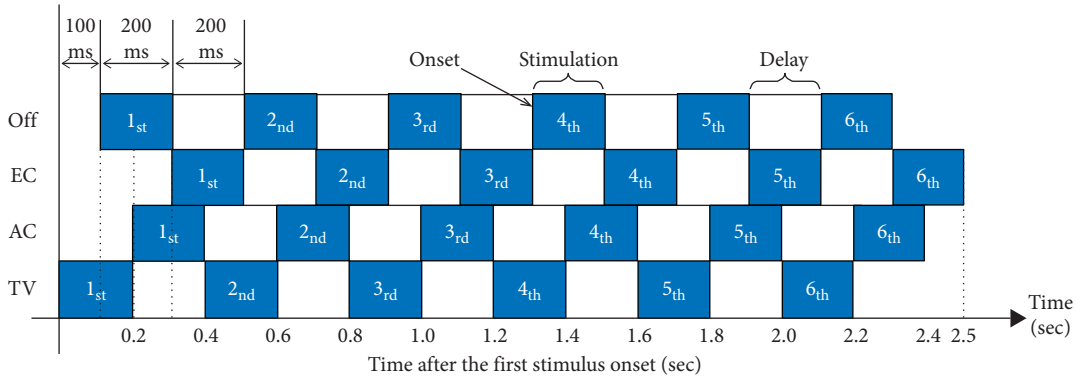


FIGURE 5: A stimulation schematic of one trial for the four options on the main screen. There are six instances of stimulation for every option in a single trial.

the bit-rate calculation in this study uses the definition of Wolpaw [62], as follows:

$$\text{bit - rate} = M \left\{ \log_2 N + P \log_2 P + (1 - P) \log_2 \left[\frac{(1 - P)}{(N - 1)} \right] \right\}, \quad (1)$$

where M indicates the number of choices made in a minute, N is the number of options, and P is the accuracy rate.

3. Results and Discussion

Table 2 shows information about all the subjects who participated in the experiment. Although the participants could ask to stop the procedure at any time, no one did. The system used the N2P3 component to interpret the output of the EEG online. However, to find the optimal solution, we analyzed the features of ERP components N200, P300, and N2P3 of all users offline. The experimental results were analyzed as follows.

3.1. Discriminating Features of ERPs. Figure 8 illustrates the discriminating features of ERPs. Figure 8(a) is the output figure obtained from the 1st trial of E14, while Figure 8(b) is the output figure from the 3rd trial of SE1.

In Figure 8(a), the red curve represents enter the TV control screen, the dotted green curve represents enter the air conditioner control screen, the dotted yellow curve represents making an emergency call, and the blue segment curve represents shut down the system.

In Figure 8(b), the red curve represents change to the next channel, the dotted green curve represents enter the TV channel shift screen, and the dotted yellow curve represents increasing the volume. The blue segmented curve is a change to the previous channel, the dotted white curve represents backing to the main screen, and the dotted gray curve represents decreasing the volume.

Figure 8(a) shows that the N200 value ($-1.7969 \mu\text{V}$) of the solid red curve (TV option) on the main screen is the lowest ERP, and P300 value ($3.5418 \mu\text{V}$) of the dotted green curve (AC option) is the highest ERP. Table 4 shows that the maximum ERP of N2P3 ($4.0814 \mu\text{V}$) is obtained from the

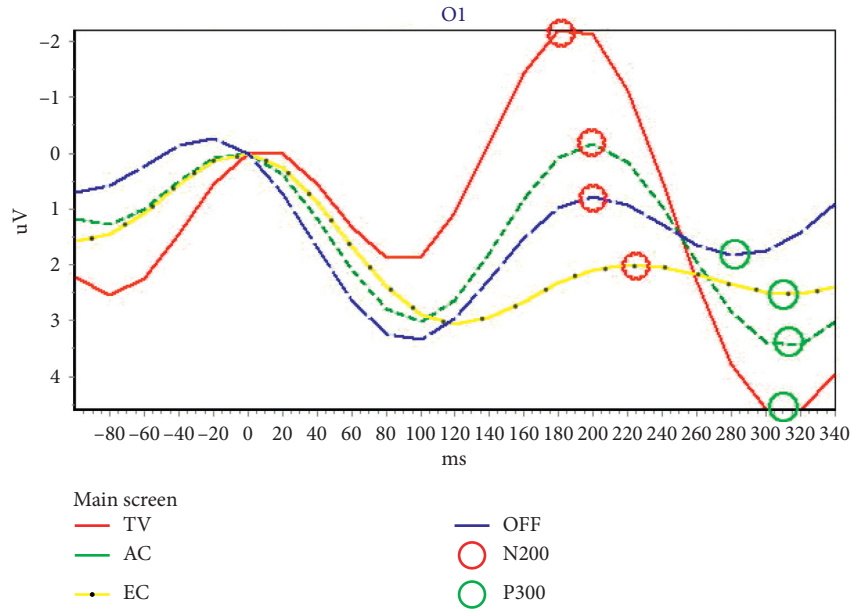


FIGURE 6: The ERPs of four options on the main screen from the output of the first trial of SE3. The red circle indicates the potential of N200, while the green circle represents the potential of P300.

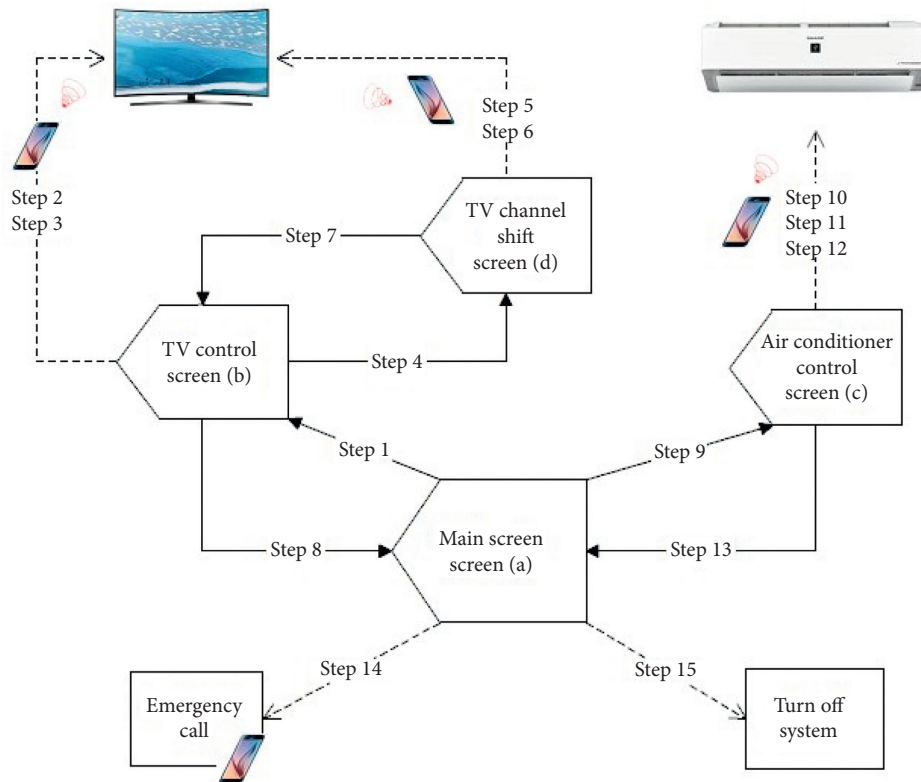


FIGURE 7: Flowchart of the vBCI operating procedures. The solid arrow line shows that the system sends an instruction to switch the screen of the system to the target GUI. The dotted arrow line shows that the system is only sending a command to do something, and the screen remains on the same GUI.

solid red curve (TV option). Thus, the user wanted to access the function of the TV control during the online experimental process. This result complies with the requirements of the experimental procedure. The offline analysis shows that the result is correct if using N200 for interpretation.

However, the result when using P300 for interpretation, AC, is wrong.

Figure 8(b) shows that the N200 value ($-1.6458 \mu V$) of the solid red curve (Next Channel) on the TV screen is the lowest ERP, and P300 value ($3.0962 \mu V$) of the dotted yellow

TABLE 3: Details of the 15 trial sequences.

Step	1	2	3	4	5	6	7	8	9	10	11	12	13	14	15
GUI	Main screen	TV screen	TV screen	TV screen	TV channel shift	TV channel shift	TV channel shift	TV screen	Main screen	Air condi.	Air condi.	Air condi.	Air condi.	Main screen	Main screen
Option to choose	Enter TV	Volume up	Next channel	Enter channel shift	Choose channel 1	Choose OK	Back TV	Back to main	To air condi.	Turn on AC	Temp down	Air Flow	Back to main	Emergency call	System off

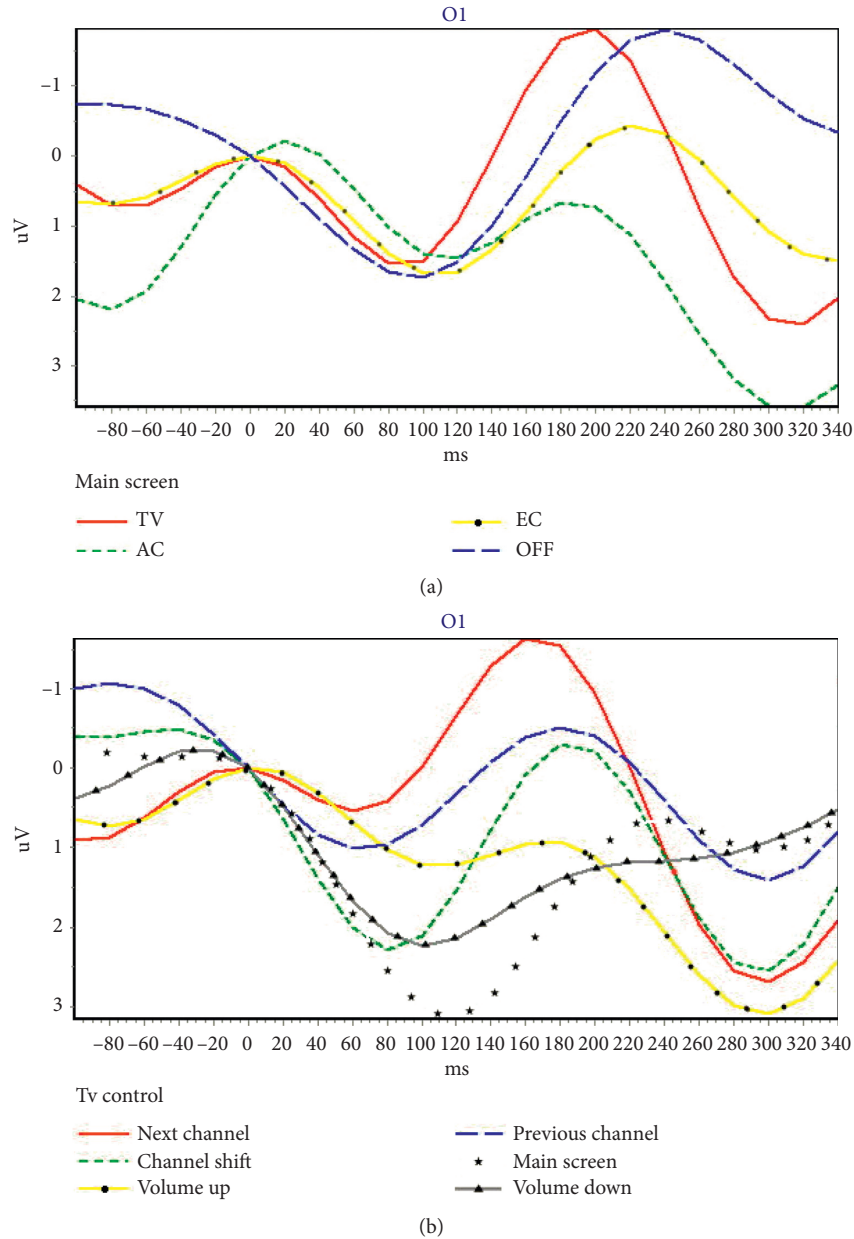


FIGURE 8: Two ERP samples from one motor-disabled subject. (a) The ERPs from the main screen of the BCI system (4 options); (b) the ERPs from TV control screen of the BCI system (6 options).

TABLE 4: The ERP values (μV) of all options in the main screen obtained from the first trial of subject E14.

Options	N200	P300	N2P3	Result	
				Online	Offline
TV	-1.7969	2.2845	4.0814	✓	N200, N2P3
AC	0.6518	3.5418	2.8900		P300
EC	0.0030	1.0302	1.0272		
Off	-1.7847	-0.9263	0.8584		

curve (volume up) is the highest ERP. Table 5 shows that the maximum ERP of N2P3 ($4.3471 \mu V$) gains from the solid red curve (next channel). Thus, it means the user wanted to access the function of the next channel during the online

experimental process. This result complies with the requirements of the experimental procedure. The offline analysis shows that the result, the solid red curve (next channel), is right if using N200 for interpretation. However, the result obtained when using P300 for interpretation, volume up, is wrong.

3.2. Experimental Results for Healthy Subjects

3.2.1. Accuracy and Bit-Rate Analysis. Fifteen healthy subjects participated in the experiment. The experimental results showed that the feature of N2P3 enabled the best discrimination. The average accuracy across all 15 users was 81.78%, meaning that of all 15 commands, 12 were

TABLE 5: The ERP values (μV) of all options in the main screen obtained from the 3rd trial of subject SE1.

Options	N200	P300	N2P3	Result	
				Online	Offline
Next channel	-1.6458	2.7013	4.3471	✓	N200, N2P3
Channel shift	-0.3196	2.5717	2.8913		
Volume up	0.9145	3.0962	2.1817		P300
Prev. channel	-0.5131	1.4089	1.9220		
Main screen	0.8788	1.0479	0.1691		
Volume down	1.3293	1.1093	-0.2200		

performed right. The precision attained by 10 of the 15 subjects was greater than 80%. The accuracy of E10 was even 100%. However, the accuracy of E1 and E15 was unacceptable. These two subjects may not be able to adapt to the BCI system or were disturbed by other factors, resulting in reduced efficiency. Figure 9 summarizes the accuracy levels and bit rate acquired by the 15 healthy subjects.

The average bit rate attained by all 15 healthy subjects is 27.11. It is better than that of other studies [25, 62, 63].

3.2.2. Analysis of Sum of Correct Choices Made by All Healthy Subjects in Each Trial. Figure 10 shows that if the system uses N2P3 to interpret the EEG, the average number of correct selections for each healthy subject was 12.27 on average, while N200 it is only 8 and 11.07 for P300. It is important to note that the 6th and 7th trials exhibited lower online performance with the system choosing the right option for only 10 of 15 users (66.67%). By contrast, all the subjects chose the correct option on the 4th trial, and the number of correct selections in 10 of all 15 trials is greater than 12 (80%). Thus, using N2P3 for interpretation is the optimal solution.

3.2.3. The Paired-Sample *t*-Test Analysis of the Results of the Targeted Option vs. Nontargeted Options. Table 6 shows the paired-sample *t*-test analysis of the ERP components of the target option and the nontarget options. The results show that the features of the ERP components, P300 and N2P3, can be used as discriminating features. However, there was a significant difference in the results between N2P3-targeted and P300-targeted. Thus, using the component N2P3 for interpretation is the optimal solution.

3.3. Experimental Results for Motor-Disabled People and ALS

3.3.1. Accuracy and Bit-Rate Analysis. Six motor-disabled people and one man with ALS participated in the experiment. The experimental results showed that the feature of N2P3 offered the best discrimination. The average accuracy across all seven users was 78.10%, meaning that of all 15 commands, 11 were performed right. However, the accuracy of SE2 is not acceptable. This subject may not be able to adapt to the BCI system or was disturbed by other factors, resulting in reduced efficiency. Figure 11 summarizes the accuracy levels acquired by the seven with physical disabilities.

The average bit rate attained by all seven disabled subjects is 22.37. Although the average bit-rate attained by the disabled group is lower than that of the healthy group, it is also better than that of other studies [25, 62, 63].

3.3.2. Analysis of Sum of Correct Choices Made by All Motor-Disabled Subjects in Each Trial. Figure 12 shows that if the system uses N2P3 to interpret the EEG, the average number of disabled subjects selecting correctly is 5.47, 2.13 for N200 and 3.67 for P300. It is important to note that the 10th and 11th trials exhibited lower performance online. By contrast, all the subjects chose the correct option in the 1st, 4th, 9th, 12th, and 14th trials. Thus, using N2P3 for interpretation is the optimal solution for motor-disabled subjects. These results are the same as those of the group of healthy subjects.

3.3.3. The Paired-Sample *t*-Test Analysis of the Results of the Targeted Option vs. Nontargeted Options. Table 7 shows the paired-sample *t*-test analysis of the ERP components of the target option and the nontarget options. Although the *p*-value (.004) of case N200 is less than 0.01, Figure 11 shows that the average accuracy is 30.48% if the system used the component N200 for interpretation. Thus, only N2P3 can be used as the discriminating feature for motor-disabled subjects.

3.4. Independent-Sample *t*-Test for the Results for the Healthy Subjects and the Motor-Disabled Subjects (including One ALS). In this study, we conducted experiments with 15 healthy subjects, six motor-disabled subjects, and one ALS. The average accuracy attained by the 15 healthy subjects was 81.78% if using N2P3 (online) for interpretation, while the average accuracy attained by the seven motor-disabled subjects was 78.10%. The disabled group has a lower accuracy level than the healthy group. However, both groups had an average accuracy of more than 75%.

We compared the results of these two independent samples, as shown in Table 8. The results show that if the system used the N200 or P300 component for interpretation, there was a significant difference in the results between the healthy group and the disabled group. That is, the system may not be acceptable for disabled people. Yet, when the system uses N2P3 for interpretation, there is no significant difference between the two groups ($t = 0.6258$, $p = 0.5385$). Thus, the proposed vBCI system appears to be suitable for our end-user, motor-disabled people, when the system uses N2P3 for interpretation online. It enables the HCS to reach a desirable level.

The average bit rate attained by all 15 healthy subjects is 27.11 (Figure 9). The average bit rate attained by all seven disabled subjects is 22.37 (Figure 11). Although the average bit rate attained by the disabled group is lower than the average bit rate attained by the healthy group, the difference is not significant ($t = 0.8793$, $p = 0.3897$).

4. Discussion

The aim of the present study is two-fold: (1) to develop a BCI-based home care system to help end-users control their

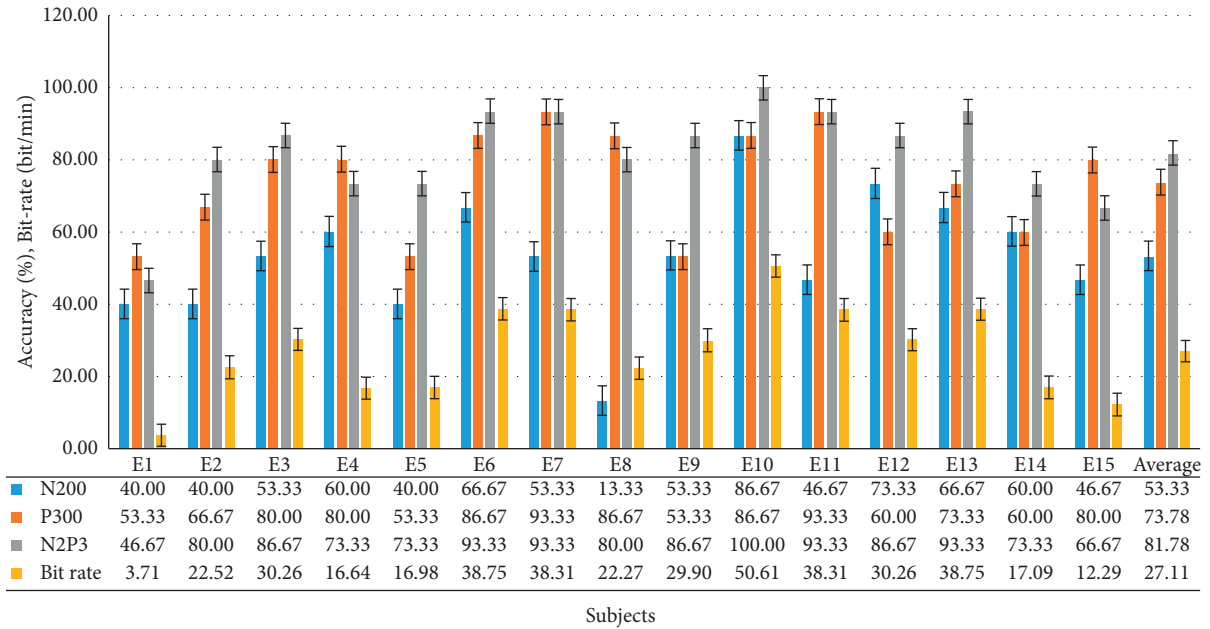


FIGURE 9: The accuracy levels and bit rate attained by all 15 healthy subjects.

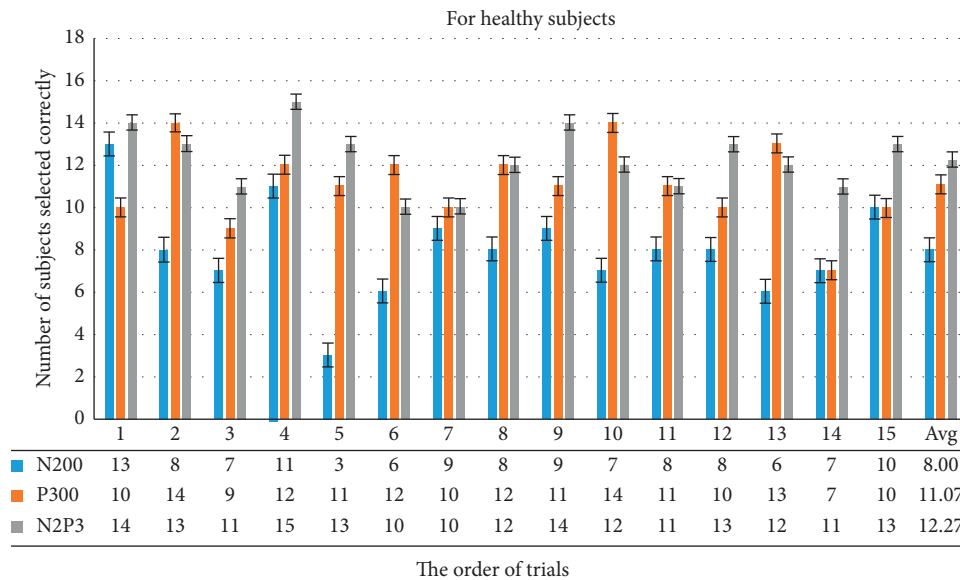


FIGURE 10: This bar chart summarizes the number of correct selections for each healthy subject for each trial. For example, if the system uses N2P3 to interpret the EEG, the choices from 14 of all 15 users are correct in the first trial, while N200 13 are correct, and only 10 are correct for P300.

TABLE 6: Paired-sample t-test results of all trials for the 15 healthy subjects. $\alpha = 0.01$, $N = 225$.

Case	T value	p value
N200 Targeted vs. nontargeted	0.747	0.467
P300 Targeted vs. nontargeted	6.225	0.000***
N2P3 Targeted vs. nontargeted	8.998	0.000***
N2P3 vs. P300 N2P3-targeted vs. P300-targeted	2.276	0.039*

* $p < 0.05$; ** $p < 0.01$; *** $p < 0.001$.

household appliances and (2) to assess whether the architecture of the HCS is easy for motor-disabled people to use.

First, we designed and developed a BCI-based home care system (HCS). We designed the HCS to make an emergency call or control the household appliances, such as TV and air

conditioner, via a smartphone. Thus, end-users can improve personal autonomy and reduce their dependence on caregivers.

Second, most previous research has not experimented with end-users. Thus, the second purpose of this study was to

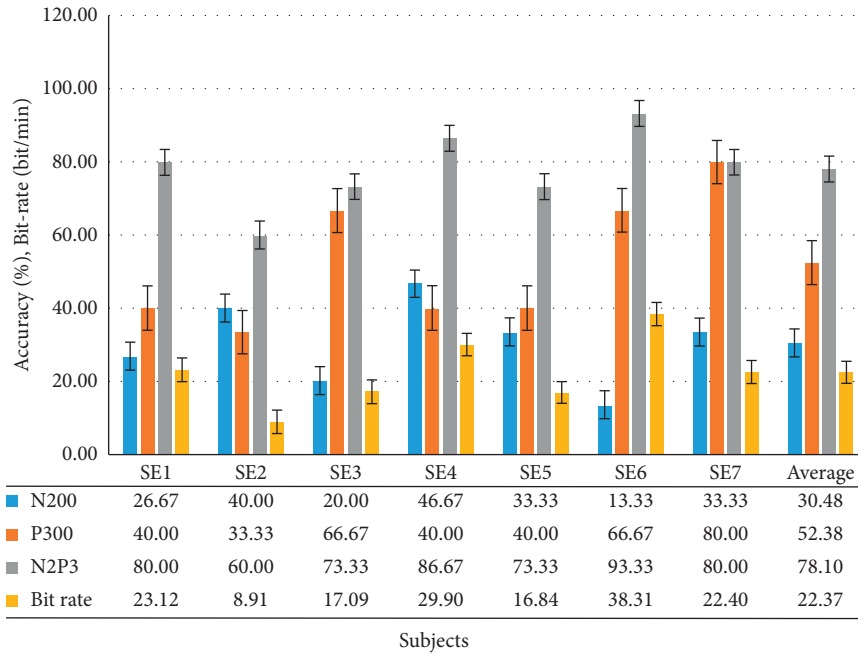


FIGURE 11: Accuracy levels and bit rate attained by all motor-disabled subjects (including one ALS, SE7).

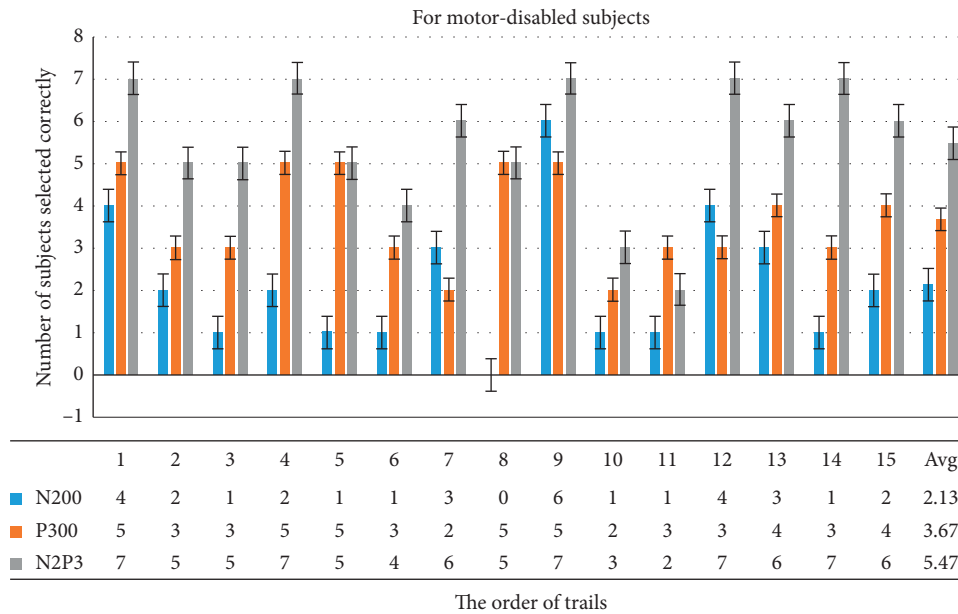


FIGURE 12: This chart summarizes the correct selections of all motor-disabled subjects for each trial. For example, if the system uses N2P3 to interpret the EEG, the choices from 7 of 7 users are correct in the first trial, while 4 are correct with N200 and 5 with P300.

assess the usefulness of the system with motor-disabled subjects. We conducted experiments with both healthy and motor-disabled subjects. One subject had ALS.

Previous researchers attempted to improve the performance of their BCI systems [7, 9, 21, 23, 60]. Thus, improving the accuracy of the HCS is the primary mission of our study. To improve the efficiency of HCS, we adjusted three details: the number of electrodes, the brain-computer interface, and the method the system uses to interpret the ERPs.

Most BCI studies use Fz, Cz, Pz, Oz, and other electrodes to collect data [9, 22, 23, 29, 34, 45, 60]. Of these, Zhang et al. also used the O1 and O2 electrodes to obtain data [10]. Based

on the previous research results of our laboratory, the ERPs acquired from electrodes O1 and O2 yield outstanding accuracy and are better than ERPs from other electrodes when we asked the user to stare at the GUI [8, 26]. Furthermore, the fewer the electrodes are, the more comfortable the user is. Thus, the system used electrode O1 only to obtain the ERP data in this study.

To use an electrode, Q1, to gain the data, we ask the user to stare at the GUI when using the system. The system asynchronously shows the stimuli to shorten stimulation times. In the HCS there are four options on the main screen, six options on the TV and AC control screen, and 12 options

TABLE 7: Paired-sample t -test results of all trials for the seven motor-disabled subjects. $\alpha = 0.01$, $N = 105$.

	Case	T value	p value
N200	Targeted vs. nontargeted	-4.509	0.004**
P300	Targeted vs. nontargeted	0.346	0.741
N2P3	Targeted vs. nontargeted	6.953	0.000***

** $p < 0.01$; *** $p < 0.001$.

TABLE 8: Independent-sample t -test of the accuracy of the healthy subjects and of the motor-disabled subjects, $\alpha = 0.01$.

	Case	F -test p value	T value	p value
N200 targeted	Healthy vs. disabled	0.1596	3.1693	0.0048**
P300 targeted	Healthy vs. disabled	0.2428	2.9396	0.0081**
N2P3 targeted	Healthy vs. disabled	0.2817	0.6258	0.5385
Bit rate	Healthy vs. disabled	0.2576	0.8793	0.3897

** $p < 0.01$; *** $p < 0.001$.

on the TV channel shift screen. Figures 10 and 12 show that the number of options on the GUI has nothing to do with the number of users correctly selecting in each trial. The average bit rate in both groups was better than that of related studies. Although the average bit rate attained by the disabled group is lower than that attained by the healthy group, the difference is not significant ($t = 0.8793$, $p = 0.3897$). Therefore, we inferred that the interface of the HCS is also applicable to motor-disabled people.

Previous studies have stated that component P300 provided an excellent level of discrimination [29, 60, 61]. However, in earlier studies in our laboratory, component N2P3 presented the best level of discrimination [8]. Thus, we compared ERP components N200, P300, and N2P3 to determine what the best feature for discrimination is.

When using component P300, the healthy and the motor-disabled subjects had an average efficiency of 73.78% (SD = 14.79) and 52.38% (SD = 18.23), respectively. Although the precision attained by 8 of the 15 healthy subjects was greater than 80%, only SE7 (ALS) obtained an accuracy of 80% when using P300 for interpretation. However, for the online experimental results (using component N2P3), the healthy and the motor-disabled subjects exhibited an average efficiency of 81.78% (SD = 13.69) and 78.10% (SD = 10.69), respectively. The precision attained by 10 of the 15 healthy subjects was greater than 80%, and the precision obtained by three of the seven motor-disabled subjects was greater than 80%. Furthermore, Figure 11 shows that, from SE1 to SE6, the accuracy using N2P3 for interpretation is the best. SE7 (ALS) had an accuracy of 80% using component N2P3 and again using P300.

Although the disabled group has a lower accuracy level than the healthy group, the difference is not significant ($t = 0.6258$, $p = 0.5385$). The average accuracy attained by the seven motor-disabled subjects was 78.10%, more than the 75% when using N2P3 for interpretation. To this point,

these results are consistent with those of Huang [8] which show that the ERP component N2P3 is the optimal solution for discrimination in the HCS. Thus, the HCS is suitable for end-users, including motor-disabled people. The HSC proposed in this study reaches a desirable level of performance when the system uses N2P3 for interpretation.

The second issue in system construction is making the system easy for end-users. This question included two key points: whether the GUI of the HCS is friendly and whether the remote controls for all appliances can be integrated into one remote control.

First, Figure 10 shows that more than 12 subjects made the right selections in 10 of 15 trials (over 80%). Figure 12 shows that more than six subjects made the right selections in 8 of 15 trials (over 85%). Most trials exhibited a high correct selection rate. Coupled with speedy bit rate, we reason that the interface in the system is easy to use.

Second, there are often two common household appliances, TVs and air conditioners, in the same room. Every home appliance has a dedicated remote control. If all home appliances can share the same remote control, the system can be easy for end-users to use. In this study, we added a smartphone to the HCS. A smartphone with IR communication technology may act as a remote control. It can emit a distinct IR wavelength to control any household appliance. Thus, we developed an app called ICAI1101 to control the TV and air conditioner using a smartphone via IR. Such a BCI system would make it easier for the end-user to control their home appliances.

ICAI1101 is first installed on a smartphone. When the user makes a choice during use, ICAI1101 can act following the user's choice. Furthermore, ICAI1101 not only makes emergency calls and controls the TV or air conditioner but can also integrate other apps. The rapid growth of the Internet and the popularity of smartphones have had an immense impact on human life in the last two decades [22]. Innumerable apps designed for smartphones reside in mobile app stores. Millions of apps are aimed at motor-disabled people. ICAI1101 can easily integrate these apps into the BCI system. In the future, we plan to integrate other apps into the BCI system. Thus, the HCS could help end-users to learn and communicate with others.

Tables 3 and 5 show that the accuracy of E1, E15, and SE2 is not acceptable. These subjects may have individual factors that resulted in lower efficiency. Development of the subsequent vBCI system should address the aforementioned personal questions. This will allow the HCS to help end-users achieve better quality of life.

5. Conclusions

In this study, we have proposed a home care system that combines BCI with a smartphone. The HCS helps end-users, motor-disabled people, make an emergency call or control their household appliances. Thus, end-users can take care of themselves with only eye muscle movement. Fifteen healthy subjects and seven motor-disabled subjects (including one with ALS) participated in clinical trials. Because of the high accuracy-rate and rapid response of the system during the

online experimentation, most subjects of both groups can rapidly complete the experimental procedure in less than the preset time, 35 minutes. In the offline analytics, the data collected enabled us to evaluate and improve the performance of the system. The results showed that the disabled group has a lower accuracy level than that of the healthy group, but the difference is not statistically significant. The average accuracy of the disabled group (78.10%) not only exceeded the chance level but was also higher than 75%. The bit-rate analysis yielded conclusions similar to those of the accuracy analysis. Thus, when a user chooses an option, the accuracy of the target option in a short period exceeds three-fourths. We, therefore, reason that the HCS is a viable system for motor-disabled people.

The HCS is a system that can be used without prior training. The bit rate of the HCS is close to that of a previous study, the Chinese Spelling System, performed in our Lab [8], and is better than that of other studies [25, 62, 63]. Such a fast bit rate and high accuracy rate make the HCS easy to use. Even if the user selects the wrong option, the system can be returned to the correct position in a short time by reselection. More importantly, only one electrode, O1, is required to measure the EEG signals, enabling the HCS to have good usability in practical use. Thus, we confirmed the feasibility and practicability of this home care system approach.

Data Availability

Data are available on request. E-mail: klhsieh@gmail.com.

Conflicts of Interest

The authors declare that there are no conflicts of interest regarding the publication of this paper.

References

- [1] M. A. Hardiman, A. Chio, A. Al-Chalabi, R. J. Pasterkamp, J. H. Veldink, and L. H. Van Den Berg, "Amyotrophic lateral sclerosis," *The Lancet*, vol. 390, no. 10107, pp. 2084–2098, 2017.
- [2] M. C. Kiernan, S. Vucic, and B. C. Cheah, "Amyotrophic lateral sclerosis," *Lancet*, vol. 377, no. 9769, pp. 942–955, 2011.
- [3] M. R. Turner, F. Agosta, P. Bede, V. Govind, D. Lulé, and E. Verstraete, "Neuroimaging in amyotrophic lateral sclerosis," *Biomarkers in Medicine*, vol. 6, no. 3, pp. 319–337, 2012.
- [4] J. Heo, H. J. Baek, S. Hong, M. H. Chang, J. S. Lee, and K. S. Park, "Music and natural sounds in an auditory steady-state response based brain-computer interface to increase user acceptance," *Computers in. Biology and Medicine*, vol. 84, pp. 45–52, 2017.
- [5] K. C. Chung, S. F. Shi, Y. Y. Tang, and K. Y. Wang, "An experience nursing a patient with amyotrophic lateral sclerosis using the theory of self-care," *Journal of Nursing*, vol. 52, no. 3, pp. 82–89, 2005.
- [6] E. V. Hobson and C. J. McDermott, "Supportive and symptomatic management of amyotrophic lateral sclerosis," *Nature Reviews Neurology*, vol. 12, no. 9, pp. 526–538, 2016.
- [7] J. Ma, Y. Zhang, A. Cichocki, and F. Matsuno, "A novel EOG/EEG hybrid human-machine interface adopting eye movements and ERPs: application to robot control," *IEEE Transactions on Biomedical Engineering*, vol. 62, no. 3, pp. 876–889, 2015.
- [8] T. Huang, *Design of Chinese Spelling System Based on ERPs*, National University of Tainan, Tainan, Taiwan, 2011.
- [9] E. Yin, Z. Zhou, J. Jiang, F. Chen, Y. Liu, and D. Hu, "A speedy hybrid BCI spelling approach combining P300 and SSVEP," *IEEE Transactions on Bio-Medical Engineering*, vol. 61, no. 2, pp. 473–483, 2014.
- [10] R. Zhang, Q. Wang, K. L. Shenghong He et al., "A BCI-based environmental control system for patients with severe spinal cord injuries," *IEEE Transactions on Biomedical Engineering*, vol. 64, no. 8, pp. 1959–1971, 2017.
- [11] R. E. Nordgren, W. R. Markesbery, K. Fukuda, and A. G. Reeves, "Seven Cases of Cerebromedullospinal Disconnection: The 'locked-In' Syndrome," *Neurology*, vol. 21, no. 11, p. 1140, 1971.
- [12] E. Smith and M. Delargy, "Locked-in syndrome," *British Medical Journal*, vol. 330, no. 7488, pp. 406–409, 2005.
- [13] G. Bauer, F. Gerstenbrand, and E. Rimpl, "Varieties of the locked-in syndrome," *Journal of Neurology*, vol. 221, no. 2, pp. 77–91, 1979.
- [14] S. Zoccollella, A. Santamato, and P. Lamberti, "Current and emerging treatments for amyotrophic lateral sclerosis," *Neuropsychiatric Disease and Treatment*, vol. 5, pp. 577–595, 2009.
- [15] F. Cui, W. Zhu, Z. Zhou et al., "Frequency and risk factor analysis of cognitive and anxiety-depressive disorders in patients with amyotrophic lateral sclerosis/motor neuron disease," *Neuropsychiatric Disease and Treatment*, vol. 11, pp. 2847–2854, 2015.
- [16] K. T. Sun, T. W. Huang, and M. C. Chen, "Design of Chinese spelling system based on ERP," in *Proceedings of the 2011 11th IEEE International Conference on Bioinformatics and Bioengineering, BIBE 2011*, pp. 310–313, Taichung, Taiwan, April 2011.
- [17] J. R. Wolpaw, N. Birbaumer, D. J. McFarland, G. Pfurtscheller, and T. M. Vaughan, "Brain-computer interfaces for communication and control," *Clinical Neurophysiology*, vol. 113, no. 6, pp. 767–791, 2002.
- [18] M. G. Bleichner, M. Lundbeck, M. Selisky et al., "Exploring miniaturized EEG electrodes for brain-computer interfaces. An EEG you do not see?" *Physiological Reports*, vol. 3, no. 4, Article ID e12362, 2015.
- [19] L. A. Farwell and E. Donchin, "Talking off the top of your head: toward a mental prosthesis utilizing event-related brain potentials," *Electroencephalography and Clinical Neurophysiology*, vol. 70, no. 6, pp. 510–523, 1988.
- [20] M. Thulasidas, C. Guan, and J. Wu, "Robust classification of EEG signal for brain-computer interface," *IEEE Transactions on Neural Systems and Rehabilitation Engineering*, vol. 14, no. 1, pp. 24–29, 2006.
- [21] E. Yin, T. Zeyl, R. Saab, T. Chau, D. Hu, and Z. Zhou, "A hybrid brain-computer interface based on the fusion of P300 and SSVEP scores," *IEEE Transactions on Neural Systems and Rehabilitation Engineering*, vol. 23, no. 4, pp. 693–701, 2015.
- [22] V. Martínez-Cagigal, E. Santamaría-Vázquez, J. Gomez-Pilar, and R. Hornero, "Towards an accessible use of smartphone-based social networks through brain-computer interfaces," *Expert Systems with Applications*, vol. 120, 2019.
- [23] Y.-H. Liu, S.-H. Wang, and M.-R. Hu, "A self-paced P300 healthcare brain-computer interface system with SSVEP-based switching control and kernel FDA+SVM-based detector," *Applied Science*, vol. 6, no. 5, p. 142, 2016.

- [24] Y. Matsumoto, S. Makino, K. Mori, and T. M. Rutkowski, "Classifying p300 responses to vowel stimuli for auditory brain-computer interface," in *Proceedings of the 2013 Asia-Pacific Signal and Information Processing Association Annual Summit and Conference, APSIPA 2013*, pp. 1–5, Kaohsiung, Taiwan, October 2013.
- [25] B. Hong, F. Guo, T. Liu, X. Gao, and S. Gao, "N200-speller using motion-onset visual response," *Clinical Neurophysiology*, vol. 120, no. 9, pp. 1658–1666, 2009.
- [26] K. T. Sun, Y. H. Tai, H. W. Yang, and H. T. Lin, "Robot control by ERPs of brain waves," *International Journal of Electrical, Computer, Energetic, Electronic and Communication Engineering*, vol. 8, pp. 1233–1238, 2014.
- [27] S. Sutton, M. Braren, J. Zubin, and E. R. John, "Evoked-potential correlates of stimulus uncertainty," *Science*, vol. 150, no. 3700, pp. 1187–1188, 1965.
- [28] C. E. Lakey, D. R. Berry, and E. W. Sellers, "Manipulating attention via mindfulness induction improves P300-based brain-computer interface performance," *Journal of Neural Engineering*, vol. 8, no. 2, pp. 1–7, 2011.
- [29] J. Lu, W. Speier, X. Hu, and N. Pouratian, "The effects of stimulus timing features on P300 speller performance," *Clinical Neurophysiology*, vol. 124, no. 2, pp. 306–314, 2013.
- [30] D. V. Moretti, "Electroencephalography-driven approach to prodromal Alzheimer's disease diagnosis: from biomarker integration to network-level comprehension," *Clinical Interventions in Aging*, vol. 11, pp. 897–912, 2016.
- [31] A. Turnip and K. S. Hong, "Classifying mental activities from EEG-P300 signals using adaptive neural networks," *International Journal of Innovative Computing Information Control*, vol. 8, pp. 6429–6443, 2012.
- [32] S. Moghimi, A. Kushki, A. Marie Guerguerian, and T. Chau, "A review of EEG-Based brain-computer interfaces as access pathways for individuals with severe disabilities," *Assistive Technology*, vol. 25, no. 2, pp. 99–110, 2013.
- [33] T. W. Picton, S. Bentin, P. Berg et al., "Guidelines for using human event-related potentials to study cognition: recording standards and publication criteria," *Psychophysiology*, vol. 37, no. 2, pp. 127–152, 2000.
- [34] R. C. Panicker, S. Puthusserypady, and Y. Ying Sun, "Adaptation in P300 brain-computer interfaces: a two-classifier cotraining approach," *IEEE Transactions on Biomedical Engineering*, vol. 57, no. 12, pp. 2927–2935, 2010.
- [35] T. W. Picton, "The P300 wave of the human event-related potential," *Journal of Clinical Neurophysiology*, vol. 9, no. 4, pp. 456–479, 1992.
- [36] M. L. Gamble and S. J. Luck, "N2ac: an ERP component associated with the focusing of attention within an auditory scene," *Psychophysiology*, vol. 48, no. 8, pp. 1057–1068, 2011.
- [37] D. Regan, *Human Brain Electrophysiology: Evoked Potentials and Evoked Magnetic Fields in Science and Medicine*, Elsevier, New York, NY, USA, 1989.
- [38] "Event-related Potential," wiki https://en.wikipedia.org/wiki/Event-related_potential#cite_note-2.
- [39] S. H. Patel and P. N. Azzam, "Characterization of N200 and P300: selected studies of the event-related potential," *International Journal of Medical Sciences*, vol. 2, no. 4, pp. 147–154, 2005.
- [40] E. Donchin, K. M. Spencer, and R. Wijesinghe, "The mental prosthesis: assessing the speed of a P300-based brain-computer interface," *IEEE Transactions on Rehabilitation Engineering*, vol. 8, no. 2, pp. 174–179, 2000.
- [41] U. Hoffmann, J. M. Vesin, T. Ebrahimi, and K. Diserens, "An efficient P300-based brain-computer interface for disabled subjects," *Journal of Neuroscience Methods*, vol. 167, no. 1, pp. 115–125, 2008.
- [42] A. Combaz and M. M. VanHulle, "Simultaneous detection of P300 and steady-state visually evoked potentials for hybrid brain-computer interface," *PLoS One*, vol. 10, no. 3, 2015.
- [43] E. Halgren, K. Marinkovic, and P. Chauvel, "Generators of the late cognitive potentials in auditory and visual oddball tasks," *Electroencephalography and Clinical Neurophysiology*, vol. 106, no. 2, pp. 156–164, 1998.
- [44] S. Amiri, R. Fazel-Rezai, and V. Asadpour, "A review of hybrid brain-computer interface systems," *Advances in Human-Computer Interaction*, vol. 2013, pp. 1–8, 2013.
- [45] M. E. Thurlings, A.-M. Brouwer, J. B. F. VanErp, and P. Werkhoven, "Gaze-independent ERP-BCIs: augmenting performance through location-congruent bimodal stimuli," *Frontiers System in Neuroscience*, vol. 8, p. 143, 2014.
- [46] K. L. Hsieh, K. T. Sun, J. K. Yeh, and Y. U. Pan, "Home care by auditory Brain Computer Interface for the blind with severe physical disabilities," in *2017 International Conference On Applied System Innovation(ICASI)*, pp. 527–530, Sapporo, Japan, May 2017.
- [47] J. E. Huggins, A. A. Moinuddin, A. E. Chiodo, and P. A. Wren, "What would brain-computer interface users want: opinions and priorities of potential users with spinal cord injury," *Archives of Physical Medicine and Rehabilitation*, vol. 96, no. 3, pp. S38–S45, 2015.
- [48] Y. M. Chi, Y.-T. Wang, Y. Wang, C. Maier, T.-P. Jung, and G. Cauwenberghs, "Dry and noncontact EEG sensors for mobile brain-computer interfaces," *IEEE Transactions on Neural Systems and Rehabilitation Engineering*, vol. 20, no. 2, pp. 228–235, 2012.
- [49] Y.-T. Wang, Y. Wang, and T.-P. Jung, "A cell-phone-based brain-computer interface for communication in daily life," *In Journal of Neural Engineering*, vol. 8, no. 2, Article ID 025018, 2011.
- [50] J. Katona, D. Peter, T. Ujbanyi, and A. Kovari, "Control of incoming calls by a windows phone based brain computer interface," in *2014 IEEE 15th International Symposium on Computational Intelligence and Informatics (CINTI)*, pp. 121–125, Budapest, Hungary, November 2014.
- [51] A. Campbell, "NeuroPhone: brain-mobile phone interface using a wireless EEG headset," in *Proceedings of the Second Acm Sigcomm Workshop on Networking, Systems, and Applications on Mobile Handhelds*, pp. 3–8, New York, NY, USA, August 2010.
- [52] G. N. Jayabhavani, N. R. Raajan, and R. Rubini, "Brain mobile interfacing (BMI) system embedded with wheelchair," in *2013 IEEE Conference on Information & Communication Technologies*, pp. 1129–1133, Thuckalay, India, July 2013.
- [53] Y.-C. Kuo, *A Study on Interface Design of Digital Television Remote Control*, Tatung University, Taipei, Taiwan, 2011.
- [54] W.-K. Tey, *Design and Implementation of Low-Power Wireless Intelligent Controller for Legacy IR Appliances*, National Chiao Tung University, Hsinchu, Taiwan, 2011.
- [55] S.-K. Tseng, *Smart IR Remote Control Application for Home Electronic Appliances*, National Taipei University of Technology, Taipei, Taiwan, 2014.
- [56] I. Käthner, S. Halder, C. Hintermüller et al., "A multifunctional brain-computer interface intended for home use: an evaluation with healthy participants and potential end users with dry and gel-based electrodes," *Frontiers in Neuroscience*, vol. 11, 2017.

- [57] F. Akram, H.-S. Han, and T.-S. Kim, "A P300-based brain computer interface system for words typing," *Computers in Biology and Medicine*, vol. 45, no. 1, pp. 118–125, 2014.
- [58] G. H. Klem, H. Otto Lüders, H. H. Jasper, and C. Elger, "The ten-twenty electrode system of the international federation," *In Electroencephalography and Clinical Neurophysiology*, vol. 10, no. 2, pp. 370–375, 1958.
- [59] "Computer Workstations eTool," Occupational Safety And Health Administration, https://www.osha.gov/SLTC/etools/computerworkstations/components_monitors.html.
- [60] L.D. Silva-Sauer, L. Valero-Aguayo, A. D. L Torre-Luque, R. Ron-Angevin, and S. Varona-Moya, "Concentration on performance with P300-based BCI systems: a matter of interface features," *Applied Ergonomics*, vol. 52, pp. 325–332, 2016.
- [61] S. Gavett, Z. Wygant, S. Amiri, and R. Fazel-Rezai, "Reducing human error in P300 speller paradigm for brain-computer interface," in *Proceedings of the 34th Annual International Conference of the IEEE Engineering in Medicine and Biology Society, EMBS*, pp. 2869–2872, San Diego, CA, Aug 2012.
- [62] J. R. Wolpaw, N. Birbaumer, W. J. Heetderks et al., "Brain-computer interface technology: a review of the first international meeting," *IEEE Transactions on Rehabilitation Engineering*, vol. 8, no. 2, pp. 164–173, 2000.
- [63] W. Speier, A. Deshpande, and N. Pouratian, "A method for optimizing EEG electrode number and configuration for signal acquisition in P300 speller systems," *Clinical Neurophysiology*, vol. 126, no. 6, pp. 1171–1177, 2015.